공학박사학위논문

해상회수를 위한 저비용 소형 고고도 과학기구 시스템 개발 및 비행시험

Development and Flight Test of Low-cost Small Scientific Balloon System Suitable for Sea Recovery

2020년 2월

서울대학교 대학원

기계항공공학부

강 정 표

해상회수를 위한 저비용 소형 고고도 과학기구 시스템 개발 및 비행시험

Development and Flight Test of Low-cost Small Scientific Balloon System Suitable for Sea Recovery

지도교수 이 관 중

이 논문을 공학박사 학위논문으로 제출함

2020 년 2 월

서울대학교 대학원

기계항공공학부

강 정 표

강정표의 공학박사 학위논문을 인준함

2020 년 2 월

위 원 장 : 金奎弘

부위원장 : 李管中

위 원 : 姜昌求

위 원 : 權高範

위 원 : 蔡相賢

ABSTRACT

Development and Flight Test of Low-cost Small Scientific Balloon System Suitable for Sea Recovery

Jungpyo Kang

Mechanical and Aerospace Engineering

The Graduate School

Seoul National University

The reasonable solution to retrieve a payload of a scientific balloon regardless of safety issues and recoverability is the sea recovery strategy. The sea recovery strategy is a unique retrieval method being pioneered by the Japan Aerospace Exploration Agency (JAXA) and the Institute of Space and Astronautical Science (ISAS) for decades. This strategy has contributed to the achievement of various scientific and engineering research missions in Japan, such as in atmospheric observation and space environment simulation. However, in spite of a long history of conducting sea recovery strategy by JAXA/ISAS, to the best of the author's knowledge, there have been few published works on designing and manufacturing balloon systems suitable for sea recovery operations due to the rarity of this recovery method. In this context, a detailed description of a system for a small

zero pressure balloon (ZPB) platform designed for sea recovery operations was presented in this study. For this, a small ZPB platform using affordable commercial off-the-shelf (COTS) products were developed with careful consideration of maritime telecommunication, water resistance, short-circuit prevention, and flotation. In addition to reducing the overall cost by using COTS products, it enabled miniaturization of the telemetry, tracking, and command (TT&C) system to enhance portability.

Along with the balloon system development, a study on the balloon trajectory was conducted to establish a balloon campaign procedure focused on sea recovery operation. To this end, the trends of the balloon trajectory for five years (2014 ~ 2018) with respect to seasonal wind variations were investigated employing the numerical trajectory prediction program. Upon reflecting on the simulation results, the sea recovery operating procedures for a small ZPB in the East Sea of the Republic of Korea, which capitalized on the geographical advantage of the Ulleungdo, were suggested. With these procedures, the developed small ZPB platform demonstrated the desired performance and system reliability at sea through four flight tests, including sea recovery strategy.

Keywords: Scientific balloon, High Altitude Balloon, Flight Test, Tracking, telemetry and command system, Sea recovery

Student Number: 2016-30182.

Table of contents

List of Figures

List of tables

1. Introduction

1.1 Overview of scientific ballooning

High altitude scientific balloon is a widely used platform to carry out various scientific and engineering research goals such as space environment simulation test, space atmospheric observation and measurement [1-7]. It usually flies in stratosphere layer with expensive equipment weights from less than 0.1 ton to several tons. Compared to space environment test and exploration tools such as satellites and launch vehicles, the scientific ballooning platform has merits such as short preparation period from proposal to launch, fewer restrictions on launch sites, low price per pounds to get the payload into space, and highly reliable platform for given missions [8, 9]. Table 1 shows additional advantages of the stratospheric balloon in the perspective of balloon operation campaign.

Table 1 Comparisons on the space research platforms

	Scientific balloon	Rocket	Satellite
Operating hours	Several hours ~ A few months	Several seconds ~ minutes	Several years
Operating altitudes (km)	35 ~ 40	100 ~ 1,000	100 ~ 10,000
Payload shape restrictions	No	Depending on the pairing shape and size	Depending on the pairing shape and size
Payload capacity (kg)	10 ~ 2,000	50 ~ 150	Several tons
Total required time for a campaign	A year	Two ~ three years	A few years ~ ten years
Recoverability	Possible	Sometimes it is possible.	Impossible
Budget ($)	Hundreds of thousands	Millions of dollars	Tens of billions

Based on the aforementioned advantages, the high altitude scientific balloon has been used for decades in the national research center of advanced aerospace countries such as the United States (NASA), France (CNES), and Japan (JAXA) to perform various research objectives. In 2004, a collaborative team of nine universities consisted of USA, Italy, South Korea countries carried out Cosmic-ray energetics and mass(CREAM) project by installing a high-energy cosmic ray measurement device in the scientific balloon in Antarctica [10]. In 2009, Japan Aerospace Exploration Agency(JAXA) conducted a balloon drop test of the flexible aeroshell used for atmospheric entry vehicles to obtain data on structural strength as well as the behavior of an inflatable torus mounted on an aeroshell [11]. In 2013, Google, one of the world's leading IT companies, made a fleet consisting of dozens of scientific balloons to provide public internet services in rural and remote areas worldwide [12]. In 2014, to improve the state of the art in Mars supersonic decelerator technology, NASA's Low Density Supersonic Decelerator (LDSD) demonstration mission has been conducted by employing a scientific balloon in Hawaii [13].

Previously mentioned researches used a large size scientific balloon more than the length of 100 meters except for the Google loon which of 15 meters. Those experiments using the large size balloon require costly support facilities and equipment such as the balloon operation control building, long airstrip, hangar, and heavy launcher vehicles to operate and develop [14, 15]. In this regard, the enormous cost has hindered most of the educational institutes to perform novel

science and test the new technologies.

However, the advent of open source software / hardware ecosystems with low-cost and yet high-performance have opened a new horizon for various research and development [16-19]. Hence, the cost of scientific balloon development and operation could have been reduced to a level that is affordable for educational institutes. In 2018, the Balloon Measurement Campaigns of the Asian Tropopause Aerosol Layer (BATAL) was aimed to research the nature, formation, and transport of polluted aerosol in the upper troposphere and lower stratosphere during the Asian summer monsoon [20]. This project utilized a small-sized scientific balloon which were supported by Tata Institute of Fundamental Research (TIFR) balloon facility to carry the aerosol impactor which weighs more than 10kg. In 2005, students from university of Kentucky conducted a rubber balloon-borne drop test of the Mars prototype aircraft equipped with inflatable-rigidizable wings [21].

1.2 Balloon configurations

In general, a scientific balloon consists of an envelope, a parachute, and a payload (gondola), as shown in Fig. 1. The envelope includes an exhaust valve and a tear panel. The exhaust valve regulates the amount of buoyant gas emission to lower the altitude of the balloon, and the tear panel rips the balloon film when the flight termination is conducted. The parachute serves to slow down the freefall speed of the separated payload so that the mission equipment can be retrieved intact. The gondola consists of observational equipment for performing a specific experiment, a telecommunication device transmitting and receiving the status information of the balloon and control command from the ground station, respectively. It also contains ballasts which will be released to control the ascent speed or to go up higher altitude.

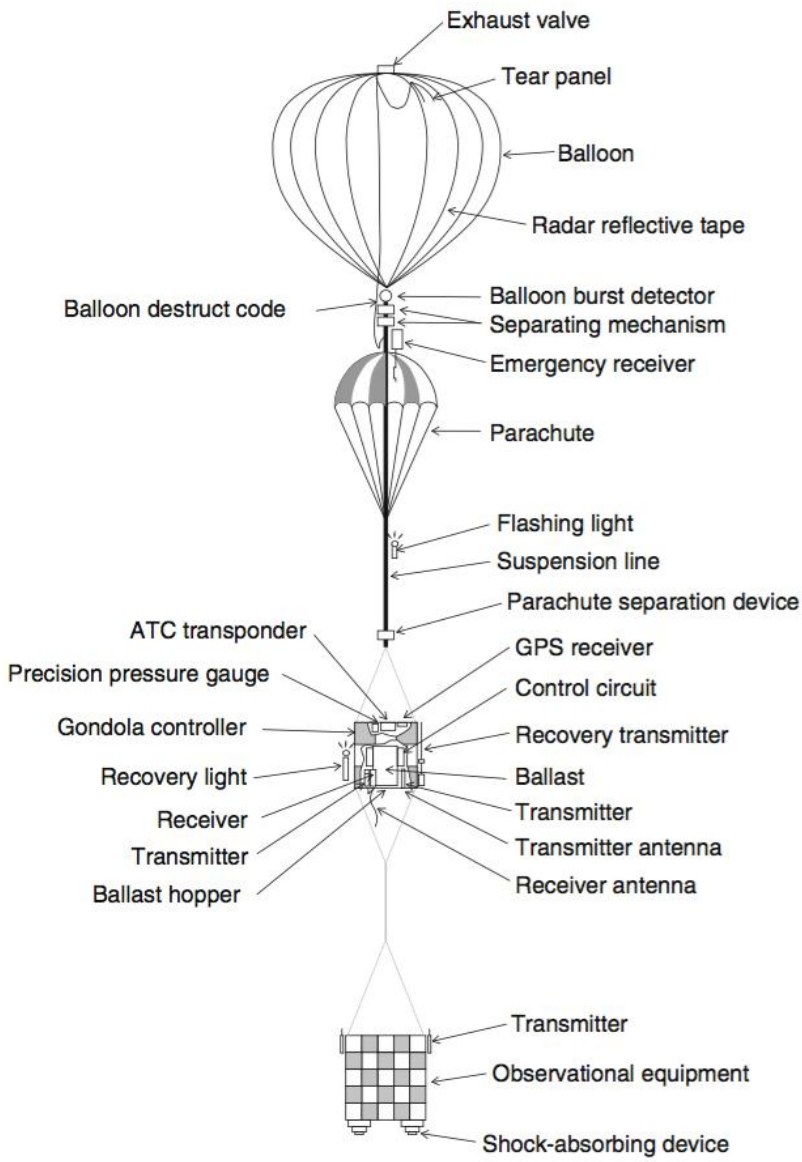

Fig. 1 Typical configuration of a balloon system [22]

The type of high altitude scientific balloon can be classified into Zero Pressure Balloon (ZPB) and Super Pressure Balloon (SPB), as shown in Fig. 2 [23]. The ZPB has a venting duct at the bottom of the envelope, so that the pressure difference between inside and outside of the envelope to be zero. The ZPB is easy to manufacture and operate compared to the SPB. However, it is an open balloon which can not escape from the Sunset effect: during the night, the volume of balloon reduces and loses buoyant force which makes dropping ballast inevitable. During the day, the volume of gas expands more than the design volume of envelope which causes gas release. The process repeats until all ballast is used up, which limits operating time.

Super-pressure balloon does not have gas ducts and is sealed completely. Since any gas can not escape from the balloon and pressure builds up as the gas expands, the SPB can operate for longer duration than the ZPB. Since super-pressure balloon should endure high pressure of buoyant gas, empirical factors should be considered to design it. Therefore, high technical maturity accumulated for decades is required for production [24].

(a) Zero Pressure Balloon (ZPB)

(b) Super Pressure Balloon (SPB)

Fig. 2 Classification of the stratospheric balloons

1.3 Motivation and scope of the dissertation

One of the better aspects of scientific balloons compared to satellite and launch vehicles is its recoverability. The retrieval of a detached payload allows easy acquisition of the mass data stored on its onboard systems as well as cost reduction through the reuse of its mission equipment [25]. Generally, ground recovery strategy is implemented for the retrieval of payload by countries with low population densities over vast geographical areas, such as the United States and Australia. As presented in Fig. 3, the facilities of scientific ballooning communities such as NASA, JAXA, and CNES have been stationed sparsely populated area around the world. These vast places are easily accessible to the recovery team [26-28].

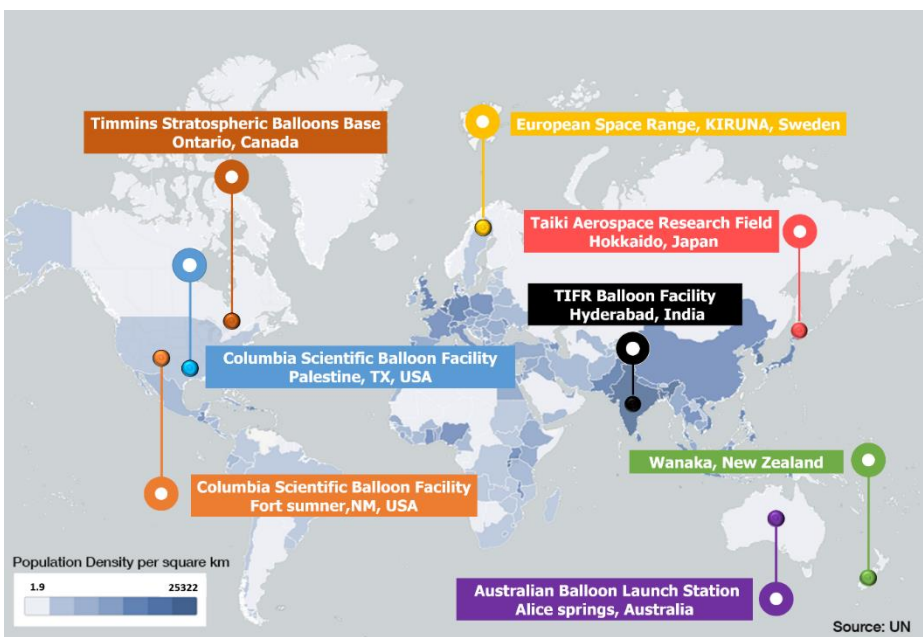

Fig. 3 The scientific ballooning base upon global population density in 2015

However, as shown in Fig. 4, ground recovery in countries with high population densities over small geographical areas, such as the Republic of Korea, may cause safety concerns such as house damage or road blockage when the detached payload is jettisoned over a populated area. In addition, Korea's rough geography, which is made of 70 % mountainous terrains and inaccessible ridges, makes it difficult to retrieve a payload after it has descended. In this regard, sea recovery is a more feasible choice for payload retrieval.

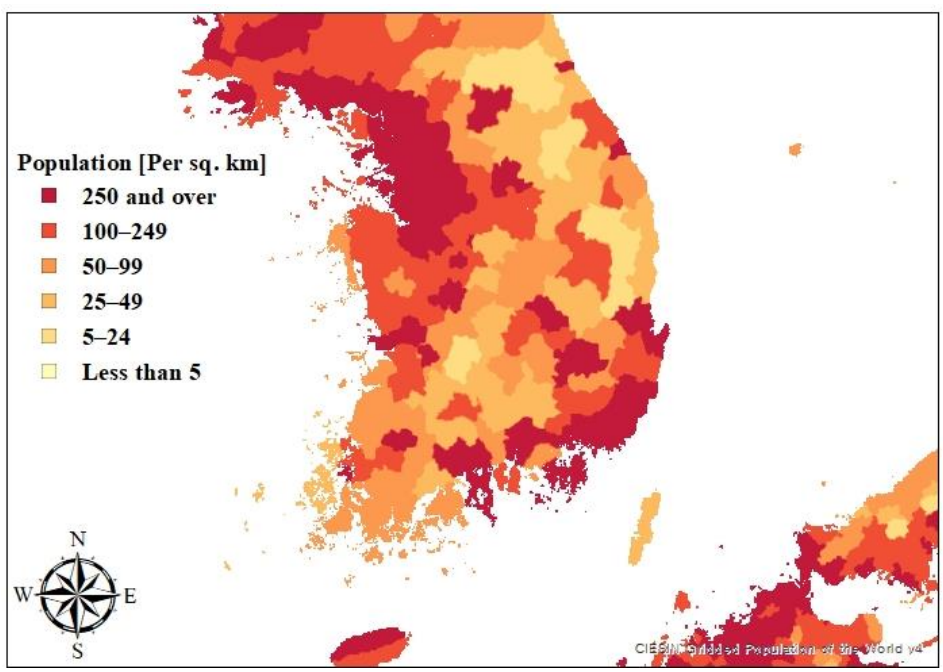

Fig. 4 Population density in the Republic of Korea as of 2015 [29]

Sea recovery is a unique retrieval method being pioneered by JAXA for decades. The strategy has helped the space research organization in successfully conducting various missions while addressing the safety issues and topographical restrictions associated with payload recovery in Japan [30].

However, in spite of there being a long history of sea recovery operations, to the best of the author's knowledge, there are few published works on the scientific balloon system development focusing on sea recovery in detail due to the rarity of this recovery strategy. Moreover, application of the scarce publications describing the generic system development of large balloons is not suitable for small balloon systems that educational institutions can afford.

In this context, this paper aims to address the detailed system development process of a small zero pressure balloon which is suitable for sea retrieval strategy with affordability. To attain this end, a small ZPB platform using commercial off-the-shelf (COTS) products was developed with careful consideration of maritime operation of the ZPB system. The developed small ZPB, titled as Seoul National University scientific BALLoon (SNUBALL), is expected to satisfy the research demands of universities that require balloons even where the terrain is unfavorable to balloon campaigns.

The SNUBALL system, which can be operational at sea, can also considerably encourage the international collaboration research projects requiring long-duration balloon flight such as scientific observation and measurement for ozone and atmospheric trace components over Antarctica and the Stratole-2 project of

the CNES for the wind observation in the equatorial tropical tropopause layer(TTL) [31, 32]. These international collaboration researches for long-duration flight can be more effectively conducted with sea recovery strategy. This strategy enables to expand balloon campaign space from domestic level to the international level by using the territorial waters of other participating nations. In this regard, it is expected to contribute to expanding the opportunities for university research institutes to participate in various international cooperation research.

This paper is organized as follows: After the introduction of Chapter 1, balloon system development was introduced in chapter 2. For the realization of the sea recovery strategy, a few salient system requirements, such as water resistance to prevent submersion, prevention of saline water-induced electrical short circuit, flotation capability to keep the payload afloat after a descent, and maritime telecommunication were taken into account in the design and manufacturing stage. To improve the completeness of the sea recovery strategy, a buzzer for detecting the gondola (suspended payload) and an auto-inflation buoy for providing additional buoyancy were included in the balloon system.

In chapter 3, pre-flight preparations focused on sea retrieval strategy was addressed. This chapter describes the towing tank test before the flight test, the developed balloon platform prototype, and the devised flight test procedure in sequence. The sea recovery procedure, which is pertinent for the Republic of Korea environment, is also suggested to minimize safety issues and a risk of losing the separated payload. Based on the devised flight test procedure, four flight tests,

including sea recovery operations, were conducted using rubber balloons and 7-m-high ZPBs to verify the operational reliability of the SNUBALL system at sea.

In chapter 4, the results of flight tests using the rubber balloon and the ZPB were investigated as a case study. The presented cases of flight tests are 28 March 2018 with a rubber balloon and 27 May 2018 with a ZPB, respectively. Based on these flight tests, some insights and lessons learned on the balloon campaign are derived. Finally, the conclusion is given in Chapter 5.

2. System development

2.1 Mission profile

SNUBALL is aimed at carrying out university-level research projects such as atmospheric aerosol measurement and airplane drop test for the Mars exploration [33]. Its target payload capacity including basic onboard equipment was determined at 50 kg, which is an appropriate weight for easy handling of light experimental equipment from educational institutions. The target altitudes vary from 20 to 30 km for given missions. The typical mission profile of SNUBALL is shown in Fig. 5. This mission profile broadly consists of launch, ascent, mission, envelope and parachute separation, and gondola retrieval at sea. After reaching the target altitude, the SNUBALL reaches level flight. The target altitude and duration of the level flight depends on the given mission purpose. For flight termination, the integrated separation system is triggered by an onboard mechanism upon receiving a command from the ground station to sever the suspension line between the envelope and the parachute. The deployed parachute then slows the descent speed of the gondola so that separated payload could be retrieved intact. For retrieving the separated envelope and gondola, the sea recovery strategy is carried out by employing a recovery boat and a global positioning system (GPS) device. The timeline for mission profile is presented as Table 2.

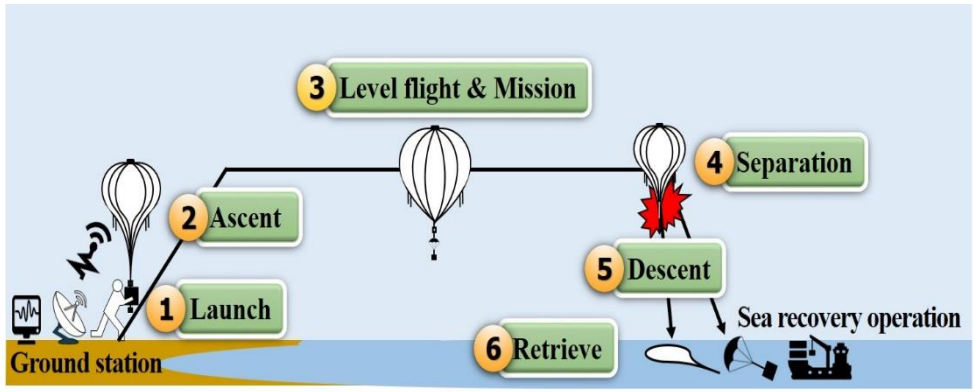

Fig. 5 Typical mission profile of SNUBALL

Table 2 Mission profile timeline

Phase	Time	Altitude [km]	Vertical speed [m/s]
Launch ~ Level flight	00:00 ~ 02:00	0 ~ Target alt.	Rate of climb 5 m/s
Level flight ~ Mission	02:00 ~ 06:00	Vary from 20 ~ 30 km for given mission	
Flight termination ~ Completion of sea recovery	06:00 ~ 11:00	Descent and sea surface	Rate of descent is less than 10 m/s

2.2 System requirement for marine operation

As previously stated in the mission profile, we aim to develop the small stratospheric balloon platform with a less than 50kg payload capacity depending on the given mission. This platform is designed to carry out university-based scientific observation and technological experimentations in the stratosphere after taking regulatory restrictions on airspace usage and geographical constraints of South Korea into account.

Therefore, the high altitude scientific balloon is exposed to extreme temperature changes, such as rapid temperature drop in the troposphere and temperature rise in the stratosphere as the flight altitude increases. It also faces low-pressure environments at an altitude of 30km where 100 times lower than ground pressure. In addition, sea-water environmental conditions that can cause undesired situation such as subversion of the floating payload by waves, and electrical shortage and corrosion by saline water, requires more robust and reliable designs. Therefore, in order to have reliable operation capabilities even in such an extreme environment, the following mission requirements should be taken into account during design and manufacturing:

1) The ZPB platform should be designed to prevent the breakage of the system due to the harsh environmental condition such as the change in internal and external pressure with the change in altitude, and a low temperature below -40°C in the stratosphere. Minor cracks on the system

are highly likely to cause the immersion of the ZPB platform at sea after splashdown.

2) The jettisoned system equipment should be able to sustain flotation and have water resistance for over 4 hours until the completion of recovery.

3) Electrical shorts caused by electrochemically active seawater should be prevented for the safety of the recovery personnel and the protection of electronic equipment.

4) The developed TT&C system should be able to secure reliable communication even in an NLOS situation for monitoring and controlling of the SNUBALL.

5) The recovery team should be able to track and discover the separated payload at sea easily.

6) The separated balloon system should withstand the shock after splashdown.

2.3 Design considerations for the sea recovery

To realize the sea recovery strategy against the aforementioned unfavorable seawater environmental condition for balloon campaign, a small ZPB platform using affordable commercial off-the-shelf (COTS) products were developed with salient considerations.

This subchapter is introduced in the following order:

1. Maritime telecommunication system (TT&C system)
2. Flotation capability to keep the payload afloat after a descent
3. Water resistance to prevent submersion
4. Prevention of saline water-induced electrical short circuit

2.3.1 Data acquisition and command system

For the realization of data acquisition and command, the TT&C system is indispensable. For the operation of a small ZPB balloon platform (SNUBALL), the following four requirements for TT&C system were considered in the design stage.

First, the development of a low-cost, compact ground station system was needed. JAXA/ISAS facilities and equipment, such as large parabolic antennas, radars, and stationary and mobile relay stations, are not compatible with SNUBALL due to financial, weight, and size constraints [22]. Affordability and size were therefore two important factors considered during the SNUBALL design process. Secondly, a telecommunication system was needed to maintain wireless

links even in an NLOS situation caused by decrease in altitude upon splashdown, obstacles such as buildings and mountains, or large distances between the balloon and ground station. As such, the completeness of sea recovery operations was ensured without signal loss. Thirdly, methods were investigated for recognizing the normal operation of critical control commands such as the operation of the integrated separation system (ISS) for flight termination or the deployment of a parachute enabling the retrieval of the balloon system without damage. Lastly, independent sea recovery operation capability of the recovery boat was considered in preparation of the communication failure with a ground station due to the remote navigation of the recovery ship, or failure of the ground station telecommunication system.

2.3.1.1 Frequency selection

The frequency band mainly used for the wireless communication module can be divided into Industry-Science-Medical (ISM) band and amateur radio band. The ISM band is widely used in industrial, scientific and medical applications, and has a wide frequency bandwidth of 2.4 GHz, 5 GHz, and so on, enabling high-speed data transmission. However, it may cause interference to other devices when used in high altitude. According to the radio regulations, the usage of the ISM band output devices which is less than 10dBm can be only used for the high altitude balloon [34]. On the other hand, the amateur frequency band is operated

by a person or organization as a radio station for hobby or research purposes. When the amateur radio driver's license is held, it can be used within 100W output freely. Since the loss is less as the frequency band is lower in the same given operating distance as in Eq. (1) showing free space loss.

$$\boldsymbol{FSL = 20log10(d) + 20log10(f) + 147.55} \quad (\mathbf{1})$$

Where d is the distance in km, and f is the frequency in MHz.

Therefore, the amateur V/UHF radio band was selected for the radio communication of the scientific balloon [35]. To ensure the reliability of long-distance transmission and reception, the downlink and uplink link margins of the UHF module are analyzed. As a result, as shown in Table 3, good link results are shown at 19 dB or more.

Table 3. Link margin for the telemetry operations.

No.	Parameter	Value
1	On-board Transmitter power	30 dBm
2	Onboard feeder losses	1 dB
3	Onboard antenna gain	2.5 dBi
4	Free space path losses for 300km	134 dB
5	Ground receiver antenna gain	13 dBi
6	Ground receiver feeder losses	1 dB
7	Ground received power (No. 1 – 2 + 3 - 4 + 5 - 6)	-90.5 dBm
8	Ground receiver sensitivity	-110 dBm
9	Link Margin for telemetry (No. 7 - 8)	19.5 dB

(a) Down link

No.	Parameter	Value
1	Command Transmitter power	30 dBm
2	Feeder losses	1 dB
3	Transmitter antenna gain	13 dBi
4	Free space path losses for 300km	134 dB
5	Onboard antenna gain	2.5 dBi
6	On-board feeder losses	1 dB
7	On-board received power (No. 1 – 2 + 3 - 4 + 5 - 6)	-90.5 dBm
8	On-board receiver sensitivity	-110 dBm
9	Link Margin for telecommand (No. 7 - 8)	19.5 dB

(b) Up-Link

Compared to the existing terrestrial networks (relay towers), the advantages of the high altitude balloon platform (HABP) in terms of communication are a larger coverage area and a less interference caused by obstacles (buildings, ground elevations). Furthermore, the balloon communication system using the V/UHF frequencies has lower latency (transmission delay) than the satellite communication platform. This feature enables the real time data acquisition and command for balloon campaigns.

To evaluate the communication capability of the balloon within the expected flight area, the line of sight (LOS) radius was calculated at the eastern border of the Incheon flight information region (FIR) by using the Eq. (2) [22, 36].

$$L = R_{er} tan\theta$$

$$\theta = cos^{-1}\left(\frac{R_{er}}{R_{er} + H_{bal}}\right) \quad (2)$$

where, L is the straight line distance from the balloon to the horizon, and R_{er} is the radius of the earth, θ is the angle between the balloon and ground station and H_{bal} is the balloon flight altitude.

Fig. 6 depicts the LOS coverage radius with altitude variation at the eastern boundary line of the Incheon FIR. It is assumed that the propagation loss of the radio waves is not considered. Even if the balloon flies at the eastern boundary line of the Incheon FIR, it was confirmed that the LOS radius is sufficient to

conduct a direct communication with the ground station of the expected launch site (Donghae-si), provided that it flies at or above an altitude of more than 10 km (265hPa). Accordingly, the target altitude of the balloon at or above this value needs to be determined for establishing a reliable communication while avoiding the jet stream region, which is not appropriate for the balloon operation.

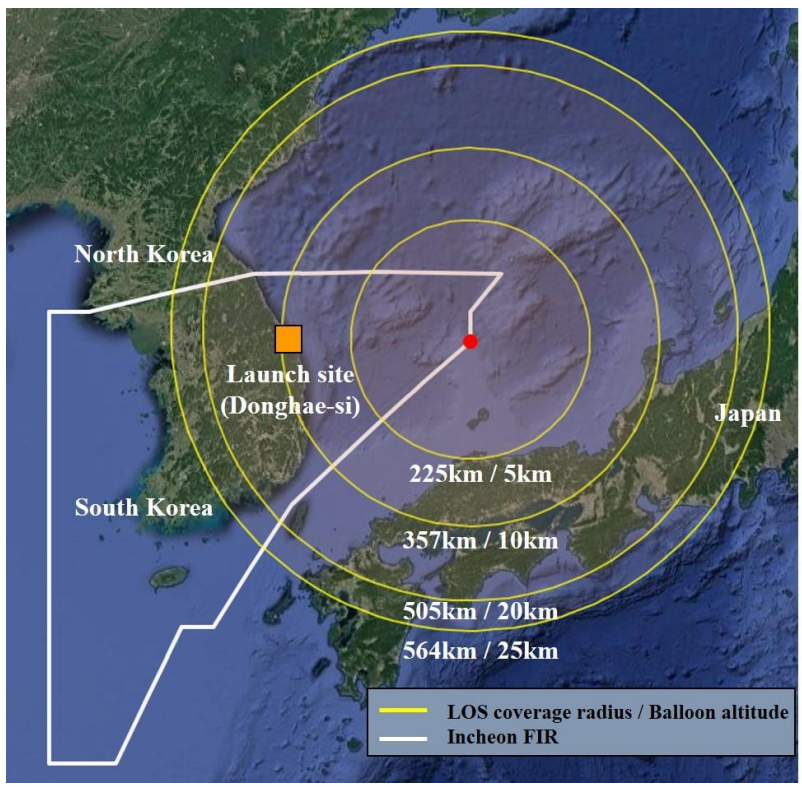

Fig. 6 Line of sight coverage radius with altitude variation at the eastern border of Incheon FIR

2.3.1.2 Development of low-cost, compact TT&C system for ground station.

For the miniaturization of the TT&C system of the ground station, affordable COTS communication products such as very-high frequency/ultra-high frequency (V/UHF) transceivers and an Iridium satellite modem were utilized, as shown in Table 4. The V/UHF transceiver features forward error correction (FEC), which controls the errors in data transmission. The UHF transceiver additionally has the frequency-hopping spread spectrum (FHSS) function, which reduces narrowband interference. The VHF and UHF transceivers are responsible for receiving image data from the balloon and transmitting the status information and command, respectively. These transceivers were connected to a VHF antenna and a UHF antenna, respectively, as depicted in Fig. 7. These antennas were used to display the received image and status information on a developed LabVIEW-based graphical user interface (GUI) program in the ground station, as shown in Fig. 8.

The compact Iridium modem is suitable for small balloon systems because it can acquire data and process commands without any large-sized telecommunication equipment. The data obtained from the Iridium module can be easily accessed via e-mail without a spacious ground station [37]. Thus, the Iridium modem has been a vital contributor in enabling the miniaturization of the ground station. In this regard, it relieves burdens on conducting scientific ballooning at the level of educational institutes.

Besides, if an unexpected malfunction occurs during the final launch check, the line replaceable unit (LRU) and pin-to-pin compatibility advantages of the COTS telecommunication devices will enable quick and easy field replacement. These modularized electronic components also contribute to cost savings by replacing only faulty parts rather than the entire system, and providing a rapid integration process.

Table 4 Selected COTS components and their specifications

Components		Dimensions (mm)	Features	Role	Operating temperature range / Cost
UHF module		37×60×13	Frequency-hopping spread spectrum (FHSS) Forward error correction (FEC)	Primary com' (Status data and command)	-40 to 85 °C / $ 5
VHF module		24×43×13	Forward error correction (FEC)	Transmit still image data	-40 to 85 °C / $ 5
Iridium module		76×51.5×19	Short bus data (SBD)	Secondary com' (Status data and command)	-40 to 85 °C / $ 290

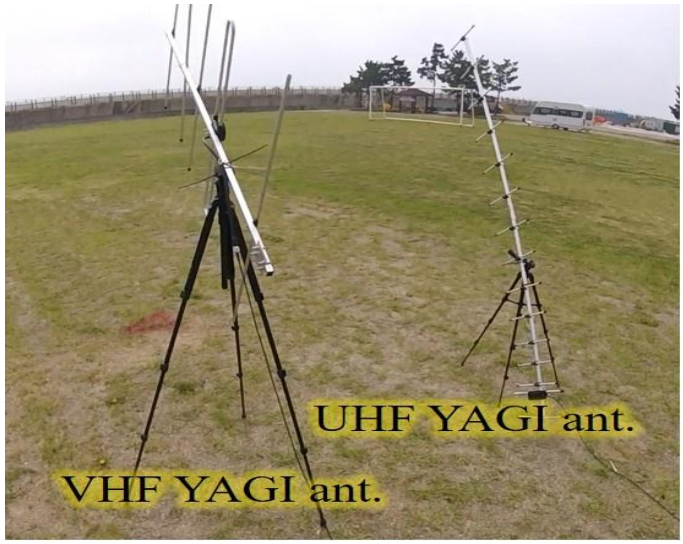

Fig. 7 V/UHF directional antennas (Yagi-Uda)

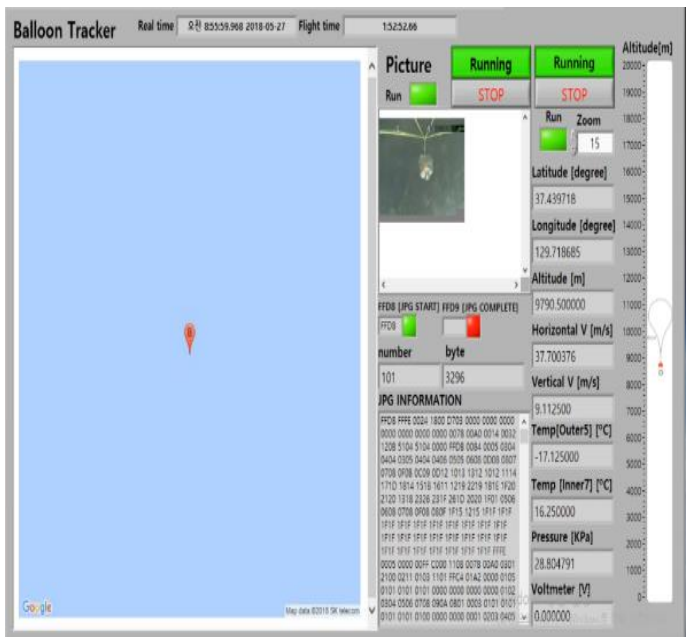

Fig. 8 Designed ground station program for TT&C system

(By using LabVIEW Program)

2.3.1.3 Measures taken in non-line-of-sight (NLOS) situation

Obstacles, balloon flying outside the communication range, and low altitude of onboard telecommunication system after flight termination is highly likely to become the NLOS situation. For preparing a counterplan for this situation, the low-orbit Iridium satellite communication system was implemented for data acquisition and command as well as detection of anomalies in the balloon system. Iridium satellite constellation consists of 66 satellites in orbit around the Earth, allowing global coverage service [38]. In addition to global coverage, several advantages offered by Iridium communication satellite systems are cost-effectiveness by COTS (commercial off-the-shelf), ease of adaptation and integration into user's systems by various data interfaces, and operational reliability under extreme environmental conditions in stratosphere [39]. In this context, the Iridium satellite system shed new light on the loss of communication problem due to NLOS situation, while it also provides affordability and a rapid development cycle.

Iridium satellite communication features short burst data (SBD). The maximum transmission and reception data are 340 bytes and 270 bytes per message, respectively [40]. Thus, its usage pertains to intercommunicating text-type status information but not for image type. In this regard, an Iridium satellite modem (RockBLOCK 9602 module) with a microcontroller was installed as a secondary telecommunication equipment in the gondola and the integrated

separation system (ISS). Fig. 9 depicts the functional diagram of the gondola TT&C system. This system is composed of a UHF transceiver and Iridium modem to telecommunicate house information and command, and a VHF transceiver to transmit real-time still image data to the ground station. Similar to the COTS full-duplex UHF transceiver, which can immediately monitor and control the balloon system, the Iridium module is designed to control the exhaust valve and ballast hopper as well as the flight termination of the balloon in conjunction with ZigBee communication.

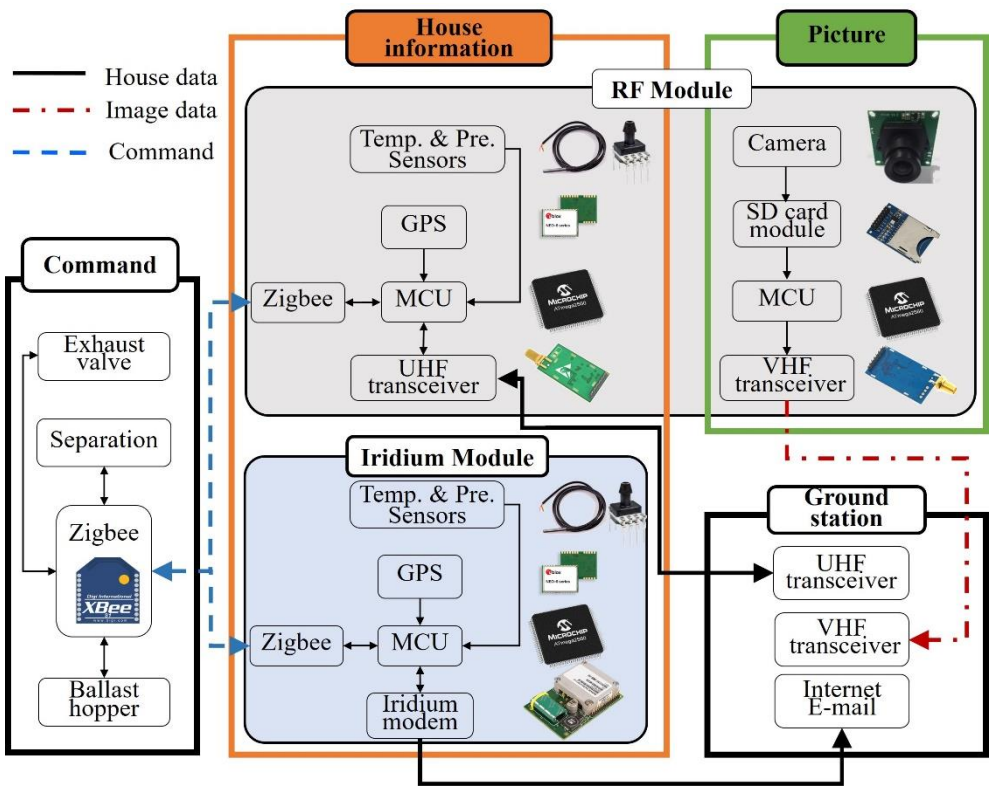

Fig. 9 Functional diagram of Gondola TT&C system

Besides the gondola, the developed integrated separation system (ISS) employing the Iridium modem made a decisive contribution to the envelope retrieval. For example, if the sea recovery operation fails due to an NLOS situation, the envelope made of a polyethylene film may not only cause marine pollution but also become a potential threat to be entangled in the propeller of ships [41]. As such, an envelope should be retrieved after the mission. Unlike for the advanced national balloon research centers, recovering the envelope at sea is a difficult task for educational institutes due to the absence of support equipment such as radar to track the envelope and helicopter to discover it quickly. However, in this study, the retrieval issue has been smoothly solved by the developed ISS connected to the envelope. The ISS transmits status information such as coordinates with altitude, temperature, and pressure via Iridium communication for tracking the envelope, as shown in Fig. 10.

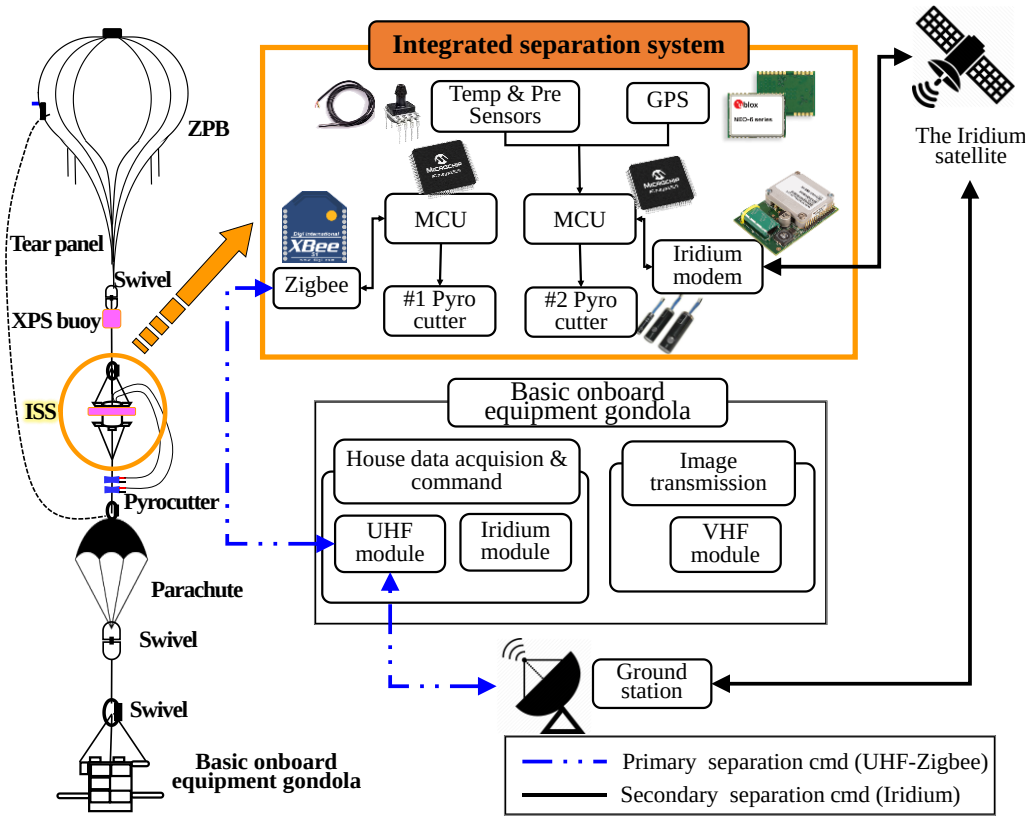

Fig. 10 Functional diagram of the ISS telemetry & command system

In addition, the ISS has a redundant wireless system for a reliable separation command in preparation for an NLOS situation. The wireless system is classified into two categories. The primary system is the Zigbee, which is a short-range wireless system. A telecommand system installed on the basic onboard equipment (BOE) gondola receives a command signal transmitted from the ground station via a UHF frequency band, and then it transmits the command to the ISS using the Zigbee. This primary system can activate the separation immediately upon receiving the command, but the command cannot be executed when it is at an NLOS situation. To address the drawback of the primary wireless communication system, the Iridium satellite communication system was selected as a secondary option for flight termination. Although this communication system is not suitable for immediate transmission and reception of data due to server processing delay or weaken satellite signal, its global communication coverage feature outweigh the shortcomings mentioned above.

2.3.1.4 Measures taken to confirm operation of received commands

To visually check the action of critical control commands such as cable-cutting of the integrated separation system (ISS) and deployment of the parachute, a universal asynchronous receiver and transmitter (UART) transistor-transistor logic (TTL) camera was used. The camera system consisted of a VHF transceiver, a camera, a microSD card, and a microcontroller unit (MCU). Since image data is only transmitted from the SNUBALL to the ground station, a half-duplex COTS VHF transceiver was employed. The images captured by the UART-TTL camera were stored in the microSD as JPEG files. The stored pictures were classified into 32-byte packets through an MCU command and then transmitted to the ground station through the VHF transceiver in real time. The time required to receive a 12 MB photo was set to 1 min. The resolution can be up to VGA (640 × 480). In this work, QVGA (320 × 240) grade, which can reduce the transmission time and allow external visual recognition, was employed. In addition to the camera, the MCUs, which were connected to the UHF transceiver and Iridium modem mounted on the gondola, were programmed to send an acknowledgment upon executing the assigned command. The received data was displayed via the developed GUI program and e-mail messages.

2.3.1.5 Shipboard TT&C system capable of conducting sea recovery operation independently

To make it capable of handling sea recovery operations independently, the recovery boat was installed with the same TT&C system as in the ground station. The developed shipboard ground station is shown in Fig. 11. It consists of a V/UHF omnidirectional antenna, V/UHF transceiver modules, and a LabVIEW-based GUI program to monitor live still images and status information. In addition to these terrestrial communication systems, an additional LabVIEW-based GUI program for Iridium satellite communication was also installed to provide the redundancy of the shipboard TT&C system. Consequently, the sea recovery operation could be performed even during an in-land ground station malfunction. Meanwhile, the minimum number of personnel to operate the TT&C system is two, which means that a relatively small number of workers can recover the payload from sea. Therefore, this system helps to reduce the human resources required by educational institutions.

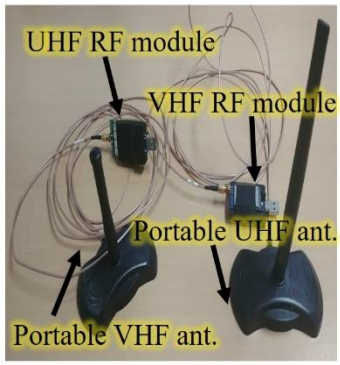

(a) Portable V/UHF omnidirectional antennas

(b) Mounted antennas

(c) The rented recovery ship

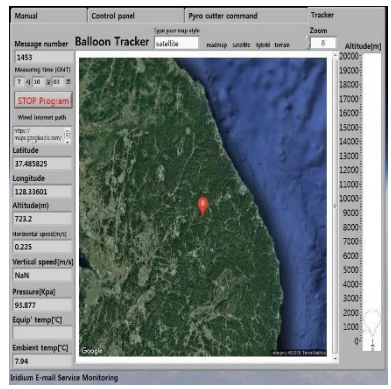

(d) Data acquisition and command GUI for Iridium satellite communication

Fig. 11 The developed shipboard TT&C system

2.3.2 Flotation

Flotation is the paramount factor in deciding the success of a sea recovery operation. Thus, buoyant materials were attached to the envelope, the integrated separation system (ISS), and the gondola, respectively.

The separated envelope after the flight termination floats above the surface of the sea for some time due to the residual air in it. However, it sinks as time elapses and becomes difficult to search for and recover. For the marine environment conservation, the envelope made of thin polyethylene film should be retrieved. Therefore, a measure was required to keep the envelope afloat until the recovery team had arrived. For this, extruded polystyrene foam (XPS) with a density of 35 kg/m^3, which provides 9700 N of buoyancy for a volume of 1 m^3 at sea, was chosen to keep the envelope afloat. Moreover, this material is a vivid pink color to improve its recognition at sea. The required buoyancy safety factor for the envelope was chosen as two times its weight to ensure successful recovery. The required XPS envelop volume was calculated from the Archimedes' principle as shown in Eq. (3).

$$\mathbf{W} = \boldsymbol{F_{Buoyancy}} = \boldsymbol{\rho g A h} \qquad (\mathbf{3})$$

Where $\boldsymbol{W}$ is the weight of the envelope, $\boldsymbol{\rho}$ is the density of the sea, $\boldsymbol{A}$ is an area of the base and $\boldsymbol{h}$ is the height of the polystyrene foam. For a 7 m / 10 kg ZPB envelope floating material weighing 4 kg, a required volume of 0.008 m^3 was calculated. It was designed as a cube with side length 20 cm for easy

manufacturing. The customized polystyrene foam was mounted on the suspension line between the base of the envelope and the integrated separation system. To prevent swaying due to turbulence during the balloon's ascent and descent, the suspension line was made to pass through the center of the buoyant material.

The ISS is developed for the retrieval of a small ZPB envelope. This system not only to conduct the flight termination but also to send GPS data of the envelope even in the NLOS situation. To transmit the location data of the envelope flawlessly after splashdown, it should stay afloat at sea. As shown in the Fig. 12, the buoyant material of the ISS was designed to maintain a stable Iridium and GPS antenna attitude even during disturbance caused by rough waves so that it could point towards the satellite in the sky at all times. It also gives additional buoyancy to the device, preventing it from submerging due to the drag force exerted on the envelope. For this reason, the slide-type buoyant material, which is lightweight and easy to attach and detach, was also made of XPS. This slide-type buoyant material was fitted with the aluminum support rod in the structural enclosure and attached to the upper lid. The volume of designed the buoyant material was 0.004 m3, which can generate a buoyancy of 40 N in sea water. This is approximately twice the required buoyancy.

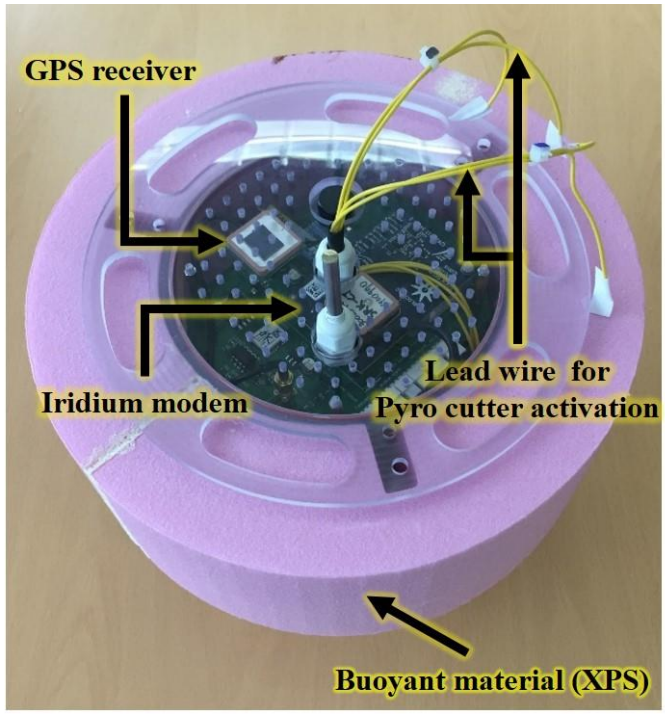

Fig. 12 Integrated separation system configuration with buoyant material

The typical gondola includes mission equipment for various research objectives, devices for telecommunication with the ground facility, and ballast to lighten the gondola weight for accelerating its ascending speed. The gondola usually carries costly equipment and records the valuable data, so it needs to be retrieved after the flight termination. In this regard, the flotation is a crucial factor to the retrieval of the gondola at sea.

The length, width, and height of the aluminum chassis for the gondola are 46 cm, 30 cm, and 30 cm, respectively. Telecommunication and aid devices included, the gondola weighs approximately 12 kg. In addition to a buoyancy of 80 N due

to the submerged volume of telecommunication and aid device enclosures, rectangular buoyant materials that can provide an additional buoyancy of 180 N fitted on the upper surface of the gondola to prevent submersion. The manufactured gondola is shown in Fig. 13.

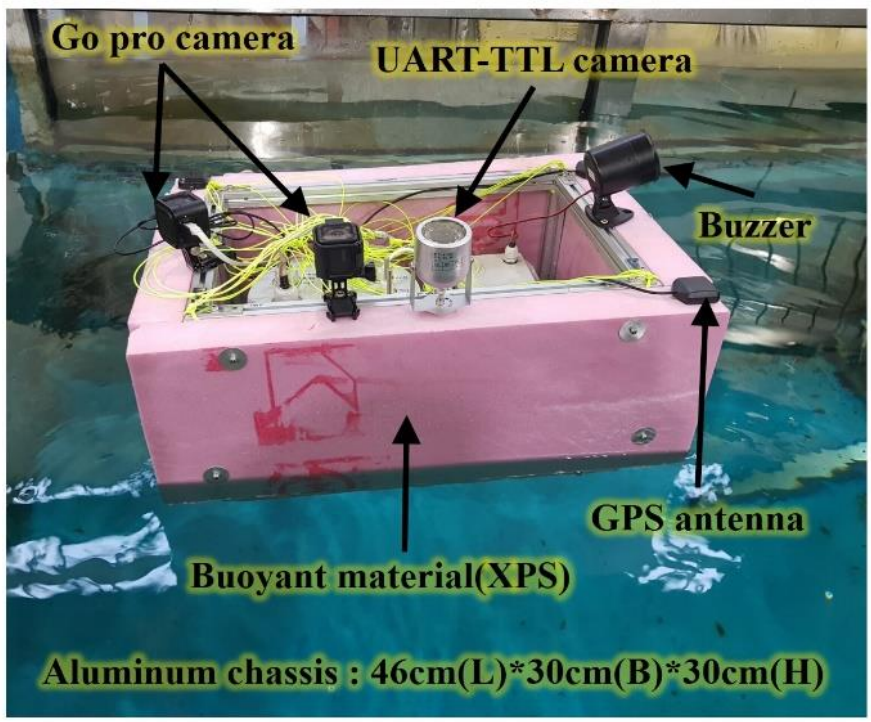

Fig. 13 Gondola in towing tank facility to check buoyancy and stability

2.3.3 Water resistance

Aside from the buoyant materials, another requirement for sea recovery is a waterproof system secured by a structural enclosure. The structural enclosure protects the electronics from submersion and short circuit upon splashdown. To this end, polycarbonate was chosen as the structural enclosure due to its high impact resistance and easy machinability. To design and manufacture an economical waterproof enclosure, a COTS polycarbonate cylinder shape was selected. After taking into account the dimensions and height of the electronics mounted on the PCB, cylindrical polycarbonate structures having an outer diameter of 150 mm and 200 mm, and a height of 150 mm and 200 mm were chosen for the telecommunication equipment of the ISS and gondola, respectively.

The structural enclosure for the gondola and the ISS consists of an upper cover, a polycarbonate cylinder, and a lower cover, as depicted in Fig. 14. The upper cover was equipped with a waterproof COTS ventilation cap (Milvent ®) to prevent stresses on its O-ring and enclosure due to the change in internal and external pressure with the change in altitude. Moreover, a cable gland was employed to place the pyro-cutter lead wire and the thermometer outside while maintaining waterproof performance. A handhold and hook point is also installed on the upper cover for the convenience of retrieving at sea.

The transparent polycarbonate cylinder allowed visual inspection of system anomalies and was bonded to the bottom lid, which was made of aluminum to withstand impact from splashdown. Moreover, three aluminum support rods were

bolted to the upper and bottom lids to prevent the detachment of these lids due to the impact.

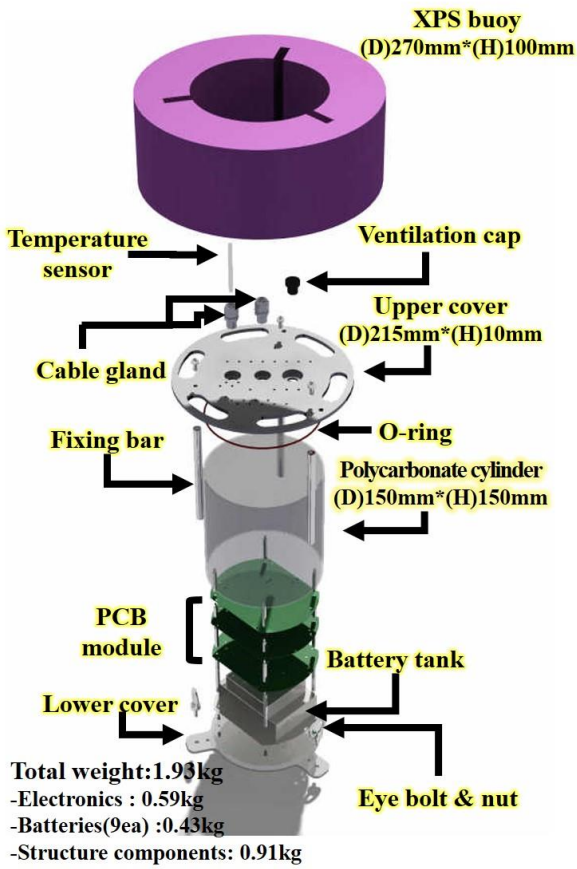

Fig. 14 Exploded view of structural enclosure for integrated separation system

2.3.4 Prevention of the short circuit

Upon splashdown, the integrated separation system (ISS) may likely suffer an electrical short since the lead wire of the cable cutter would be exposed to seawater. To ensure the performance reliability of the ISS in this situation, the power sources of the cable cutter and the electronics were divided into two power sources of 18.5 V and 5 V ratings, respectively, as shown in Fig. 15.

Separation commands received via the Zigbee or Iridium satellite communications activated the specified relay to provide all-fire currents greater than 4.5 A from the 18.5 V power supply to the # 1 or # 2 cable cutter. The 5 V power source supplies power only to the enclosed electronic equipment that such as relays, sensors, and MCU of the ISS. This enables the telecommunication electronics to transmit location and ambient information continuously, regardless of a short circuit in the cable cutter. The maximum available time for the ISS is designed to last for more than 4 hours, assuming a 50% capacity reduction of the lithium-ion battery due to low temperatures. It can operate for more than 9 hours at room temperature.

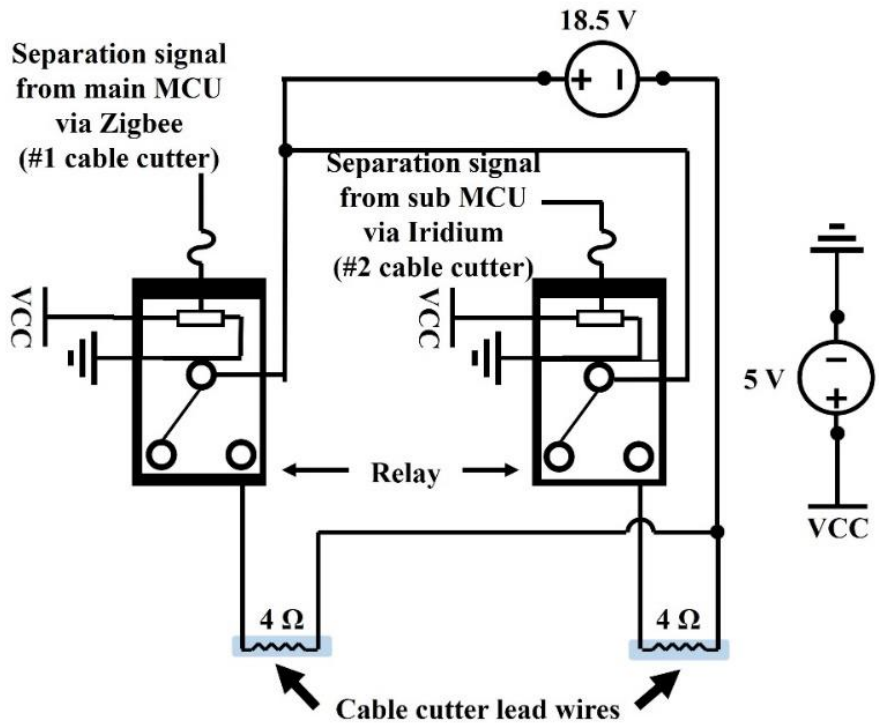

Fig. 15 Circuit diagram of the integrated separation system

2.4 Additional aid equipment for sea recovery

To perform seamless retrieval of the SNUBALL at sea, the following supplemental devices were manufactured and mounted:

2.4.1 Buzzer

For a successful sea recovery operation, the gondola was painted in a vivid color for easy identification, and the information on its position was continuously delivered to the recovery team on the ship via wireless communication. In spite of taking the measures mentioned above, visual identification of the gondola can be laborious since it is small in size and partially submerged. Therefore, to facilitate the identification of the gondola's position, an active buzzer was developed with inexpensive COTS components such as a liquid-level sensor, an active buzzer, and a watertight case, as described in Fig. 16. The liquid-level sensor mounted in the lower part of the gondola becomes a closed circuit that makes a beep sound when its conductor is immersed below the waterline of the gondola. For sea operations, an active buzzer featuring excellent waterproof performance was selected. The maximum sound intensity of the active buzzer is 120 dB, which is the pain threshold of human hearing range.

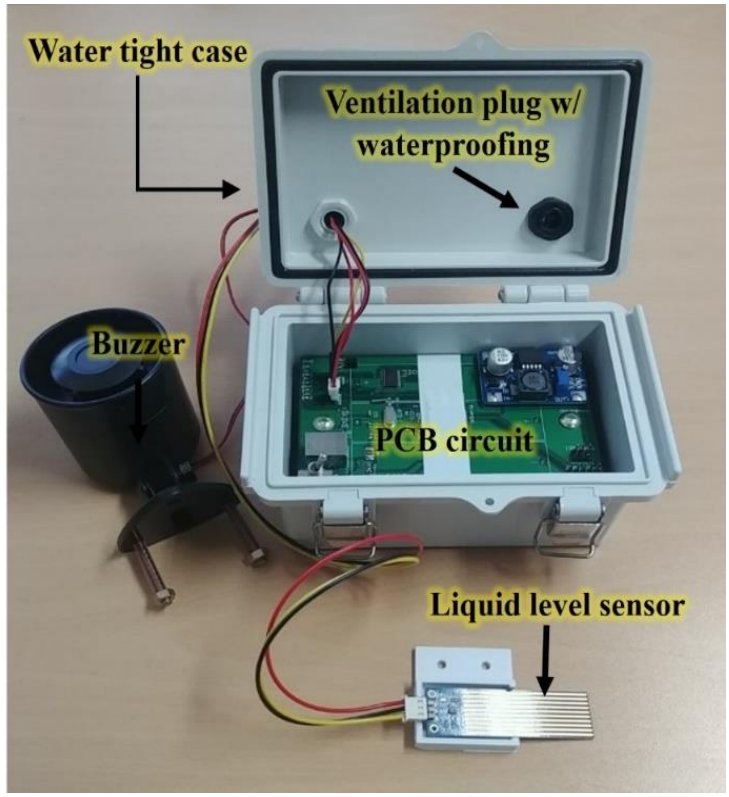

Fig. 16 Buzzer

2.4.2 Auto-inflating buoy

In case of the gondola immersion due to loss of its buoyancy after splashdown, an auto-inflating flotation device was attached. The automatic inflation system is classified into two types: water-pressure inflation and water-detecting inflation [42]. As the balloon ascends among to the atmospheric layer containing clouds, it is exposed to high humidity. Therefore, a water-pressure automatic inflation system was selected instead of a water-detecting inflation device because the latter may expand in the air due to moisture. It is shown in Fig. 17. The commercial automatic inflation system was tethered to the lower part of the gondola by a water-soluble string. After landing in the sea, the system detected the pressure difference, and then activated a CO2 gas cylinder that expands the lifejackets providing buoyancy. The structural integrity of the gas cylinder was verified in a low-pressure chamber before the flight test. For this ground test, an environmental condition of less than 1 kPa (7.5 Torr), which is about one-hundredth of the atmospheric pressure, was set as shown in Fig. 18. The results revealed no breakage or leakage of the gas cylinder.

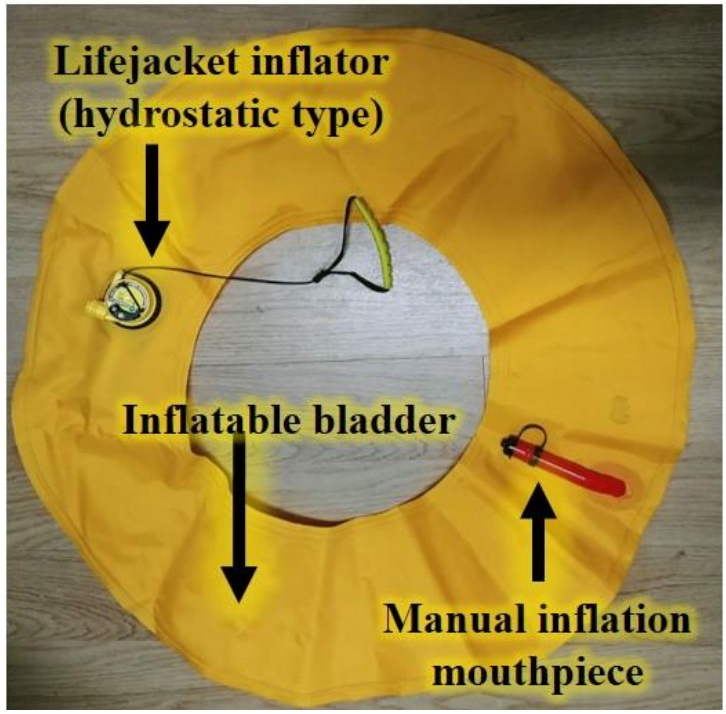

Fig. 17 Water-pressure automatic inflation system

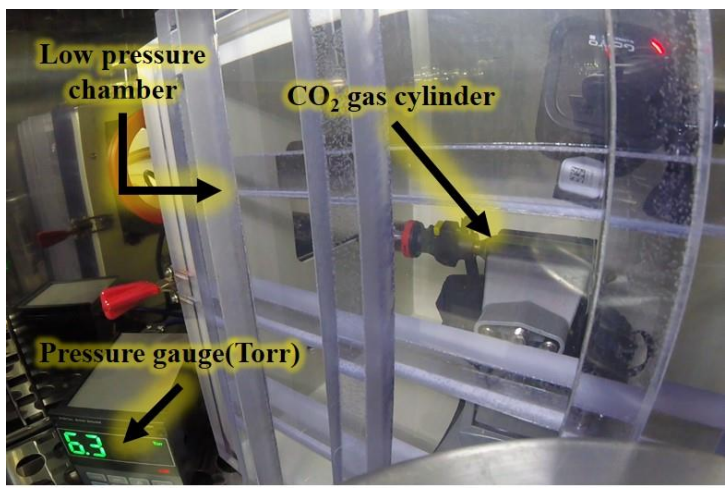

Fig. 18 CO2 gas cylinder ground test in low-pressure chamber

2.4.3 Portable backup GPS-Iridium tracker

Since the gondola is partially immersed, the tracking equipment inside it is vulnerable to electrical shorts when the water-resistance function fails. Therefore, a backup GPS-Iridium tracker was developed and installed to in case the gondola tracking system malfunctioned. It was designed to report the position of the gondola every 2 min via e-mail. The transmitting interval of the tracker can be adjusted according to the user's intention. For example, it is possible to set the reporting cycle as a unit of an hour for a long-duration mission or as a unit of a second for collecting a large amount of data within a short time. It was tethered to the surface of the gondola by a water-soluble string. Upon splashdown, the water-soluble string dissolved to separate the backup GPS-Iridium tracker from the gondola. The tracker detached from the gondola was connected by a thin, high strength 3-m-long rope. Consequently, it holds the GPS and Iridium antennas above the sea surface regardless of the gondola’s attitude.

3. Pre-flight preparation for sea retrieval strategy

Along with the balloon system development, four feasible sea recovery operating procedures were devised in order to realize the balloon campaign at sea in South Korea. To verify the operational reliability of the SNUBALL system at sea and the designed sea recovery operation procedure, four flight tests were performed, including a marine recovery operation using rubber balloons and 7-meter-high ZPBs.

3.1 Towing tank test before flight

The integrated separation system and gondola developed by taking into account flotation, water-resistance, and short-circuit prevention in the design stage were tested in a towing tank of 110 m length and 3.5 m depth prior to the flight test [43]. In order to check their floating posture and impact resistance, the integrated separation system and gondola were free felled at a height of five meters, assuming a terminal velocity of 10 m/s, which is twice the target speed. The results did not report any breakage of the buoyant materials, integrated separation system, or gondola due to the freefall. Moreover, the integrated separation system and gondola maintained stable posture even in simulated waves of height 0.3 m. Additionally, no short circuits occurred for 3 h during the water tank test. Throughout the test, the capability of the balloon system in a maritime environment was confirmed before the flight test.

3.2 Platform for flight test

3.2.1 Zero pressure balloon

Fig. 19 describes the manufactured SNUBALL platform used in the flight test of 27 May, 2018. The developed SNUBALL platform weighed 20.16 kg with a height of 28.1 m. The 7-m-high envelope was designed to reach an altitude of 20 km given 10kg payload. This balloon platform was manufactured as a part of a step-by-step approach strategy before making 15-m- high, 50kg payload balloon envelope, and focused on verification of the balloon system for sea recovery. The mass of the envelope was 4 kg, and the volume of the full inflated envelope was 168 m^3. The mass suspended by the envelope was approximately 16.16 kg. For a stable climb rate of 5 m/s, 3.7 kg of helium gas was injected into the envelope. The lower part of the envelope was equipped with a buoyancy material made of XPS. Upon splashdown, the floating material prevents not only the sinking of the envelope but also the submergence of the connected integrated separation system. The developed integrated separation system was located 5 m below the envelope and supplied power to two cable cutters. After taking into account the weight of the telecommunication system and the ancillary equipment mounted on the gondola, a 4.8 m diameter parachute with a drag coefficient of 1.5 was used to decelerate the gondola. The terminal velocity of gondola was calculated as approximately 4.5 m/s. Aside from the TT&C system in the gondola, an ATC transponder for aviation safety, a buzzer for easy identification, an auto-inflating

buoy for providing additional buoyancy, and the developed portable backup Iridium tracker were also mounted.

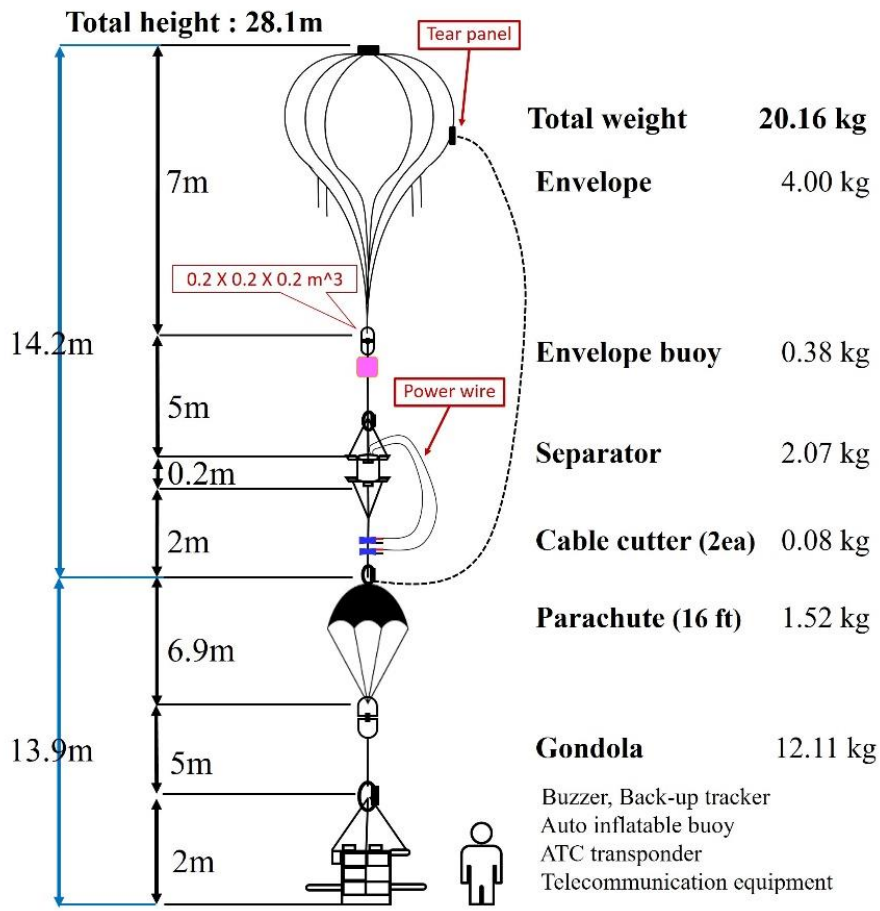

Fig. 19 The zero pressure balloon system configuration

3.2.2 Rubber balloon

The purpose of the two flight tests using a rubber balloon was to assess the performance of the developed ISS and to pre-exercise the sea recovery procedure in preparation for the 7-meter ZPB flight tests. A commercial rubber balloon weighing 1.5 kilograms was used to test the ISS performance in the sky and at sea. Unlike the separated envelope of the ZPB could serve as a parachute, the rubber envelope of the ISS burst or fly away after flight termination. Thus, a parachute was connected to slow down the freefall speed of the separated the ISS so that it can be retrieved intact, as presented in Fig 20.

Rubber balloons can be equipped with not only the ISS but also small mission equipment, making it easy and affordable to use as a stand-alone platform for research in educational institutions. According to International Civil Aviation Organization Aviation Annex 2, a balloon carries a payload less than 4 kg is classified as small balloons. A small balloon has less operating limitations compared to a heavy balloon in the aspect of flight permission and a fail-safe equipment. In this regard, the ISS for was designed to meet the weight constraints of 2kg. This constraint was determined to accommodate the scientific and engineering payload weighs less than 2kg, such as a CubeSats, an aerosol impactor, and an ozone sensor.

Owing to the achievement of weight reduction, rapid flight cycle with mission flexibility becomes possible for the rubber balloon campaign. Universal joints

using eyebolts and nuts were bolted on the protruded bases of the ISS lower part to improve the compatibility with other experimental equipment.

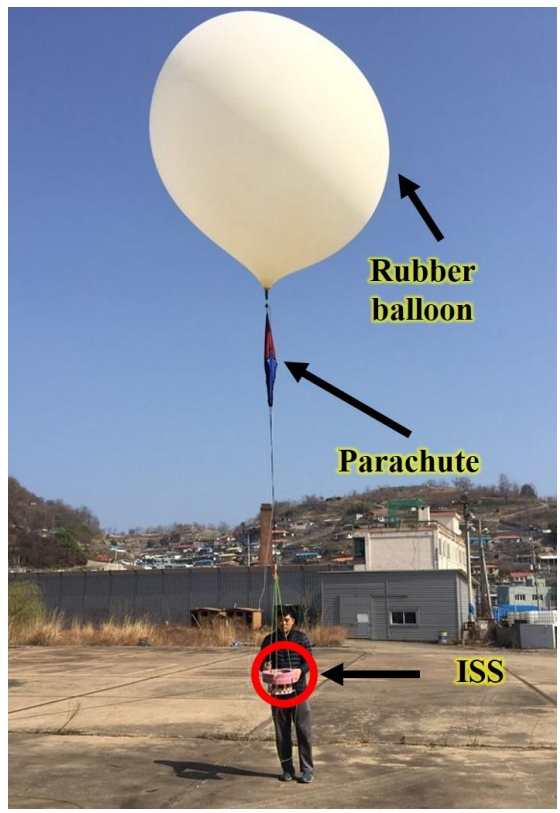

Fig. 20 Rubber balloon system configuration

3.3. Establishing balloon campaign procedure focused on sea recovery operation

3.3.1 Wind environment study

According to the result of wind environment study for scientific balloon campaign, which was thoroughly addressed in appendix A , the lowest wind speed (at or below 12 m/s) was recorded at an altitude of 20 hPa (25km MSL). It also noted that the South Korea, which located in the mid-latitude location, has the wind characteristic of prevailing western wind in all four seasons. However, the wind direction was changed westward at or above 18.5km altitude while constantly blowing eastward in the below of its altitude. This wind characteristic enables the returning of a launched balloon to the launch area. This behavior of the balloon is called as boomerang flight. This phenomenon could make a considerable contribution to the extension of the endurance of the balloon within approved airspace in South Korea. In addition, the time and effort for the retrieval of the payload after completing a given mission could also be drastically saved through this returning behavior of the balloon

Based on the wind study, the launch of the ZPB from the west part of South Korea has been excluded due to the fact that the westerlies could result in balloon trajectories flying over populated areas. Therefore, the Donghae-si, which is located the east coast of South Korea, was tentatively designated as a launch site for the operation of the small scientific balloon. In addition, this place facing the sea is pertinent launch site where the safety issues that may arise due to any abnormal behavior of the balloon during the launch could be minimized.

3.3.2. Scientific balloon trajectory simulations

To establish balloon campaign operation and sea recovery procedures at the tentative launch site, the simulation program introduced in Lee et al.'s work was used [44]. Balloon flight model is illustrated in appendix B

The specifications and the flight simulation information of the small balloon are listed in Table 5. The total mass of the balloon is 18.06kg with the fully inflated volume of 443 m^3. The target altitude of small ZPB was chosen as 25km with 10kg payload. The flight window of the balloon campaign for conducting the university based researches was chosen 6 hours after taking into considerations of followings: airspace infringement to neighboring countries, the time required to reach the target altitude, 2 ~ 3 hours of the mission flight time, and additional flight time for a contingency which requires the extension of the given mission. To investigate seasonal trends of the ZPB trajectories, the daily flight simulation for 5 years from 2014 to 2018 was performed. The weather data employed in the simulations were given by the Global Forecast System (GFS) model of the National Centers for Environmental Prediction, and the simulation implemented the GFS analysis file [45].

Table 5 Balloon specification and flight simulation information

Parameter	Value
Balloon specification	
Payload	10 kg
Free lift percentage	10 %
Lifting gas mass (Helium)	2.69 kg
Total mass	18.06 kg
Maximum volume	443m^3
Flight simulation information	
Target altitude	25km
Flight termination	6 hrs after launch
Launch site	Donghae-si
Launch time	KST 09:00 and 21:00, (UTC+9)

As an example of balloon trajectory simulation results, the winter and summer of 2018 are presented respectively, as shown in Fig 21, 22. The red line, which represents the daily flight paths of the balloons, showed the tendency of the balloon's movement. The yellow circles denote the position of the balloon when the 6 hours elapsed after the launch.

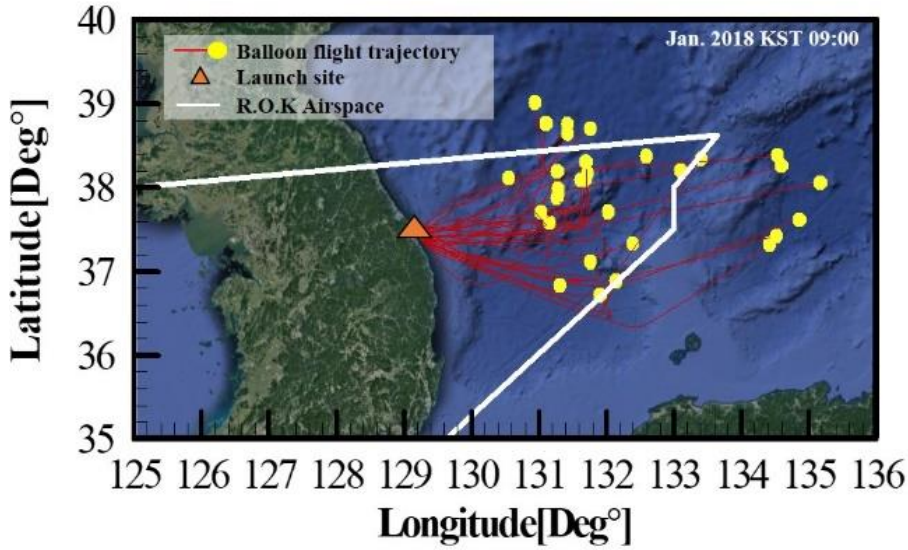

Fig. 21 Predicted trajectories on January 2018 (winter), KST 09:00, UTC+9

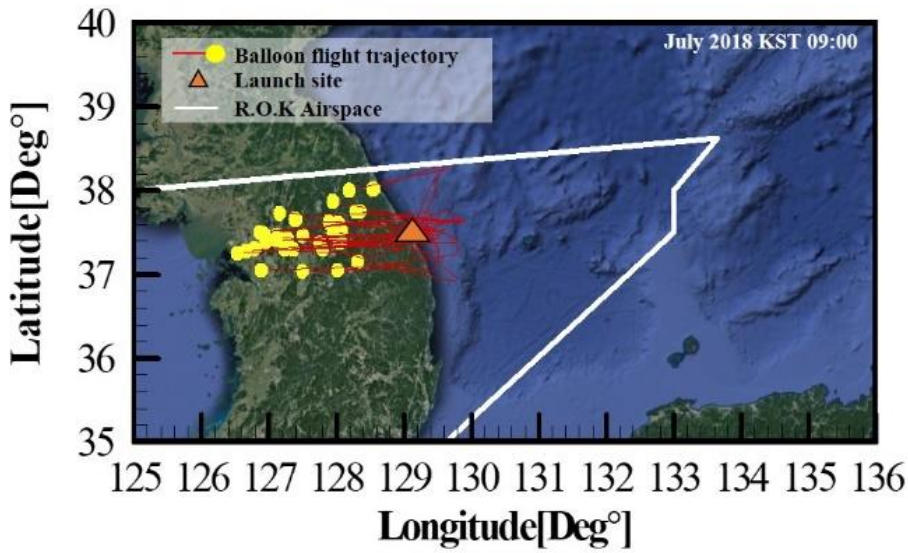

Fig. 22 Predicted trajectories on July 2018 (summer), KST 09:00, UTC+9

The simulation results depict distinctive trends in the summer and winter. The balloon moves notably eastward in winter. It results in several balloon flights crossed over the borderline of the Incheon FIR. These airspace violations were caused by the jet stream, which becomes stronger in winter due to an increment of the temperature difference between the polar region and the equatorial region.

Unlike the trajectories in winter, in summer, the boomerang flight trajectory flies excessively towards the shore. This result is not compatible with the purpose of sea-based operation in terms of safety and recovery efficiency. In a realistic balloon campaign in summer, several balloon trajectories flying above the land could be minimized by make the balloon descend to the altitude where the westward wind is dominant via releasing lift gas. Conducting flight termination before reaching the coastline is also an alternative.

However, there may be a need to support a rubber balloon operation without ballast and exhaust valves or to support experiments that require a certain period of flight time at an altitude of eastward wind. Taking these into consideration, the balloon trajectory simulations were also conducted assuming that a balloon launched from the Ulleungdo. Fig. 23 shows the trajectory simulation results of the Ulleungdo in June, 2018. It can be noted that the distance traveled in the direction of the shore was considerably reduced compared to that of launching in the tentative launch site (Donghae-si).

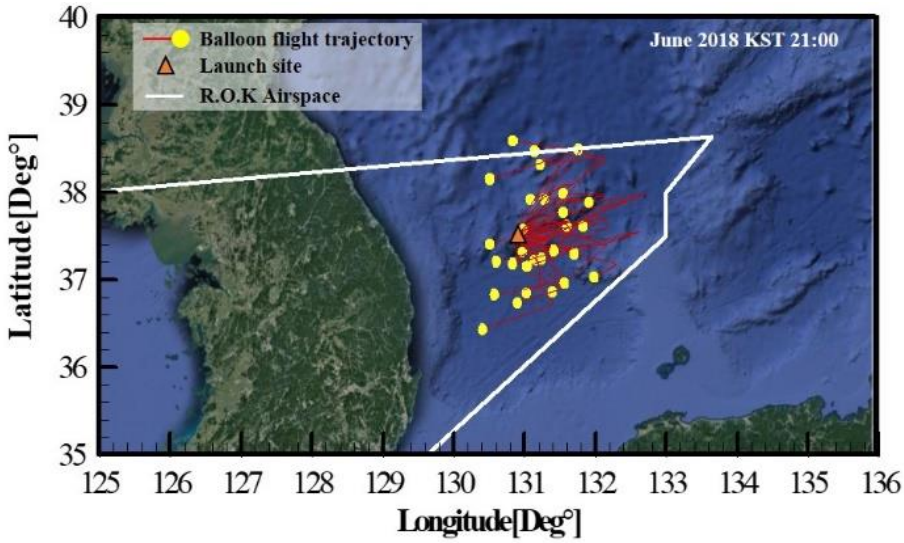

Fig. 23 Predicted trajectories on June 2018 (summer), KST 21:00, UTC+9

On the whole, the simulation results could hardly be the same as the actual balloon flight because there exist uncertainties in balloon trajectory prediction. The uncertainties include operational uncertainty, uncertainty in the prediction model, environmental uncertainty, and manufactural uncertainty. In this context, it should be pointed out that balloon trajectory simulation results are only one of the references for assisting balloon campaign.

3.3.3. Establishing viable sea recovery operations in South Korea

Reflecting on the trajectory simulation results, the four viable sea recovery operating procedures considering seasonal wind environment and safety issues were established as follows.

First, the balloon is launched from the east coast of the South Korea peninsula and retrieved in the vicinity of Ulleungdo in winter, as shown Fig. 24. This sea recovery procedure is recommended for the retrieval of the balloon system which was continuously flied eastward due to the strong westerlies. For the retrieval of the jettisoned balloon system, the geographical advantage of the Ulleungdo was employed. The pre-deployed recovery team at the Ulleungdo are supposed to be waited in the vicinity of the expected landing area while tracking the balloon system. Flight termination is executed when the balloon approaches close enough to the expected landing area, or before flying out of an approved temporary airspace. This strategy is suitable for short flight missions of less than 4 hours considering the strong winds in winter and approved airspace.

Secondly, the balloon is launched from east coast of the South Korea peninsula and retrieved in the vicinity of the launch site coast in summer, as depicted in Fig.25. Flight termination takes place when the balloon flies back close to the near coast of the launch site due to the boomerang effect. After then, the sea recovery team near the launch area is intended to conduct the retrieval operation. This sea recovery procedure with the boomerang effect could make a remarkable contribution to save time and effort.

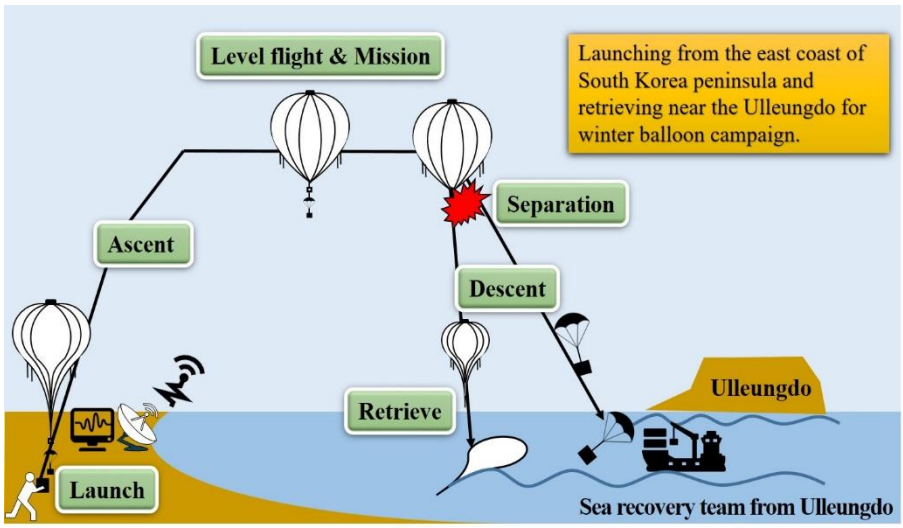

Fig. 24 Launch from the east coast and retrieve near the Ulleungdo(Winter)

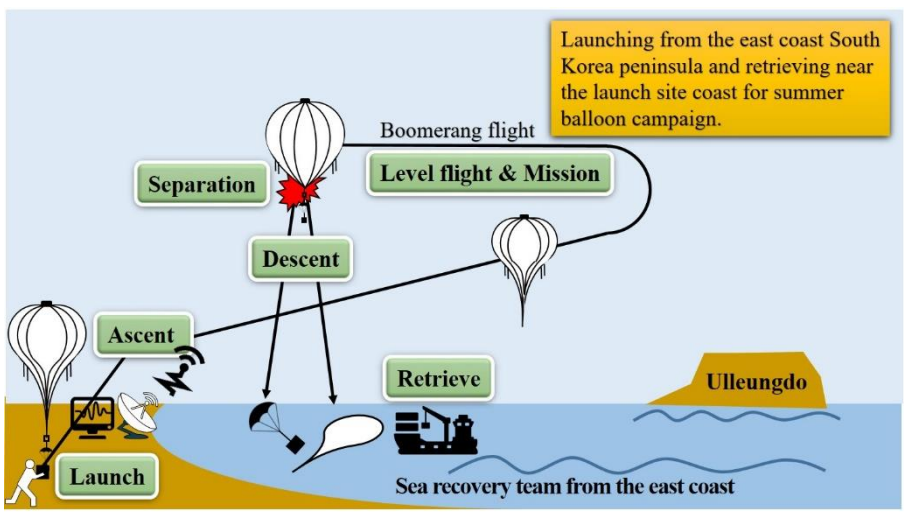

Fig. 25 Launch from the east coast and retrieve near the east coast(summer)

Lastly, a procedure for launching a balloon from Ulleungdo, which is located in the center of the Incheon FIR eastern sector, was established. This procedure was devised to prevent the excessive shoreward flight of balloons in summer due to boomerang effect. Two retrieval locations can be selected by the experiments demands: One is retrieving a jettisoned balloon near the east coast of the Korean peninsula for both the ease of sea recovery strategy, the other is retrieving jettisoned payload near the Ulleungdo for the longer flight time at the target altitude, as presented in Fig. 26,27. In this regard, this method could benefit from the geographical advantage of the Ulleungdo in terms of longer endurance in flight and faster sea recovery operation in summer. However, it should be noted that this procedure has the disadvantage of mobility in transportation. For instance, sea shipping of personnel and equipment to the Ulleungdo are required.

Details on trajectory simulation results for establishing sea recovery operation procedures can be found in Appendix C with operational feasibility.

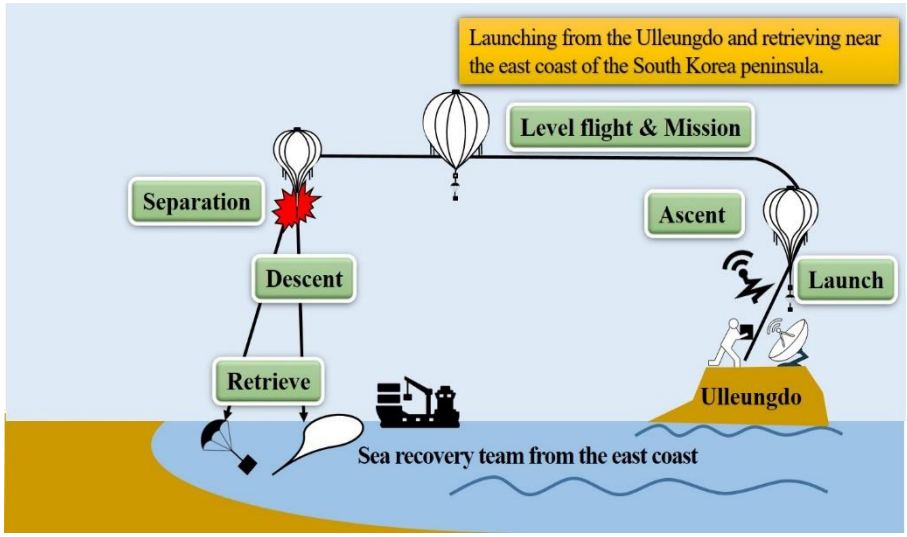

Fig. 26 Launch from the Ulleungdo and retrieve near the east coast (summer)

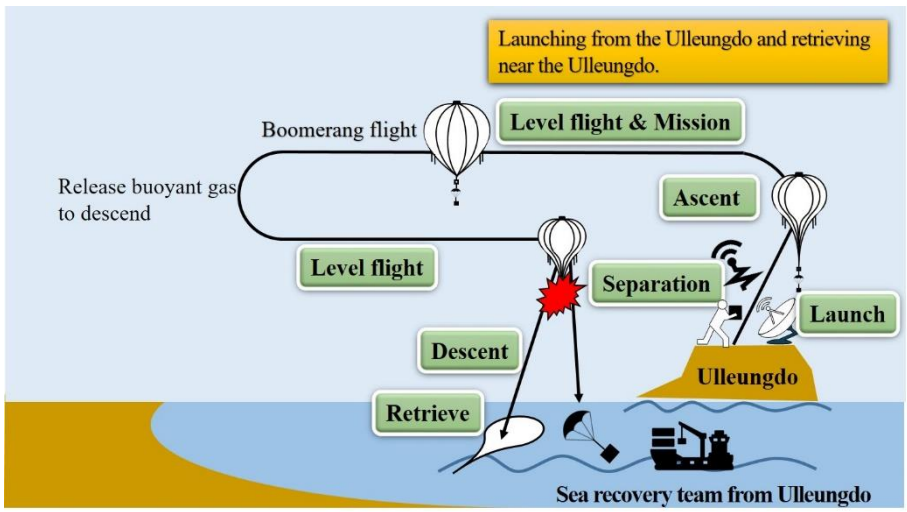

Fig. 27 Launch from the Ulleungdo and retrieve near the Ulleungdo (summer)

3.4. Flight test procedure for the SNUBALL

3.4.1 Pre-launch phase

The flowchart of the pre-launch phase is depicted in Fig.28. After determining the mission profile such as flight time, target altitude, and the payload, the available launch window with favorable weather for balloon campaign is selected.

The Samcheok's closed shipyard facility was chosen for the launch site after taking the safety issues and support facility into account. This place not only provides a hangar for accommodating balloons, but also is located in an area facing the sea where the safety issues that may arise due to any abnormal behavior of the balloon during the launch could be minimized. Thereafter, the predicted flight path is reviewed with respect to safety concerns such as airspace violation during flight, house damage or road blockage of the jettisoned payload. Furthermore, the predicted landing area of the balloon system after flight termination are also examined for the recovery operation. To this end, the balloon trajectory prediction program was employed. The predicted flight trajectory of the ZPB on 27 May 2018 is described in Fig. 29.

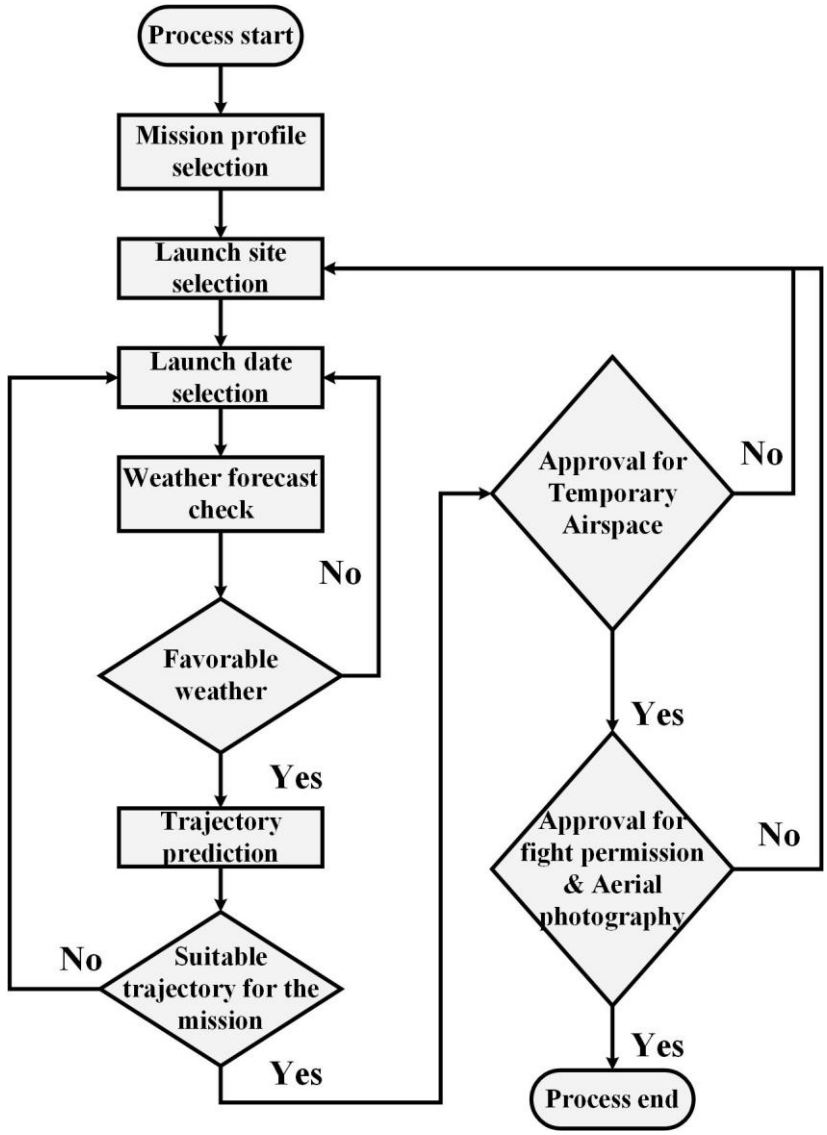

Fig. 28 The flowchart of the pre-launch phase

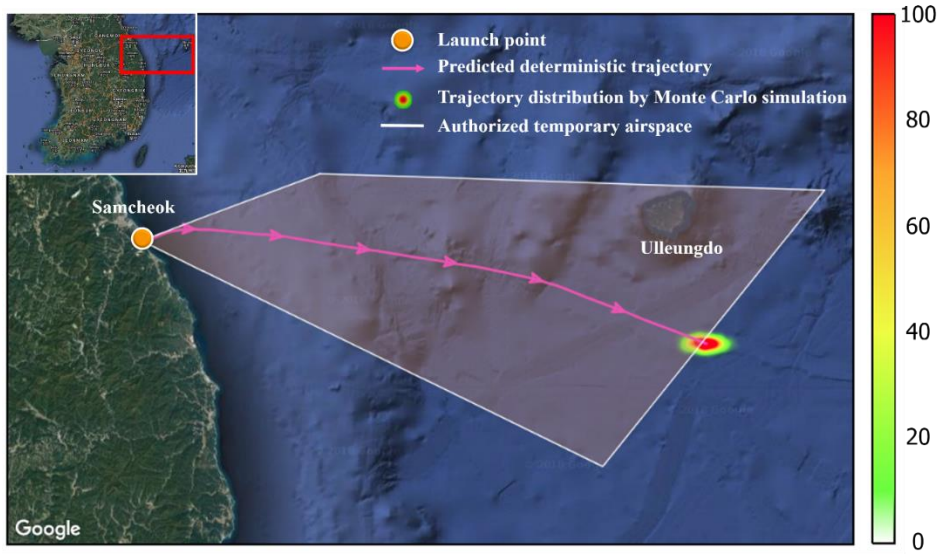

Fig. 29. The predicted flight trajectory of the ZPB on 27 May 2018

If the probability of safety problems due to the balloon's predicted flight trajectory is low and the gondola can be recovered after the flight termination, an administrative procedure for the approval of temporary airspace is carried out [46, 47]. After receiving the approval for using a temporary airspace and flight permission, the launch can be conducted in Samcheok's closed shipyard facility, as shown in Fig. 30.

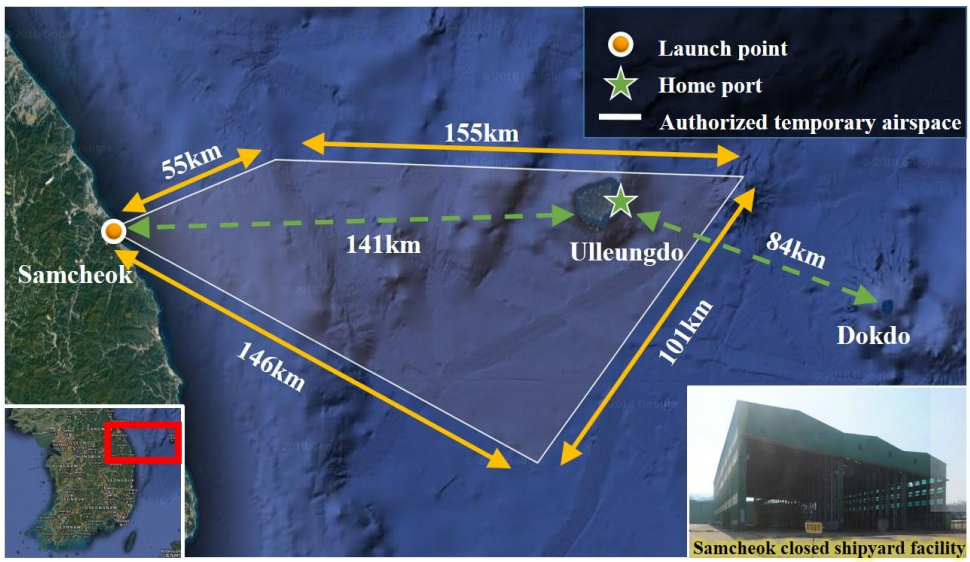

Fig. 30 Launch sites and the airspace of East sea.

3.4.2 Launch phase

Helium injection procedure should be done with extremely carefulness since the film of a balloon envelope is vulnerable to damage. The handling and launching procedures of the small-sized scientific balloon on the ground are as follows:

(1) Move the envelope to a hangar to prevent wind induced damage of the envelope.

(2) Installation of the protective mat on the ground to prevent ripping of envelope.

(3) Visual damage inspection before injecting helium.

(4) After coupling the suspension line attached lower part of the envelope with a weight on the ground, proceed with the helium injection and leakage test.

(5) After operation check of all electronic equipment, attach it to the suspension line.

(6) Unfasten the weight preventing the ascent of the envelope.

(7) Launch the balloon after moving it outside of the hangar.

(8) Monitor the status of the balloon during the given mission.

National research institutes such as NASA and JAXA use equipment such as a mobile launch vehicle when launching a balloon, to prevent damage by the ground wind fluctuations and to smooth the launch process. NASA uses a dynamic

launching method that the stationary roller vehicle releases the balloon and then the launcher moves downwind of the apex of the balloon for releasing the gondola. On the contrary to this, JAXA/ISAS conducts a static launching method that the roller vehicle moves toward the stationary launcher, which is a suitable for a narrow launch field [22, 48]

Since the Samcheok launch site also possesses a small open field for launching a balloon, a similar to the static launch method of JAXA/ISAS was implemented for this balloon campaign without both the roller vehicle and launcher. As depicted in Fig. 31, the workers stationed at the position 4, 3, and 2 are sequentially moved to the person at position 1 until the balloon envelope is erected vertically over the gondola. When the wind state on the ground is favorable, the gondola is carefully released from the person holding the suspension line at position 1. It should be noted that the bottom of the gondola is not collided with the ground to prevent damage

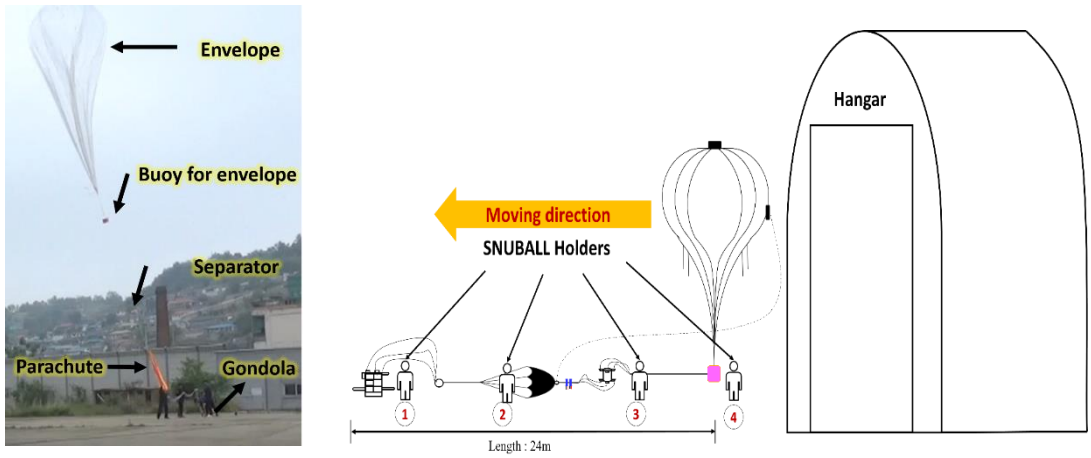

Fig. 31 Launching methodology for the SNUBALL

3.4.3 Flight termination and recovery phase

After completing a given mission according to an experiment purpose, flight termination is carried out by activating the UHF or satellite communication to jettison the payload. To safely retrieve the payload intact, a pertinent parachute providing sufficient drag force is required. Typically, the terminal velocity of 5 ~ 7 m/s is recommended for a safe recovery of a payload. As mentioned earlier, the sea recovery strategy is a reasonable solution after taking into the domestic environment, which consists of the mountainous terrain and highly populated areas, condition consideration.

The sea recovery team for the SNUBALL consists of two people. These workers board a rented fishing boat at the Ulleungdo. The maximum speed of the boat and the displacement are 15 knots (27.8 km/h) and 5 tons, respectively. The sea recovery team can communicate with the ground station with respect to vital information for tracking, for instance, the location of the boat and the balloon, and the on-scene sea state. This information is exchanged in real-time using a mobile phone messenger application. Although mobile phone communications are available in most areas of the East Sea, the Iridium satellite phone is also prepared in case of communication failure due to out of service area. As mentioned earlier, the portable TT & C system for the balloon tracking operation is also equipped in the recovery boat. Consequently, the sea recovery operation can be independently conducted even in preparation for a malfunction situation of the GS.

In spite of valuable equipment embarked on the gondola is in a watertight case, it is recommended that the gondola should be retrieved as soon as possible to minimize the drift after splashdown. This drift may cause problems such as penetrating a restricted area at sea and entanglement with a fishing net or other ship's propeller. The envelope is may more hazardous to ships or fishing nets owing to its poor visibility at sea. In this regard, the envelope made of thin polyethylene film should be retrieved for the conservation of the marine environment as well as the prevention of the problems mentioned above. In general, the sea recovery operation for the gondola, carrying valuable experimental equipment, is performed prior to the retrieval of the envelope. However, the priority of recovery may be changed for reasons such as the number of vessels available, the travel distance from the envelope or gondola to the recovery boat.

Table 6 depicts the established search and recovery operation timeline for the retrieval of the SNUBALL, provided that one recovery boat is available.

Table 6. The general sea recovery operation sequence for the SNUBALL

Elapsed time(Min.)	Operation
H – 120	The recovery team departs towards the expected landing point.
H – 60	Arrive and stay near the expected landing point
H	Flight termination Tracking the location of the descending gondola and envelope Envelope splashdown
H + 30	Search and recovery operation for the envelope starts by the sea recovery team.
H + 50	Gondola splashdown Search and recovery operation for the gondola starts by the sea recovery team
H + 60	Search and recovery boat returns to the port
H + 180	Search and recovery boat returned to the port

The H-time is defined as the fight termination. Mostly, the recovery team departs to a standby point near the expected landing point before the flight termination. The standby point at sea is selected after considering the flight direction of the balloon calculated by the trajectory prediction program. In order to reduce the travel distance difference between the expected landing point and the standby point after the launch, the recovery team moves continuously while tracking the position of the balloon in real time.

As the flight termination is executed at the H-time, the balloon envelope and the gondola begins to descend. After splashdown of the envelope and the gondola, the recovery team approaches the landing point. The floating gondola and envelope drifts slowly in the direction of the sea surface wind. Therefore, the recovery boat should approach downwind to avoid a situation in which both the gondola and the envelope go beneath the ship, causing difficulties in retrieval operation. It also should be noted that the ship's propeller is stopped to prevent the entanglement with the strings of the flight system such as a suspension line and a cord of the parachute.

The strings attached both the gondola and the envelope are elevated by a stick with a hook for retrieval. Afterward, these strings are pulled by worker's hands to put on the deck of the recovery boat. The average time from the access to the landed gondola or the envelope to a completion of retrieval takes less than 10 minutes since the SNUBALL is a small-sized balloon.

The delay of the sea recovery operation is greatly affected by the distance between the recovery boat and the jettisoned envelope or gondola. Overall, it takes at least 5 hours to completion of the sea recovery operation. After towing the envelope and gondola in the deck of the ship, the electronic equipment should be turned off or the battery should be disconnected for safety while returning to the homeport.

3.4.4 Flight test outline

As presented in Table 7, four flight tests including sea recovery operations, were conducted using rubber balloons and 7-m-high ZPBs to verify the operational reliability of the SNUBALL system at sea.

In rubber balloon flight tests, the mission objectives were to verify the flight termination function of the integrated separation system via the Iridium satellite communication while monitoring the tracking ability for the retrieval of a small ZPB after splashdown. In addition to these aims, the sea recovery operation strategy capitalizing on the geographical advantage of the Ulleungdo was demonstrated. In these flight tests, the sea recovery operation, which is launching a balloon from the east coast of the South Korea peninsula and retrieving near Ulleungdo, was conducted due to administrative issues such as research schedule and airspace approval.

Based on a successful demonstration of the ISS employing rubber balloon flights, the ZPB flight tests were followed. The mission of the balloon flight was

to ascend to an altitude of 20 km, collect atmospheric and its flight behavior data, and terminate the flight less than 3 h after launch to exercise the retrieval operation of the payload and envelope. After choosing the launch window for the balloon mission with favorable weather, the predicted flight path was reviewed using the balloon trajectory prediction program. The launch was carried out in Samcheok's closed shipyard facility, after receiving the approval for using a temporary airspace and flight permission.

In the ZPB flight tests, opening the exhaust valve and dropping the ballast to control the rate of climb was not considered due to the short flight mission time and insufficient payload of the 7 m class scientific balloon

Table 7. The summary of the flight test results.

Date	'18.3.27 (Tues.)	'18.3.28. (Weds.)	'18.4.28 (Sat.)	'18.5.27 (Sun.)
Flight distance [km]	95	138	200	204
Maximum Altitude [km]	27.1	27.8	17.4	16.4
Total elapsed time from a launch to completion of sea recovery [min.]	332 (10:22~ 15:54)	190 (09:52~ 13:02)	185 (08:03~ 11:08)	310 (08:10~ 13:20)
Sea Recovery	Success	Success	Fail (Adverse sea state)	Success
Received data	Location Ambient data Video		Location Ambient data Video Photo	
Telecommand	Iridium		RF, Iridium	
Envelope type	Rubber (1.5kg)		ZPB (20km/10kg)	

4. Results and discussion of the flight tests

In order to validate the design considerations for the sea recovery, the results of flight tests using the rubber balloon and the ZPB were investigated as a case study in this chapter. The presented cases of flight tests are 28 March 2018 with a rubber balloon and 27 May 2018 with a ZPB, respectively.

4.1 28 March 2018 with a rubber balloon

Fig. 32 describe the flight path of the rubber balloon with timeline on 27 March 2018. The rubber balloon flew about 139 km after launching from Samcheok and quickly recovered from a point 5 km west of Ulleungdo. It took 187 minutes from launch to the completion of the ISS retrieval. In particular, it took only 19 minutes to retrieve the ISS after the splashdown by virtue of favorable weather conditions and a rapid access of the recovery boat. This recovery operation was recorded as the shortest time to completion of the sea recovery in our balloon campaigns.

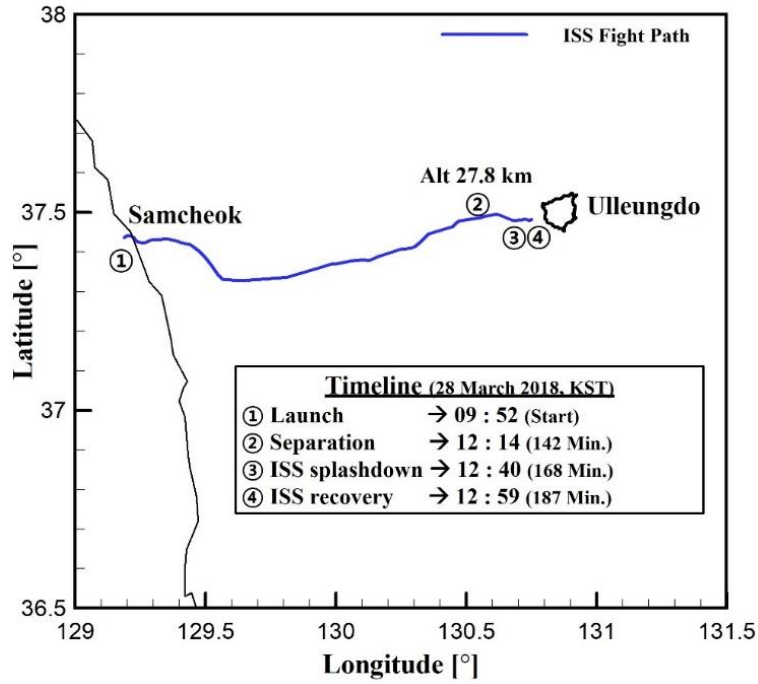

Fig. 32 Sea recovery operation timeline for rubber balloon on 28 March 2018

The altitude and vertical speed variation over elapsed time after launch of the ISS on 28 March is depicted in Fig.33. Based on these data, the rubber balloon ascended for 142 minutes at an ascent speed of 3.5m/s on average. The highest altitude was recorded at 27.8 km. This value was measured just before commencing the flight termination command at 142 minutes later after launching. After the execution of the separation command, a descent rate of the ISS was recorded up to 54 m/s. It is ascribed to the fact that standard atmosphere pressure at an altitude of 28 km is only 1.6 % of the ground atmosphere pressure. Consequently, the low drag in high altitude resulted in accelerating the descent speed of the separated payload. The descent speed of the separated ISS was getting slower owing to the increased drag values as altitude decreases. At an altitude of 10 km where has one-fourth of the ground atmosphere pressure value the descent rate of 10 m/s was recorded. After this, it recorded a descent speed of 9.2 m/s just before the splashdown. The initial assumption of the impact test that the maximum descent speed is less than a speed of 10 m/s was well comparable with this result.

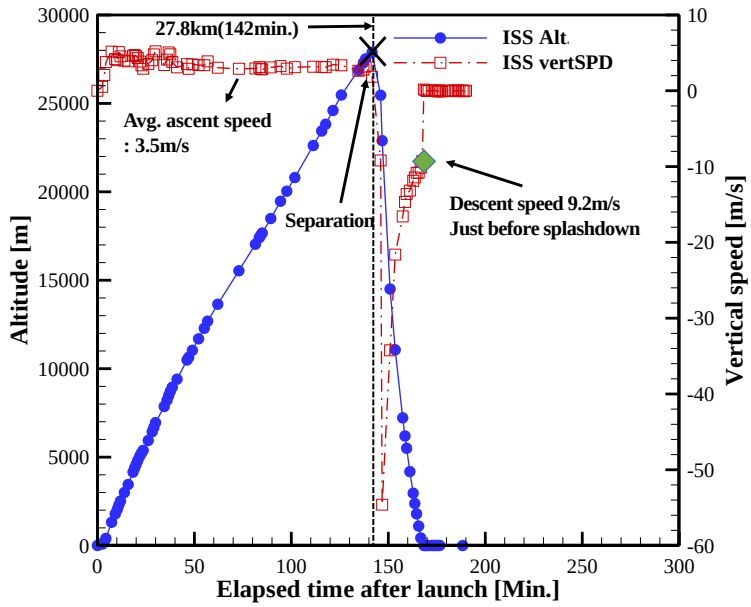

Fig. 33 Altitude and vertical speed variation over elapsed time after launch (28 March 2018, Rubber balloon)

4.2 27 May 2018 with a zero pressure balloon

Fig. 34 shows the flight path of the ZPB platform with the timeline. The envelope and the BOE were retrieved at the distance of 156 km and 201km from the Samcheok launch site, respectively. To minimize the travel distance, the pre-deployed recovery boat in the vicinity of Ulleungdo retrieved the envelope, after which the gondola was recovered. Overall, the balloon campaign took 310 minutes from launch to the completion of a sea recovery operation.

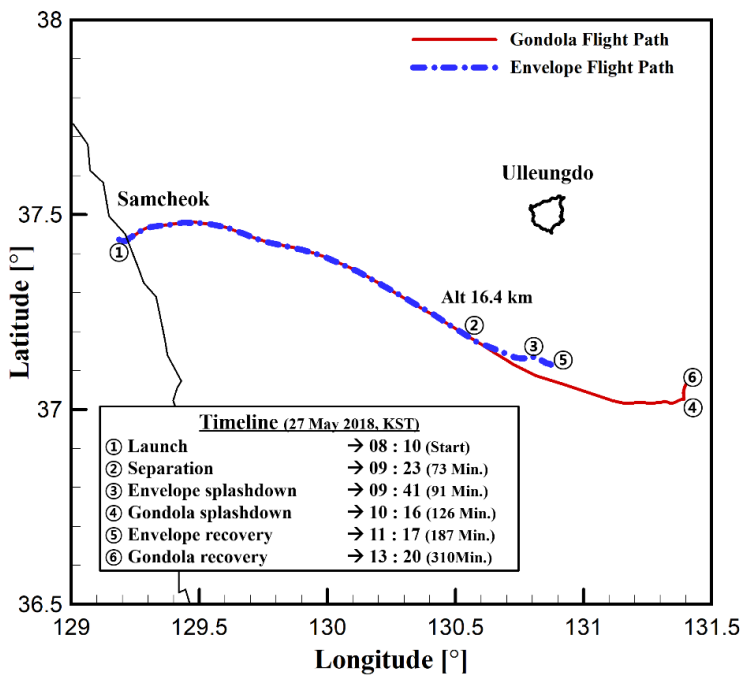

Fig. 34 The 7-m-high ZPB sea recovery operation timeline on 27 May, 2018

The altitude and vertical speed variation over elapsed time after launch of the the 7-m-high ZPB is also depicted in Fig.35. The ZPB ascended for 70 minutes at a speed of 3.7 m/s on average. However, based on the GPS horizontal velocity data installed on the gondola, a significant increase in the wind speed was noticed as the balloon ascended. Altitude over horizontal speed based on the GPS data is shown in Fig. 36. The horizontal speed of the ZPB was recorded at or above 35 m/s after reaching an altitude of 10 km After that, the maximum horizontal speed of 60 m/s which is equivalent value to the winter season was noted at an altitude of 12 km, albeit the flight test was conducted in the spring season.

It could be speculated that the subtropical jet stream was blowing strongly during the flight test. In this regard, the flight test ended at 73 minutes after the launch, which is earlier than expected. This was done due to concerns of airspace violations. The highest altitude was recorded at 16.4 km. A descent rate of the ISS on 27 May was recorded up to 19 m/s. This maximum value of speed in the vertical direction was 35 % slower than which on 28 March. Accordingly, the relatively high drag at an altitude of 15 km led to a lower descent speed than which on 28 March. After conducting the flight termination command successfully, the integrated separation system with the envelope landed with a terminal velocity of 5 m/s. The gondola also landed in the sea with a terminal velocity of 4 m/s.

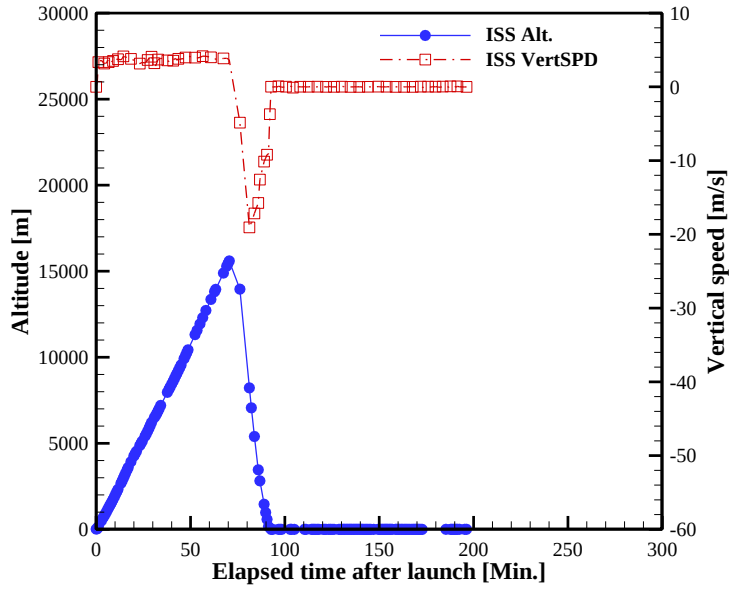

Fig. 35 Altitude and vertical speed variation over elapsed time after launch (27 May 2018, Zero pressure balloon)

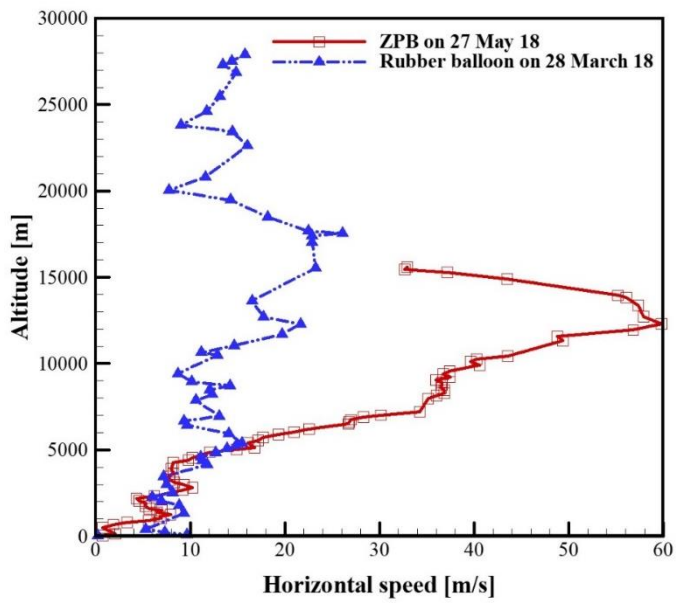

Fig. 36 Horizontal speed variation over altitude

During the sea recovery operation, neither the ISS nor the gondola submerged due to the breakage of the structure upon splashdown, which is due to the excellent impact resistance of the cylindrical polycarbonate enclosure. Owing to the installed ventilation plugs, no damage was also observed due to pressure differences inside and outside the enclosure. This plug allowed air to pass through inside and outside the enclosure impeccably while maintaining waterproofness. As illustrated in Figure 37, the measured internal pressure showed a linear decrease with increasing altitude.

The ISS and gondola maintained stable posture even during turbulence in the sea. This can be ascribed to the fact that the ISS drifted away 4 km for 96 min while reporting the location and ambient information successfully. The gondola also showed the same behavior while drifting away 5 km for 184 min. This result also showed that the divided power source helped prevent short circuit.

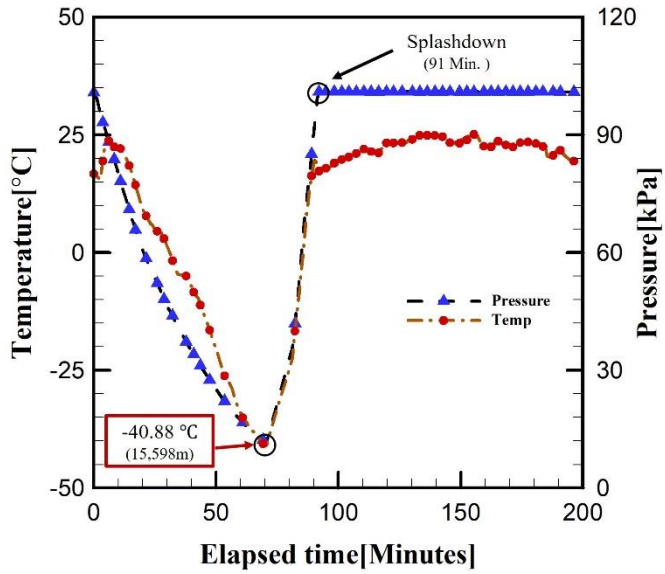

(a) Integrated separation system

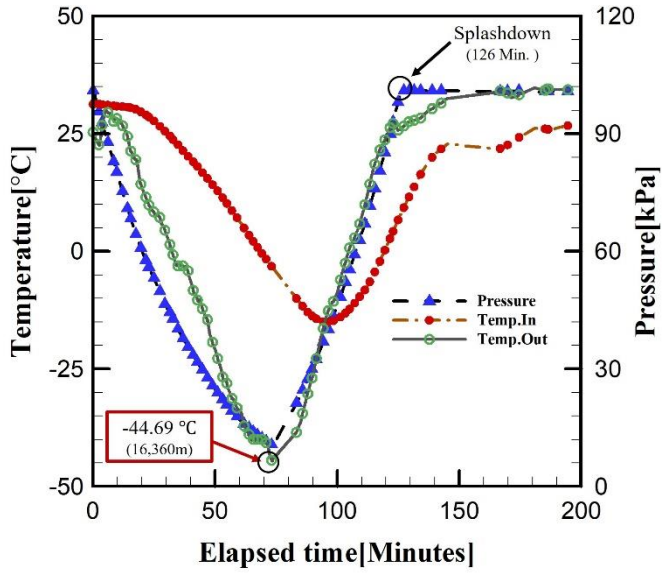

(b) Gondola

Fig. 37 Temperature and pressure variation over elapsed time

After the flight termination, the loss of communication in the NLOS situation occurred at a balloon altitude of less than 11 km and distance of 122 km from the ground station. Handling this situation, the Iridium satellite communication implemented as a secondary communication system functioned acceptably in monitoring the status of the SNUBALL by e-mail, albeit momentary dropouts were incurred due to the weaken signal quality of the Iridium satellite during the flight. This issue will be addressed in the chapter 5 in detail. Through the Iridium satellite communication, the position of the ISS and gondola, which drifted after the splashdown, as shown in Fig. 38, was monitored precisely.

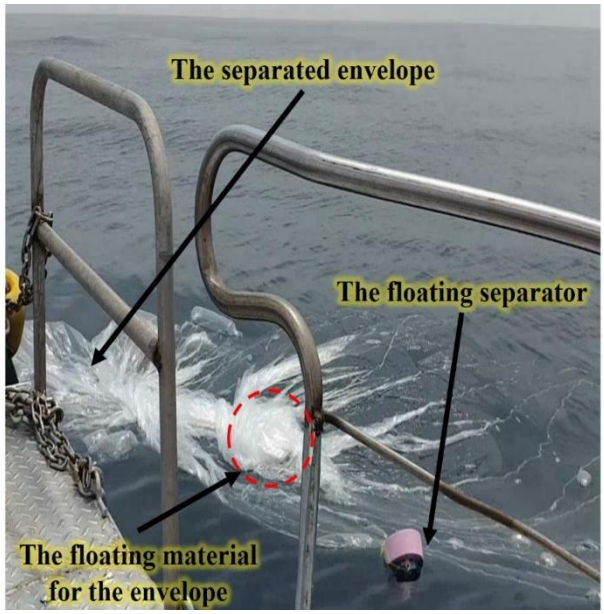

(a) Floating ISS and envelope

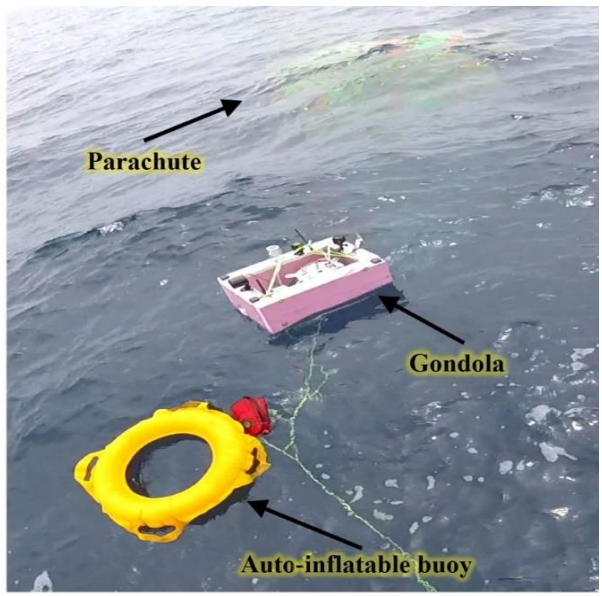

(b) Floating gondola and expanded auto-inflatable buoy

Fig. 38 Retrieval of ISS and gondola

Besides the shipboard V/UHF TT&C system, the Iridium communication system also enabled the easy installation and rapid movement of ground station with excellent portability, since it does not require any supporting equipment except a laptop to receive e-mails. Owing to this portability and convenience, the installation and operation of the ground station in vehicles such as ships and automobiles were simple. Thus, the recovery team on the boat was able to perform sea recovery operation independently without support from ground station. This contributed to reduction in the required workforce of the recovery team. In addition, this system is the E-mail based network which does not require to construct a spacious ground station for data acquisition and command. In this regard, it relieves burdens on conducting scientific ballooning at the level of educational institutes.

The auto-inflating buoy installed to provide additional buoyancy also operated and expanded successfully without problems, even after exposure to low-temperature and low-pressure environments. Meanwhile, the active buzzer continuously made a loud beeping sound of 120 dBs. This alarm sound aided the visual contact of the small, partially-submerged gondola, which the recovery team had difficulties with earlier.

The still images taken by the UART–TTL camera to visually inspect the operation of critical control commands such as the ISS operation and parachute deployment is shown in Fig. 39(a). This picture is a real-time still image received from the UART camera in the gondola from an altitude of 5 km. It showed full

still image data without any loss. However, the image data loss attributed to an interference occurred intermittently as the balloon flew away, as shown in Fig. 39(b). In this regard, additional equipment will be developed to automatically track the moving balloon to reduce the loss of photographic data in the future.

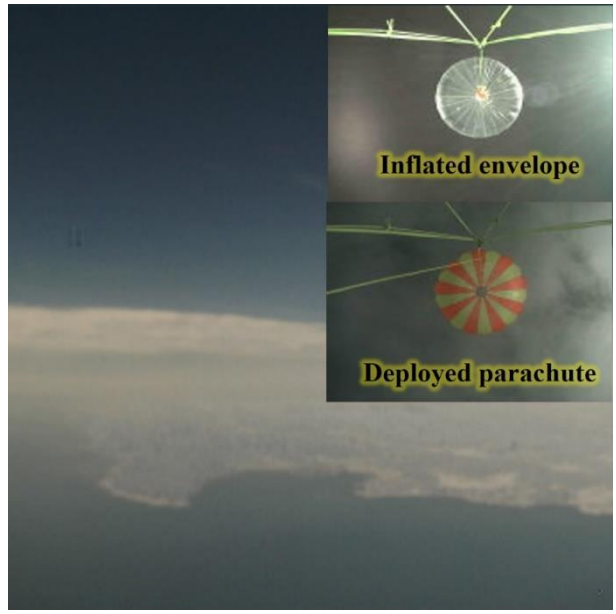

(a) Normal image data

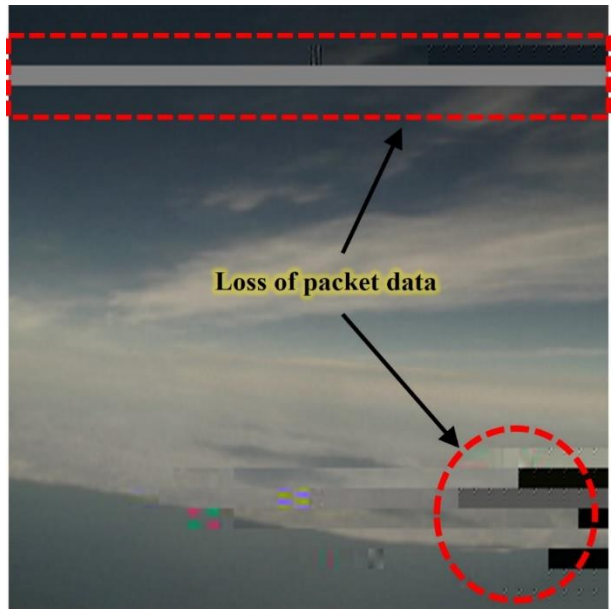

(b) Missed image data

Fig. 39 Live streaming still images from the UART camera in the gondola

4.3. Lessons learned

4.3.1. The delay of the Iridium satellite communication

Based on the aforementioned two flight results, telemetry and telecommand system showed desired performance with respect to obtaining of the status information such as GPS position, atmosphere pressure and temperature.

However, unlike UHF-Zigbee communication, which is performed instantaneously after receiving a separation command, satellite communication delay was observed. This phenomenon is shown in Fig. 40, which presents the changes in altitude with operating time on 27 May.

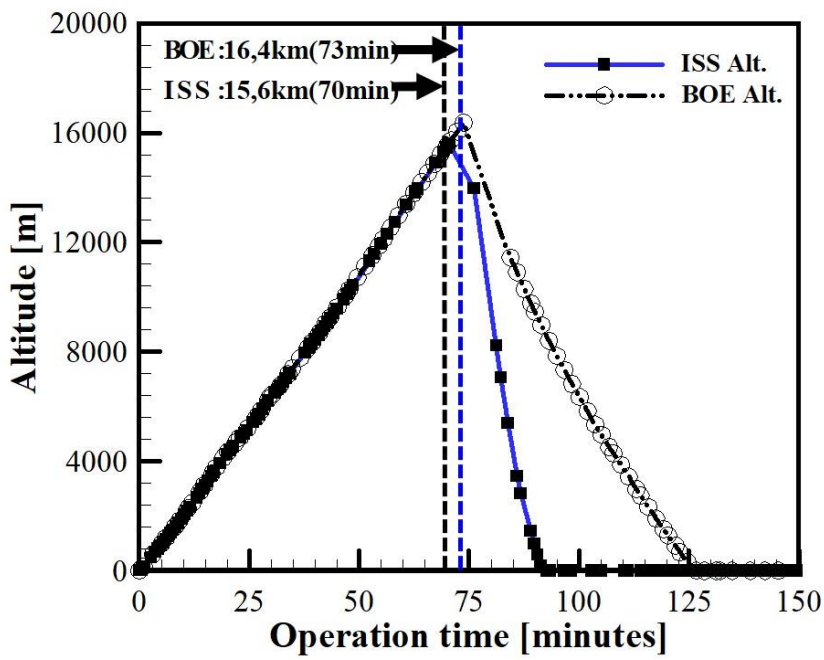

Fig. 40 Altitude variation with operation time of the integrated separation system (ISS) and basic onboard equipment (BOE), 27 May 2018

The ISS reached 15.6 km at 70 minutes, while the gondola went up to 16.4 km at 73 minutes. In this regard, it was conceivable that the latest status information was not transmitted timely due to the communication delay. The required time for receiving the ISS data via E-mail after measuring the GPS time is about 10 seconds under the ideal condition with maximum signal quality, as depicted in Fig. 41. However, it was found that the average elapsed time varied from 38 to 127 seconds on average during the 4 flight tests, as shown in the Table 8.

Through a further investigation into this delay issue, it could be inferred that the chance of the Iridium satellite system dropout is increased as the altitude goes up. In other words, the higher the altitude, the lower the signal strength. Fig 42 shows the distribution of elapsed time for receiving e-mail according to altitude. The average elapsed time for receiving e-mail took 173 seconds in the altitude from 20km to 28km. This value was 1.8 times higher than the total elapsed time for receiving the status information e-mail. A similar phenomenon was also reported in Andrew's work [49], albeit no definitive explanation has been found to account for the occasional dropout. In addition to this, processing time in the modem including signaling channel negotiations from the modem to the satellite was speculated to make it take a longer time [50, 51].

Accordingly, it could be concluded that weaken signal strength and sever processing delay brought these particular results. For this reason, it should be noted that an execution delay of control commands and reception delay of the

status information may occur according to the signal strength of the Iridium satellite modem.

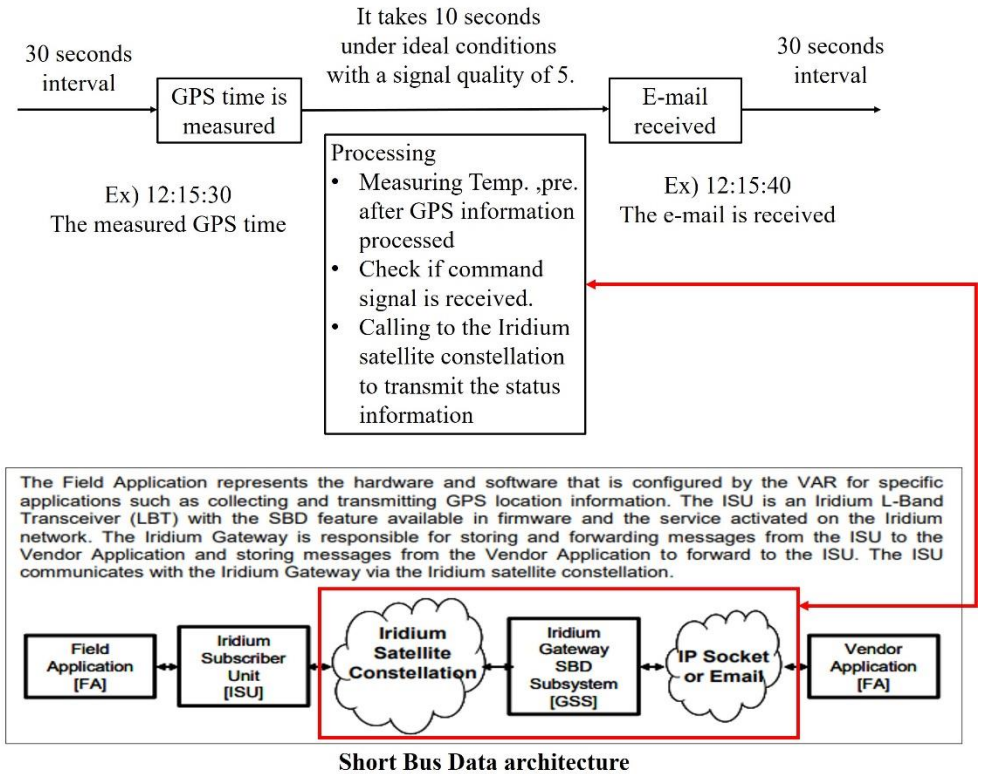

Fig. 41 The processing time for the Iridium telecommand in the ISS

Table 8 Average elapsed time for receiving the status information via e-mail

Date	‘18.3.27 (Tues.)	‘18.3.28. (Weds.)	’18.4.28 (Sat.)	’18.5.27 (Sun.)
Maximum Altitude [km]	27.1	27.8	17.4	16.4
Total elapsed time [seconds]	127	97	50	38

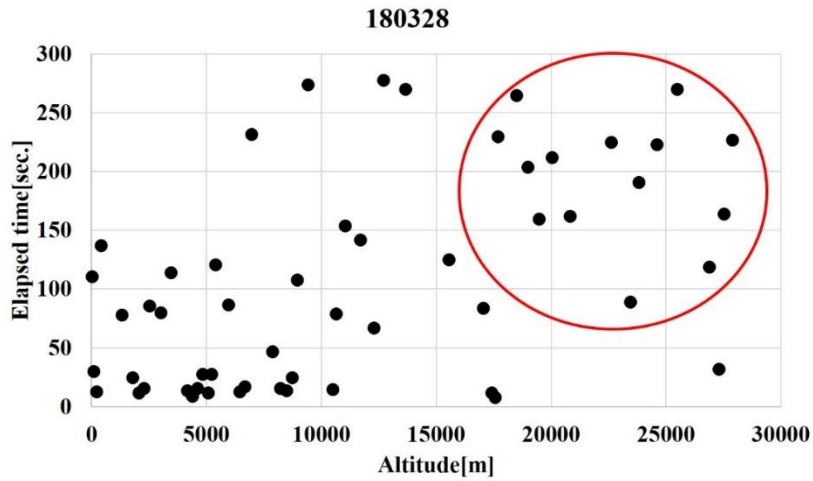

(a)

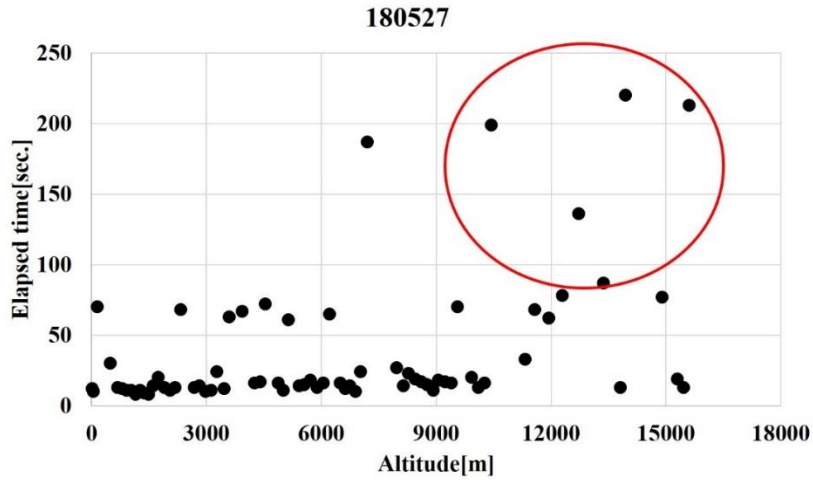

(b)

Fig. 42 Distribution of elapsed time for receiving e-mail according to altitude

4.3.2. Discrepancies on the predicted trajectory VS obtained flight path

As discussed previously, it can be seen that some discrepancies between the predicted balloon trajectory and the real flight path happen. As the time of flight operation elapses, the discrepancy is aggravated, as illustrated in Fig 43. The maximum horizontal distance between the predicted trajectory and the real flight path recorded 20km at the time of 70minute elapsed after launch. If the flight termination to prevent airspace violation had not been executed earlier, the discrepancy in the horizontal distance would have been far greater.

It can be confirmed again that the simulation results could hardly be the same as the actual balloon flight because there exist uncertainties in balloon trajectory prediction [44]. The uncertainties include operational uncertainty, uncertainty in the prediction model, environmental uncertainty, and manufactural uncertainty. Thus, it should be noted that balloon trajectory simulation results are only one of the references for assisting balloon campaign.

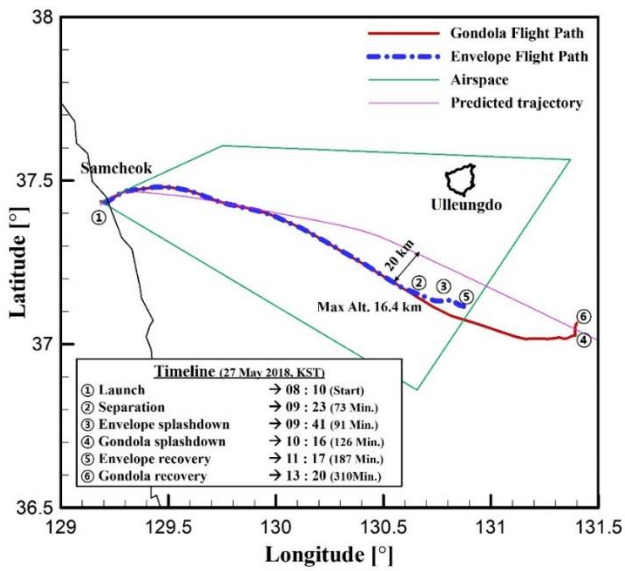

Fig. 43 Flight trajectory comparisons

4.3.3. Establishment of weather minimum for the sea recovery operation

A fishing boat with a displacement of 5 tons was available to educational institutions considering the budget limitation and ease of rent-a-ship. However, in the third flight took place on the 27th April 2018, the operation of small recovery ship with a displacement of less than 5 tons was restricted due to deteriorating maritime conditions, which resulted in failure to recover payloads. This failure is attributed to the enforcement of an impractical plan without considering a performance of a recovery ship in an unfavorable sea state. The high wind and wave weaken the work efficiency of the sea recovery workers. Moreover, the severe pitching and rolling of the ship by high waves can cause the falling overboard of the workers who pull the landed envelope or the payload up to the deck of the ship.

In this context, a standard operating procedure for a small recover ship was established after taking into the weather condition based on the maritime law in the Republic of Korea considerations. According to the maritime law in the Republic of Korea, wind and wave advisory will take effect under the following weather condition:

1) Wind of 14m/s or more sustains for over 3 hours at sea

2) Significant wave height is expected to be over 3m

After issuance of the wind and wave advisory, ships with a displacement of 2,000 tons or less will be restricted in their operation. Thus, the small recovery

ship can be used to retrieve the payload when the observed values on the wind and wave is below the stipulated weather conditions.

However, the following criteria, which are somewhat lower value than the stipulated maritime law standard were established after taking the capability of a recovery ship, efficiency of recovery work, and safety of the worker into account.

1. Wind of 10 m/s or less sustains Beaufort number 5 (Fresh breeze equivalent to the sustained wind of 10 m/s or less)
2. The wave height of 2m or less

The newly established weather minimum was applied on the 28 May 2018 flight test under the conditions that the sustained wind of 6m/s or less and the wave height of 1 m or less. This flight test was demonstrated successfully with respect to the sea recovery operation, albeit it took more than 4hours to navigate on the sea due to the balloon trajectory flew away considerably from the south of the Ulleungdo.

4.3.4. Emergency measures to prevent airspace violation

Temporary airspace and hours of use for the flight test before the start of the balloon campaign are approved in cooperation with the relevant agencies of the Ministry of Land, Infrastructure, and Transport. However, it is difficult to secure sufficient airspace and time for the flight test of an unstable prototype at the level of universities. Therefore, approved airspace size is generally insufficient to achieve flight test objectives. Moreover, favorable flight time, when the wind speed is weak during the twilight, for balloon campaign is restricted due to the flight schedule of other aircrafts.

In this context, it is possible to push ahead with the launch during high wind speeds, as in the flight test on May 27, leaving the temporary airspace. Accordingly, the flight should be terminated earlier than the target flight time to comply with the airspace regulations, and the ground station should take the following actions.

1) Monitor the flight status on the airways around the balloon flight path before the end of the flight.

2) Execute the flight termination if there is no threat to other aircraft on the airways

3) Notify the balloon location and the completion of air space use due to early flight termination to the relevant aircraft control agency.

5. Concluding remarks

5.1. Summary

Since the balloon can be recovered after a mission, it can achieve cost reduction through the reuse of its mission equipment and retrieve mass experimental data stored on test equipment which is not possible for satellites and space launch vehicles. By virtue of these advantages, the scientific balloon has contributed greatly to the various scientific and engineering researches

Sea recovery is a distinctive method to alleviate concerns regarding the safety and recoverability of a scientific payload. Despite its long history, published data with respect to the design and manufacturing of balloon systems suitable for sea recovery operation is scarce. Even these rare works address only large-scale and high-priced balloon systems available only to national research institutes.

Therefore, this study attempted to present the detailed system development of a small zero-pressure balloon (ZPB) prototype flight train which is designed to suit sea recovery with affordability. This prototype, which will be employed for university-based researches, was titled as Seoul National University scientific BALLoon (SNUBALL).

This paper was addressed as followings:

Firstly, based on the SNUBALL campaign, the system development process has been presented after considering the salient requirements such as maritime telecommunication, water resistance, buoyant materials, and short-circuit

prevention. To construct a low-cost compact maritime communication system, COTS transceiver modules were used. The Iridium satellite communication modem was employed to tackle an NLOS situation. A UART–TTL camera was used to visually inspect the operation of critical control commands. In addition to this, a portable TT&C system was installed on the recovery boat to conduct independent data acquisition and tracking of the balloon, which greatly aided the recovery team. The employment of the COTS products reduced not only the financial budget of developing the balloon system but also the overall size and weight of the balloon system. Circular polycarbonate cylinders were used to provide excellent impact and water resistance to the system to withstand the splashdown. To provide buoyancy to the envelope, separator, and gondola, XPS was utilized as the material. Exposure of electronic devices to sea water was minimized, except for the ISS. To mitigate this and prevent short circuit, the ISS's power source was divided into two power sources of different voltages. An active buzzer, auto-inflation buoy, and a backup GPS-Iridium tracker were developed and mounted as supplementary equipment for flawless sea recovery.

Secondly, viable sea recovery operating procedures were established. To this end, the annual average wind data analysis and numerical trajectory prediction was conducted, respectively. Wind data analysis contributed to selecting the east coast of the South Korea peninsula as a launch site (Samcheok). After determining the launch site, the flight simulations for the period of five years (2014~2018) were performed with the NOAA' GFS data. Reflecting on the trajectory

simulation results, four feasible sea recovery operating procedures, which capitalizing on the geographical advantage of the Ulleung-do, were established as follows.

1) A balloon is launched from the east coast of the South Korea peninsula and retrieved in the vicinity of Ulleungdo in winter. This sea recovery procedure is recommended for the retrieval of the balloon system, which was continuously flown eastward due to the strong westerlies.

2) The balloon is launched from the east coast of the South Korea peninsula and retrieved in the vicinity of the launch site coast in summer. Flight termination takes place when the balloon flies back close to the nearshore of the launch site due to the boomerang effect.

3) A balloon is launched from Ulleungdo, and retrieved near the east coast of the South Korea peninsula in summer. This procedure was devised to tackle the excessive shoreward flight of balloons in summer due to the boomerang effect. Recovering the jettisoned payload near Ulleungdo contributes to the ease of sea recovery operations. Retrieved payload is shipped to east coast directly after completion of sea recovery. In this regard, this has the advantage of requiring less transportation and required manpower from east coast to Ulleungdo for a balloon campaign

4) A balloon is launched from Ulleungdo, which is located in the center of the Incheon FIR eastern sector, and retrieved near the sea of Ulleungdo. This procedure could satisfy a mission profile demand for the longer flight time during

a balloon campaign. Given these sea recovery operation procedures in both winter and summer, it seems plausible that a safe and sustainable balloon campaign for university-based research within the eastern airspace of South Korea can be possible.

Lastly, the established balloon campaign focused on the aforementioned sea recovery operations, and the flight test results of the developed balloon system were presented. For seasonal and administrative reasons, only the first sea recovery method (Launching from the east coast and retrieving near the Ulleungdo) was performed, but the designed sea recovery operational procedures were validated by four flight tests. And it showed potential for success on the other unexercised sea recovery operating procedures. The developed balloon system showed no leakage, submergence, or short-circuiting of the balloon system during both the water tank test and actual flight tests. Based on the results of these tests, the developed ZPB system was found to be ideally suited for sea recovery. Consequently, it was able to master the sea recovery procedure as well as the system reliability verification of the balloon at sea through four flight tests. Owing to the presented process, which focused on designing a small ZPB to suit sea recovery, conducting the scientific balloon campaign in countries with topographical limitations such as small and tough geographic areas, such as with South Korea, becomes possible.

5.2. Future works

In this study, the developed small ZPB platform demonstrated the desired performance and system reliability at sea through four flight tests including sea recovery strategy. Thus, the usefulness of balloon system suited for sea recovery strategy in the Republic of Korea was attested. However, there is still room for practical usage of the developed balloon system for sea recovery because this is in the early stage of research.

Firstly, it was assumed that the balloon flight mission is less than four hours to support university-based researches. In practice, however, a long-duration balloon flight more than tens of hours is required to assist various studies. Long duration flight can be divided into two types. The first is the continuous flight pattern regardless of airspace limitations. In this case, international agreements to fly over sovereign territories are required to conduct the global ballooning [52, 53]. Accordingly, this flight pattern has limitations that can only be implemented in exceptional circumstances, such as international joint research or flight in the Antarctic. The second flight pattern is long-duration flight by employing the boomerang effect within the designated airspace. Although this pattern can be only available in the summer season by virtue of the boomerang effect, there is the advantage of not having to consult with neighboring countries regarding the use of airspace. When the balloon moves excessively in the west direction at an altitude of more than 15 km, buoyant gas is discharged to make the balloon descend to an altitude of eastward wind prevails. After moving to the eastward for

a certain distance, the ballast is released to make the balloon climb to an altitude of westward wind prevails. Through this series of ascending and descending cycles, it is possible to conduct a long-duration flight of more than tens of hours. To this end, manufacturing and flight test on venting and ballast valves are required.

Secondly, the manufactured balloon in this study is 10kg / 20km (payload/target altitude) class. The envelope has a height of 7m and a volume of 168m^3. This envelope size was manufactured as a part of a step-by-step approach strategy before making 50kg payload and 25km target altitude balloon envelope due to low manufacturing maturity. For broader applications on university-based researches, therefore, medium-sized balloons, which have a payload of 50kg or more and a target altitude of 25km or more, should be manufactured and tested. However, this arise the problems of storage about the mid-sized balloon which is calculated more than 15m high and 1840m^3 volume. In particular, the Samcheok's closed shipyard have a height of 15 m. This means the envelope at the height of more than 15m is not accommodated. Therefore, a large hangar facility should be furnished to prevent damage to the envelope due to wind gusts during gas inflation [54]. On the other hand, it is laborious to transfer the medium-sized balloon from the hangar to the launch spot by manpower safely. In this regard, the mechanical launcher should be furnished for both fastening balloon to avoid damage due to wind gust and minimizing personnel injuries due to the drag force by the inflated balloon.

Lastly, practical research plans using this developed balloon system with sea recovery strategy are should be performed more frequently to provide lessons for a certain degree of modifications and technology upgrades. Considering the current limitations on the balloon campaign, such as the designated airspace and short flight window in the Republic of Korea, the most feasible research plan is drop test of the MARS exploration airplane [55]. Since the balloon can simulate the low-density environment, it is possible to verify the complete system functionality of the MARS exploration airplane as well as to acquire data on the behavior of the vehicle. In the near future, a cooperative balloon campaign with the MARS exploration airplane laboratory is expected to encourage the practical usage of the developed balloon.

Appendix A: Wind Environment

To explore the wind environment that the balloon encountered during operation, the radiosonde wind data of Oasn-si was chosen due to its comprehensive data for the period of 5years, albeit its location is far from the launch site. The wind profile in the stratosphere is less varied spatially, whereas it can significantly differ at the ground level due to topography, surface heating differences, and local winds such as land and sea breeze, mountain and valley winds [56-59]. From this point of view, it is viable to use the wind data of Osan-si as a representative value for recognizing the tendency of the wind profile the balloon will face in the stratosphere [60] . Fig. A1 presents the seasonal mean wind profile for the period of 2014-2018 at Osan-si. These wind data were measured by a radiosonde at Korea Standard Time (KST) 09:00 and 21:00, respectively. This time was chosen as the representative value of day and night time.

The months of the four season in the northern hemisphere are generally categorized as follows: a) Spring: March, April, and May; b) Summer: June, July, and August; c) Autumn: September, October, November; d) Winter: December, January, and February [61]. To clearly distinguish the variations of the seasonal wind profile, January, April, July, and October were selected to represent spring, summer, autumn, and winter, respectively.

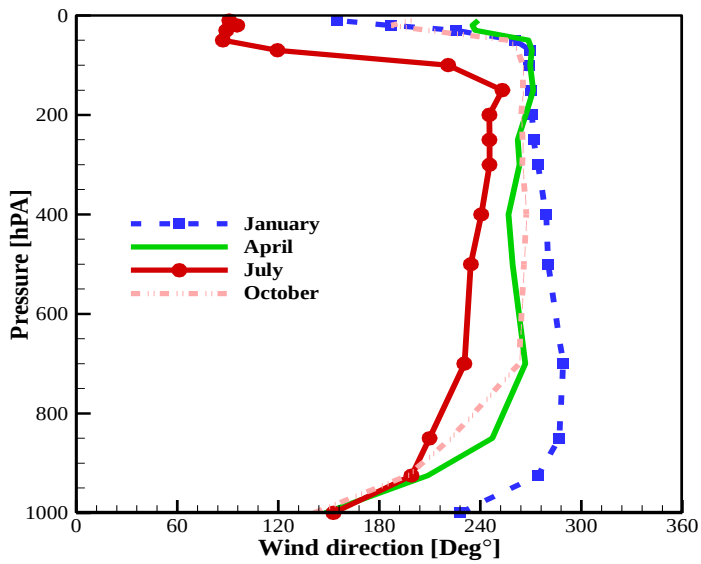

(a) Seasonal mean wind direction variation with the altitude, KST 09:00

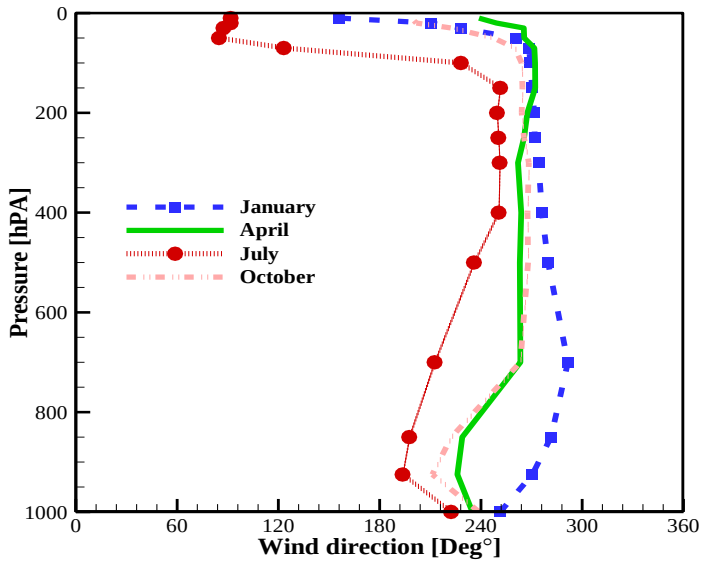

(b) Seasonal mean wind direction variation with the altitude, KST 21:00

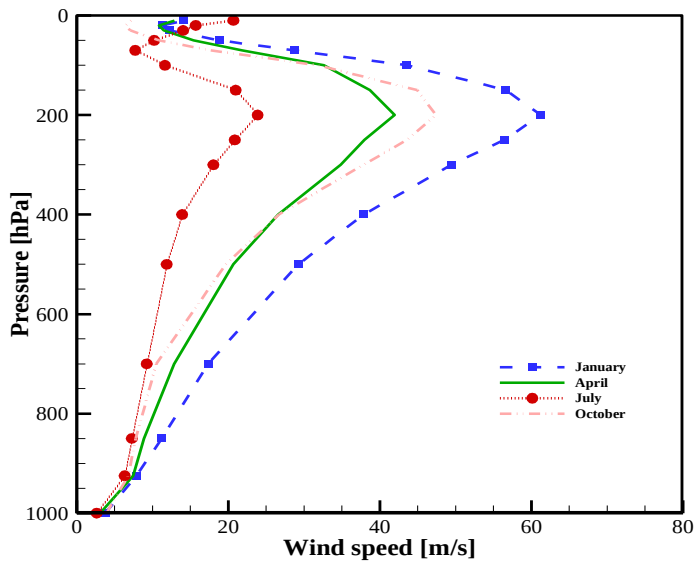

(c) Seasonal mean wind speed variation with the altitude, KST 09:00

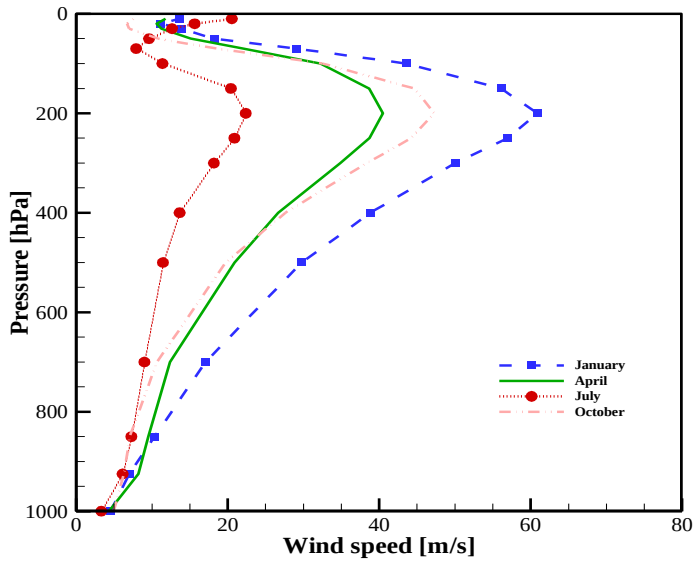

(d) Seasonal mean wind speed variation with the altitude, KST 21:00

Fig. A1 Seasonal mean wind profile for the period of 2014-2018 at Osan-si, South Korea

As shown in Fig A1(a) and (b), the prevailing winds blow predominantly from 180° to 300° at all altitudes throughout the year. This phenomenon, known as westerlies, appeared in the middle latitudes between 30° and 60°. Consequently, it is highly likely that the LTA platform whose trajectory is determined by the wind direction moves eastward. In the summer, however, eastward winds (almost blows from 90°) become dominant at or above 70 hPa (about 18.5 km MSL). This is attributed to the expansion of the eastward winds region from lower to higher latitude in summer. Accordingly, this weather phenomenon causes the balloon flying towards the eastward direction to return to the launch site due to the westward wind blowing at or above 18.5 km altitude. This behavior of the balloon is referred to as boomerang flight [62]. This phenomenon could make a considerable contribution to the extension of the endurance of the balloon within approved airspace in South Korea. In addition, the time and effort for the retrieval of the payload after completing a given mission could also be drastically saved through this returning behavior of the balloon.

Seasonal mean wind speed variations with the altitudes are shown in Fig. A1(c) and (d). The maximum wind speed can be noted at a pressure altitude of 200 hPa (about 12 km MSL) throughout all four seasons [63]. The reason for this phenomenon is the jet stream which blows intensively eastward. In particular, the average wind speed in winter was recorded approximately 60 m/s at that altitude, which was 2.7 times faster than the maximum wind speed in summer. In this

context, the time exposed at a pressure altitude of 200hPa should be minimized to enable mission flight time longer without airspace violation.

Wind speeds significantly weaken at or above 150 hPa pressure altitude. At a pressure altitude of 50 hPa (20 km MSL), all four seasons wind speed were recorded at or below 20 m/s. The lowest wind speed, which was at or below 12 m/s, was measured at an altitude of 20 hPa (25km MSL), and then it was slightly increased again as altitude goes up. In this regard, at an altitude of 20 hPa, the flight distance could be minimized due to the slowest wind speed. Therefore, it is very likely that the required flight time (6hrs) can be satisfied without breaking the airspace regulation. In this context, the target altitude of the simulation was determined to be 25 km.

Appendix B: Balloon Flight Model for Trajectory Prediction

A high altitude balloon is a LTA vehicle. Thus, its motion is determined by both the buoyant force of lifting gas and aerodynamic drag of the balloon. To precisely calculate these force acting on the balloon, the surface area and volume which was designed by its mission requirements also should be taken into account. Lifting capacity is also influenced by the density of the buoyant gas. The density of the lifting gas is a function of the temperature of the gas. Therefore, it is imperative to calculate the radiative and convective heat transfers between the balloon and its surrounding environment for achieving reasonable accuracy. For a preliminary study to analyze the operational feasibility of balloon operation, the simulation program introduced in Lee et al.'s work was used [44]. In the following section, the dynamic and thermal model was briefly introduced.

B.1 The Dynamic Model for Balloon

The value of the buoyant force can be defined using the following equation:

$$\boldsymbol{F_{buoyant} = \rho_{air} \cdot volume_{bal} \cdot g} \quad \textbf{(1)}$$

When V_{bal} and u_{wind} represent the absolute velocity components of the balloon and the wind, respectively, the magnitude of the relative velocity of the balloon, $V_{rel,}$, can be calculated as follows:

$$\boldsymbol{V_{rel} = u_{wind} - V_{bal}} \quad (\mathbf{2})$$

Then, the magnitude of the drag force and its components are determined with the following equations:

$$\boldsymbol{Drag = \frac{1}{2} \cdot \rho_{air} \cdot V^2{}_{rel} \cdot C_d \cdot A_{top}} \quad (\mathbf{3})$$

where the reference area $\mathbf{A_{top}} = \boldsymbol{\pi r_{max}^2}$ is the top projected area.

The balloon system mass, which is the sum of a payload mass, balloon mass, and ballast mass, is $m_{G.}$ The mass of the lifting gas is m_g, therein, the mass of the total balloon system M_{total} is defined by

$$\boldsymbol{M_{total} = m_G + m_g} \quad (\mathbf{4})$$

In the motion equations, the mass of air which is caused by the acceleration of the balloon immersed in the air should be considered as well. Therefore, $M_{virtual}$ is introduced using the following equation:

$$\boldsymbol{M_{virtual} = M_{total} + C_{virtual} \cdot \rho_{air} \cdot volume_{bal}} \quad (\mathbf{5})$$

According to the Palumbo et al.'s Analysis Code for High-Altitude Balloons (ACHAB), the virtual mass coefficient $C_{virtual}$ is considered a mean value. In this study, a value of 0.37 was used after referring to his work[64]. Consequently, the equation of the motion for a balloon can be written as follows:

$$\ddot{x} = \frac{Drag_x}{M_{virtual}}$$

$$\ddot{y} = \frac{Drag_y}{M_{virtual}}$$

$$\ddot{z} = \frac{F_{buoyant} - M_{total} \cdot g \ + Drag_z}{M_{virtual}} \tag{6}$$

B.2 Thermal Model for Balloon

In this study, it is assumed that the lifting gas is transparent, and the effect of radiant heat transfer is negligible. Therefore, the temperature of the gas is only influenced by the internal free convection, Q_{conInt}, which occur inside of the balloon film. Accordingly, the following equation can be used to calculate the temperature of the lifting gas:

$$\frac{dT_{gas}}{dt} = \frac{Q_{conInt}}{C_v \cdot m_{gas}} + (\gamma - 1) \cdot \frac{T_{gas}}{\rho_{gas}} \cdot \frac{d\rho_{gas}}{dt} \tag{7}$$

The mass, temperature, and density of the lifting gas are denoted by m_{gas}, T_{gas}, and ρ_{gas}, respectively. The specific heat at a constant volume of the buoyant gas is

represented by C_v. $\boldsymbol{\gamma}$ is the specific heat ratio. If there is no interaction between the lifting gas and the film, Eq. (8) depicts the adiabatic temperature change of the gas.

To calculate the temperature of the envelope film, the simple transient energy-balance equation was introduced:

$$\frac{\boldsymbol{dT_{film}}}{\boldsymbol{dt}} = \frac{\boldsymbol{Q_{sun} + Q_{albedo} + Q_{IRplanet} + Q_{IRfilm} + Q_{conExt} - Q_{conInt} - Q_{IRout}}}{\boldsymbol{C_f \cdot m_{film}}} \quad (8)$$

In Eq. (9), Q_{sun} is the absorbed direct solar heat, Q_{albedo} is the absorbed albedo heat, $Q_{IRplanet}$ is the absorbed planetary IR heat, Q_{IRfilm} is the absorbed IR self-glow from the interior, $Q_{convExt}$ is the convectional heat flux between the film and the atmosphere, $Q_{convInt}$ is the convectional heat between the film and the lifting gas, and Q_{IRout} is the emitted IR energy from the balloon film. The specific heat of the film material is represented by C_f. Further details also can be noted in Farley's, Roberto Palumbo et al.'s works [64-66].

Appendix C: Trajectory simulation results in detail

Although flight simulations for the period of 5 years (2014-2018) were conducted, the case study of this chapter described only the winter and summer of 2018 to show the seasonal variation of the balloon trajectories clearly.

The simulation results of the balloon launched from the Donghae-si in January and July of 2018 with different launch time (KST 0900, 11:00) are shown in from Fig. C1 to Fig.C6, respectively. As previously mentioned, January and July were chosen to represent winter, and summer, respectively. The red line, which represents the daily flight paths of the balloons, showed the tendency of the balloon's movement. The yellow circles denote the position of the balloon when the 6 hours elapsed after the launch.

The simulation results depict distinctive trends in the summer and winter. The balloon moves notably eastward in winter regardless of day and night time, as shown in Fig. C1 and C2. Thus, several balloon flights crossed over the borderline of the Incheon FIR. These airspace violations were caused by the jet stream, which becomes stronger in winter due to an increment of the temperature difference between the polar region and the equatorial region.

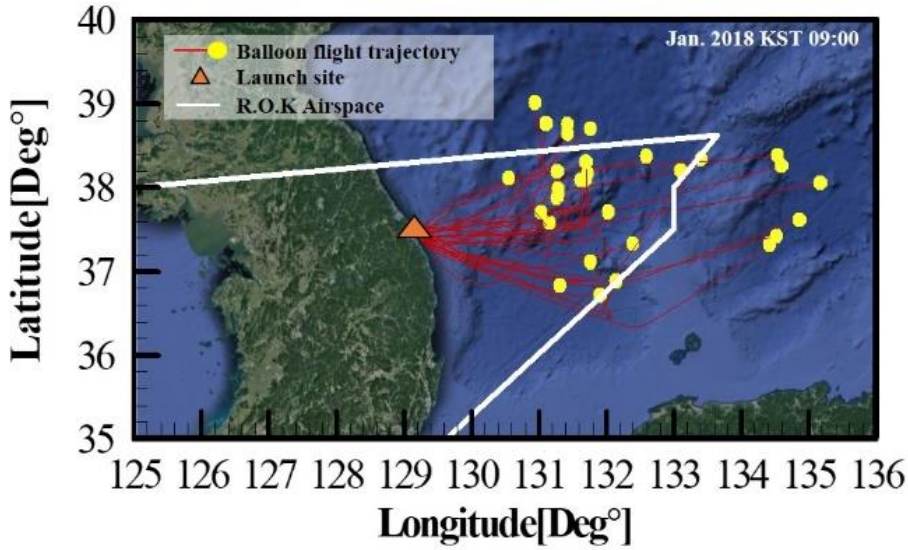

Fig. C1 Predicted trajectories on January 2018 (winter), KST 09:00, UTC+9

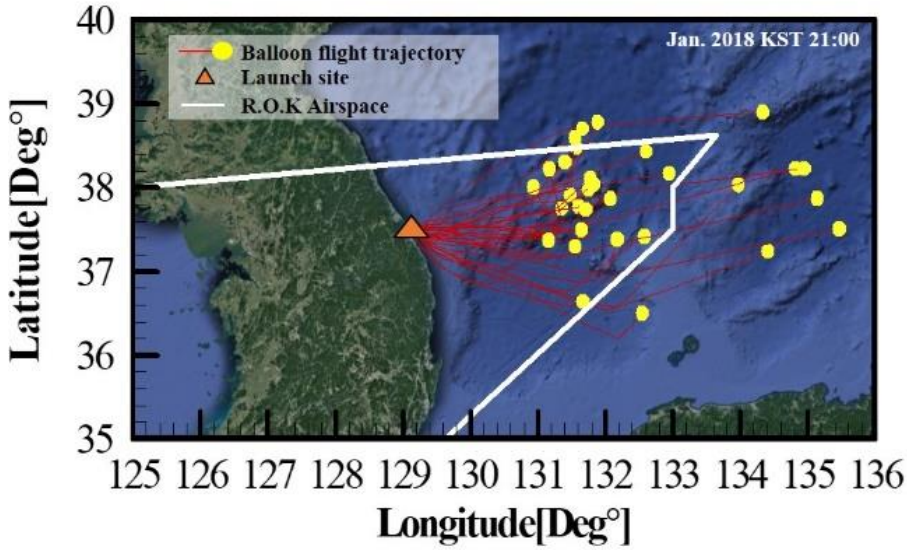

Fig. C2 Predicted trajectories on January 2018 (winter), KST 21:00, UTC+9

The differences in longitude and latitude distributions with altitude are presented in Fig. C3 (a), (b), (c), and (d). On these figures, one can observe that the movement of the balloon significantly depends on the altitude range from 5 to 15km. It is natural consequences since the balloons flying at this altitude range face strong wind environment, which was introduced in section 2.1. In particular, in Fig. C3(a) and (b), the gradient of the altitude over longitude at an altitude of 10 ~15km is the lowest. This implies that the balloons move farther in the longitude-wise than the vertical direction due to the strong jet stream. The predicted trajectories of the balloons in the longitude-wise showed no significant differences between day and night time. One reason for this would be that the longitudinal wind velocity components with altitudes less varied during these flight windows.

On the other hand, the predicted balloon trajectories in the latitude direction with the altitude changes showed more broad distributions at nighttime than the daytime, as indicated in Fig. C3(c) and (d). This phenomenon could be explained by the ideal gas equation Volume = ($m_{gas}R_{gas}T_{gas}$ / P). The volume of the balloon envelope, which determines the buoyant force of the balloon, is affected by the temperature of the buoyant gas. Owing to the absence of the thermal energy from sunlight at night, the temperature of the buoyant gas inside the balloon is lower than that of the daytime. Accordingly, the volume of the balloon is relatively smaller than that of the daytime during the ascent phase, resulting in less buoyant force. This connotes that the balloon could be exposed longer time in the

troposphere where the strong wind blows; hence, it seems that the flight trajectories in the latitudinal direction are distributed more broadly than that of the daytime.

In this simulation results in winter showed the tendency of the flight trajectories that traveled distance of the longitudinal direction is greater than that of the latitudinal. These particular results were led by the longitudinal velocity component of the jet stream which is far stronger than that of latitudinal in winter. In this respect, it is conceivable that the required mission flight without crossing the eastern border of the Incheon FIR is achieved by shortening the exposed flight time in the troposphere with a high rate of climb. To this end, following methods such as injecting more buoyant gas into the balloon envelope, or dropping ballasts could be implemented to increase the ascending speed in realistic balloon campaign [67].

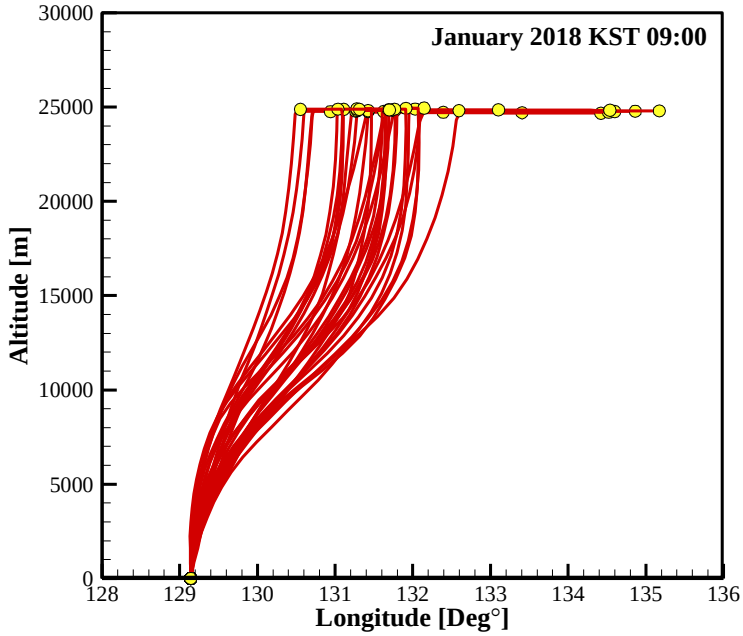

(a) Longitude variation with altitude

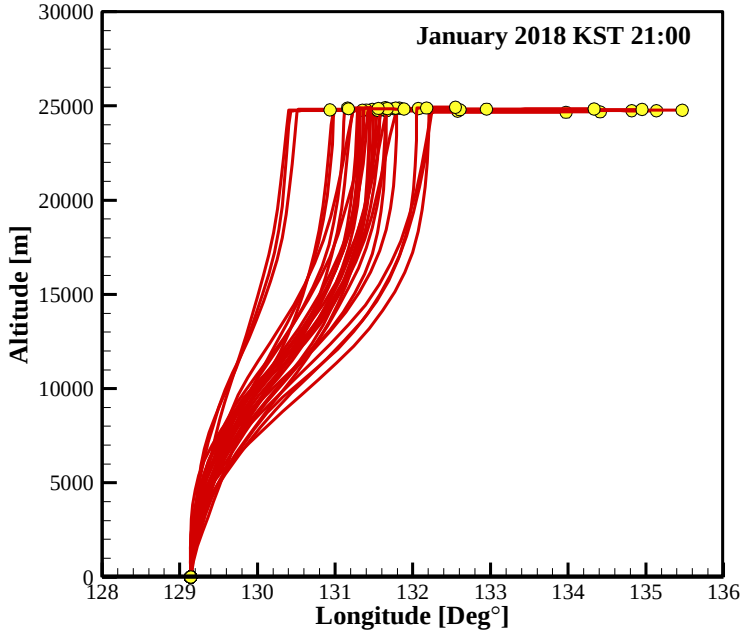

(b) Longitude variation with altitude

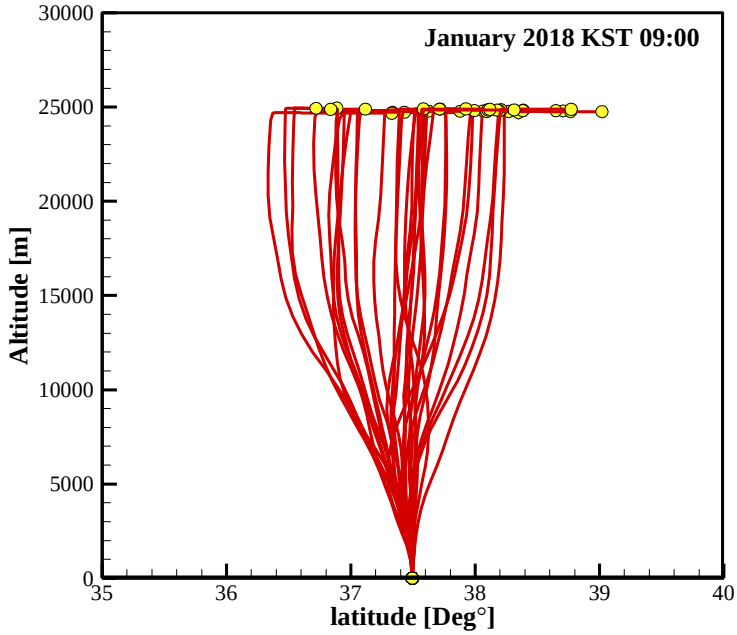

(c) Latitude variation with altitude

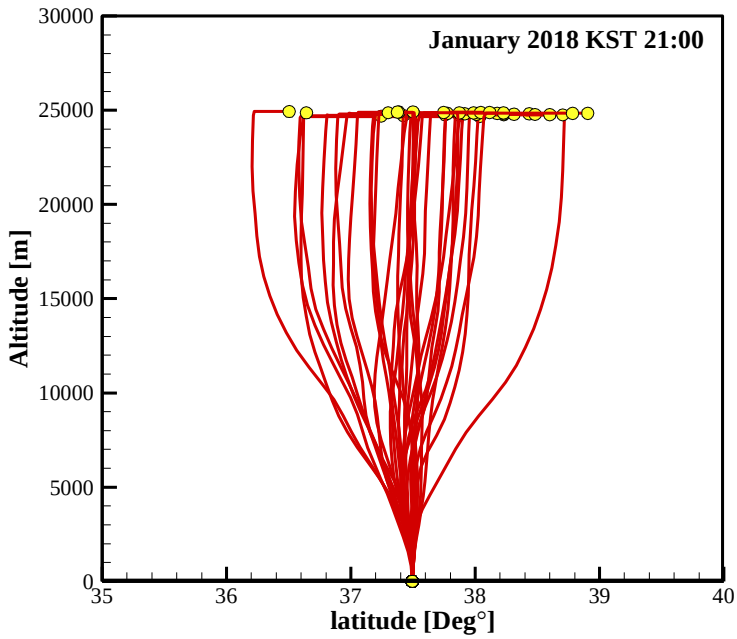

(d) Latitude variation with altitude

Fig. C3 Flight simulation results in winter (Launching from the Donghae-si, January 2018 KST 09:00 , 21:00, UTC+9)

Unlike the trajectories in winter, in summer, the balloons change its direction westward at or above 15km altitude while moving eastward in the early stage of flight, as depicted in Fig. C4 and C5. This phenomenon is known for the boomerang flight, as stated earlier. Therefore, there is no risk of crossing the approved airspace in summer.

The differences in longitude and latitude distributions with altitude are presented in Fig. C6 (a), (b), (c), and (d). The predicted balloon trajectories in the longitudinal direction in summer also showed no significant differences between day and night time like that of winter.

Unlike the more broadly distributed trajectory trends of the winter nighttime for the latitude-wise balloon trajectories over altitude, summer nighttime trends revealed no notable difference with the daytime trends. It is conceivable that the reason for the narrow distribution in the latitudinal direction at both day and night is the slow wind speed. The lowest wind speed spectrum appears in summer throughout the year. Since travel distance is proportional to wind speed and the time the balloon faces the wind, it is a logical consequence that the shortest travel distance is recorded in summer.

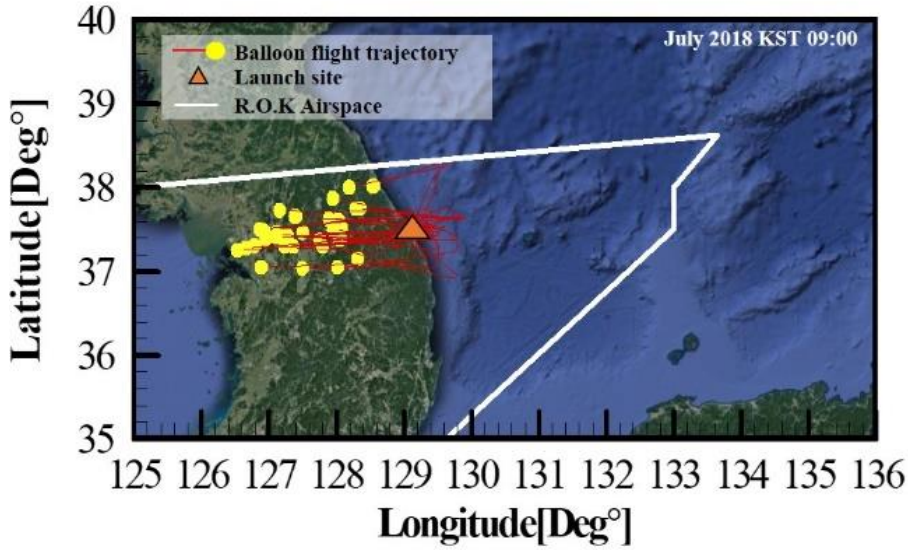

Fig. C4 Predicted trajectories on July 2018 (summer), KST 09:00, UTC+9

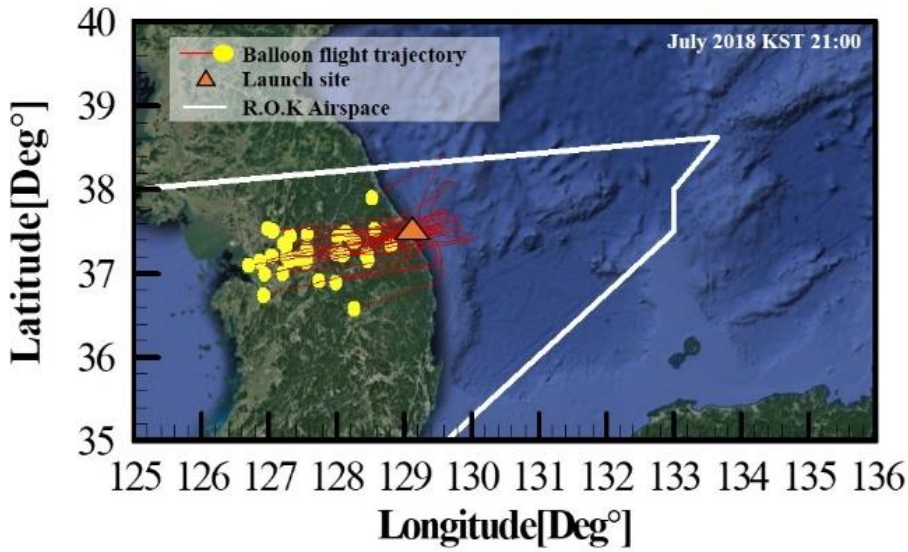

Fig. C5 Predicted trajectories on July 2018 (summer), KST 21:00, UTC+9

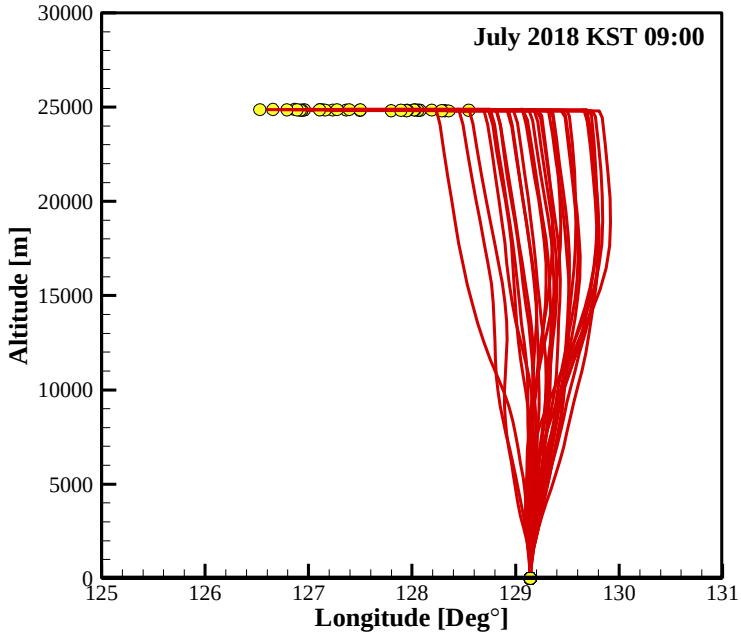

(a) Longitude variation with altitude

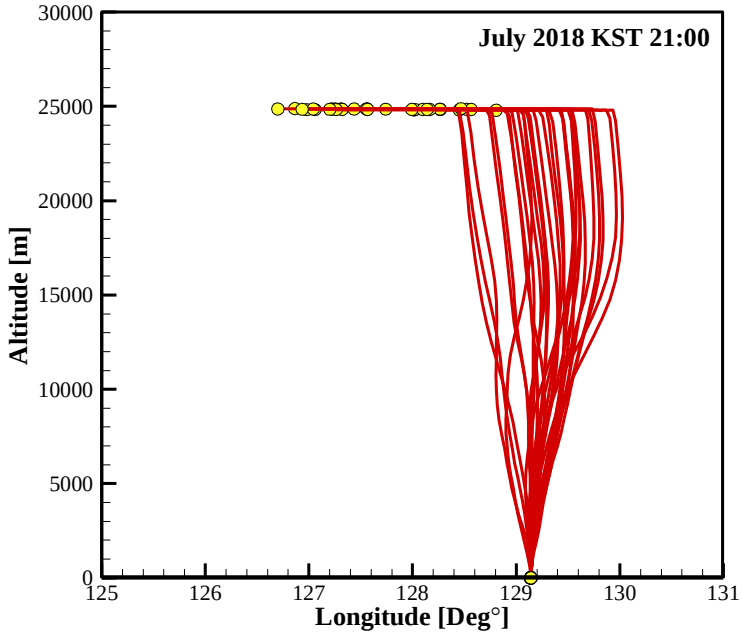

(b) Longitude variation with altitude

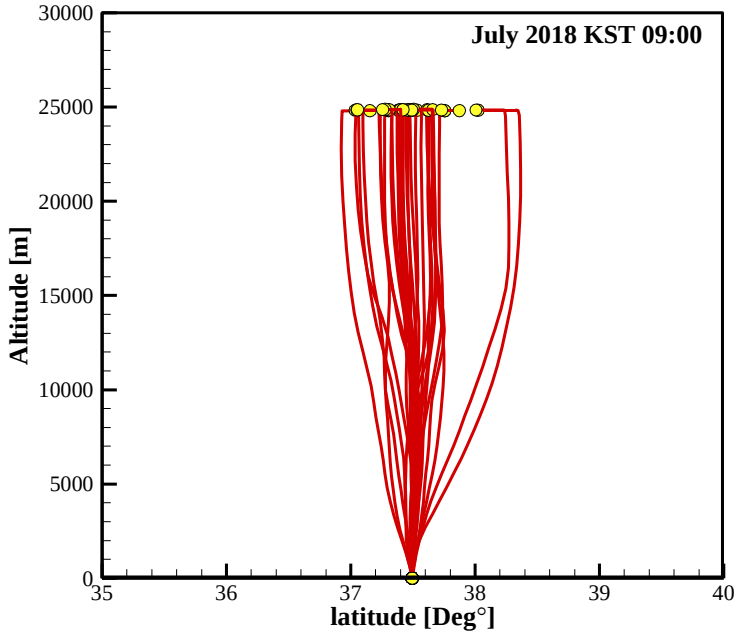

(c) Latitude variation with altitude

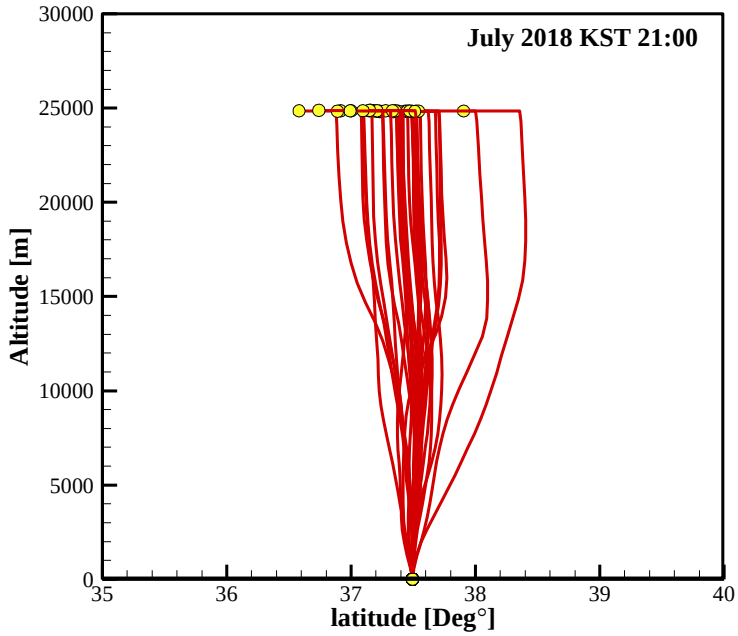

(d) Latitude variation with altitude

Fig. C6 Flight simulation results in summer (Launching from Donghae-si, July 2018 KST 09:00, 21:00, UTC+9)

As previously mentioned, several balloon trajectories crossed the boundary line of the Incheon FIR in winter. Strong winds such as the winter's jet stream will impact on the operational feasibility of the balloon campaign negatively. To tackle these concerns, the results of the daily flight simulation for 5 years from 2014 to 2018 were thoroughly investigated with respect to airspace violation.

Fig. C7 indicates the monthly operational feasibility, and elapsed time at the moment of airspace violation after launch, respectively. The operation feasibility of December recorded the lowest value, approximately 50%. Afterward, the values increased from 71 to 78% as the spring season is coming. It recorded operational feasibility over 97% without airspace violation within the required mission time (6 hrs) from May to October (from late spring to mid-autumn season), after that it decreased again in winter.

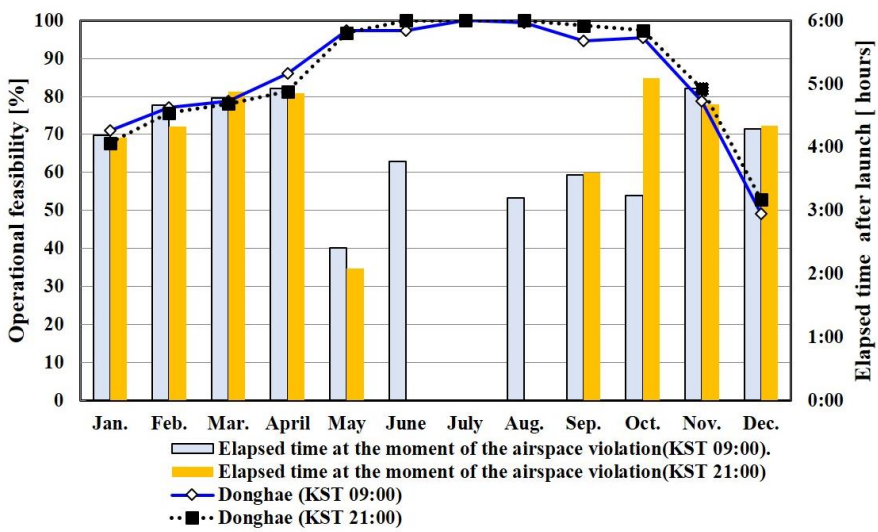

Fig. C7 Monthly flight simulation results based on the wind data for 2014~2018 years

Even though the value of operational feasibility in winter was the lowest the whole year, it seems acceptable values upon considering both the limited operation days of a recovery boat due to adverse sea state in winter and average elapsed flying time at the moment of airspace violation. The average elapsed flying time of the balloon in those periods after launch was 4:40, which was shorter than the expected 6 hours for the expected mission. Although other experiments with long flight time windows are not available in winter, certain space environmental tests, such as the MARS exploration airplane drop test, can be covered in that flight window.

In case of the airspace infringement between May and October, the elapsed time after the launch was recorded as taking three hours on average. This result was generally attributed to the fact that the wind blowing from the south make the balloons penetrate the north border of the Incheon FIR, which is approximately 38° north. Such cases are negligible with regard to the value of operational feasibility.

The nature of boomerang flights returning to the launch site can realize a great savings of time and effort for retrieving payload in summer and solves airspace violation problems. However, as demonstrated in Fig. C4 and C5, if the boomerang flight trajectory moves too much towards the shore, it is not compatible with the purpose of sea-based operation in terms of safety and recovery efficiency. Taking these into consideration, launching a balloon at the Ulleungdo was devised for balloon operations in summer. This method could

benefit from the geographical advantage of the Ulleungdo, which is located in the center of the Incheon FIR eastern sector. Fig. C8 (a), (b), and (c) show the trajectory simulation results of the Ulleungdo for June, July, August, respectively. It can be observed that balloons move westward without violating the boundary line of the Incheon FIR by virtue of the boomerang flight. Furthermore, the distance traveled in the direction of the shore was considerably reduced compared to that of launching in the Donghae-si. In realistic balloon campaign in summer, several balloon trajectories flying above the land could be minimized by controlling the rate of climb speed via employing dropping ballasts and exhausting lift gas, along with conducting the flight termination.

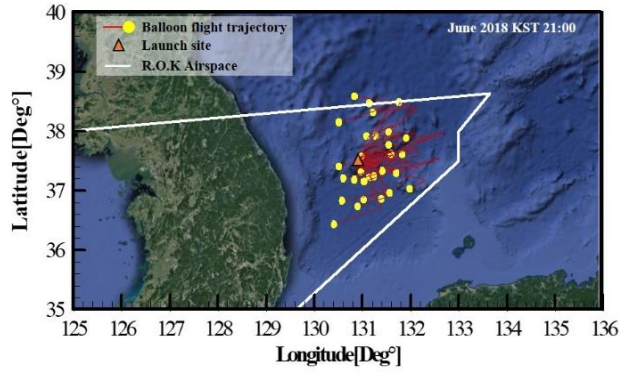

(a) Predicted trajectories of June 2018 KST 21:00

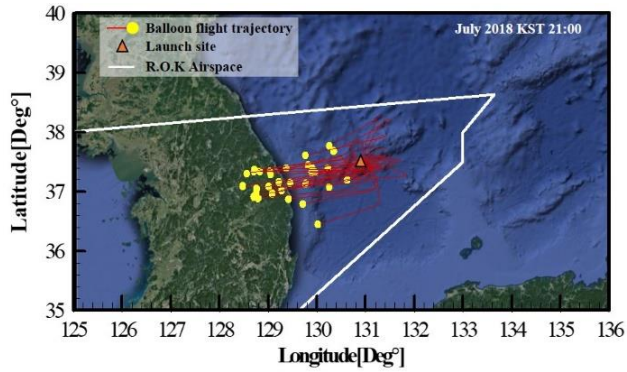

(b) Predicted trajectories of July 2018 KST 21:00

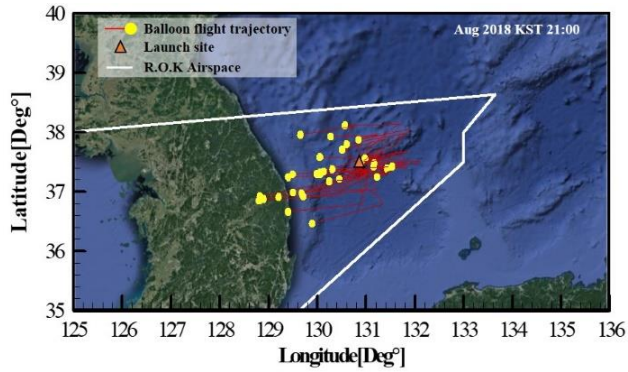

(c) Predicted trajectories of August 2018 KST 21:00

Fig. C8 Flight simulation results in the summer season (Launching from Ulleung-do, KST 21:00)

Appendix D: The manufacturing of the balloon

D.1 The envelope design algorithm of SNUBALL

To design a small-sized zero pressure balloon, a Σ-shape natural shape balloon design algorithm which maintains the inverted teardrop-like shape from partial to full inflation was followed.

The flow chart of envelope design is depicted in Fig. D1.

1) To carry out a given mission, the target altitude, the weight of the payload loaded on the balloon, and the density and thickness of the polyethylene film need to be determined.

2) To find the natural shape parameter of dimensionless length ($\boldsymbol{\lambda}$), weight (Σ_e) and buoyancy ($\boldsymbol{b_g}$), guessing for the envelope length ($\boldsymbol{l_s}$) and initial angle ($\boldsymbol{\theta_0}$) is conducted.

3) As presented in the Eq. 1, the ordinary differential equations (ODEs) associated with the relationship among the tension $\tilde{T}_\theta$, weight Σ_e, and buoyant force b_g of the balloon film should be solved to determine the shape of the envelope.

$$\tilde{r}\tilde{T}_\theta \frac{d\theta}{d\tilde{s}} = -k\sum_e \tilde{r}\frac{d\tilde{r}}{d\tilde{s}} - (\tilde{z} - \tilde{z}_b)\tilde{r} \qquad \text{Eq. (1)}$$

where, $\tilde{r} = \frac{r}{\lambda}$, $\tilde{z} = \frac{z}{\lambda}$, $\tilde{z}_b = \frac{z_b}{\lambda}$, $\tilde{s} = \frac{s}{\lambda}$

$$\tilde{T}_\theta = \frac{T_\theta}{b_g\lambda^2}, \quad k = (2\pi)^{-\frac{1}{3}}, \sum_e = \frac{w_e g}{k b_g \lambda}$$

4) If the initial angle and the length of the envelope are incorrectly calculated, the procedure is iterated until the proper shape is obtained. After this iteration process, the final envelope shape is derived.

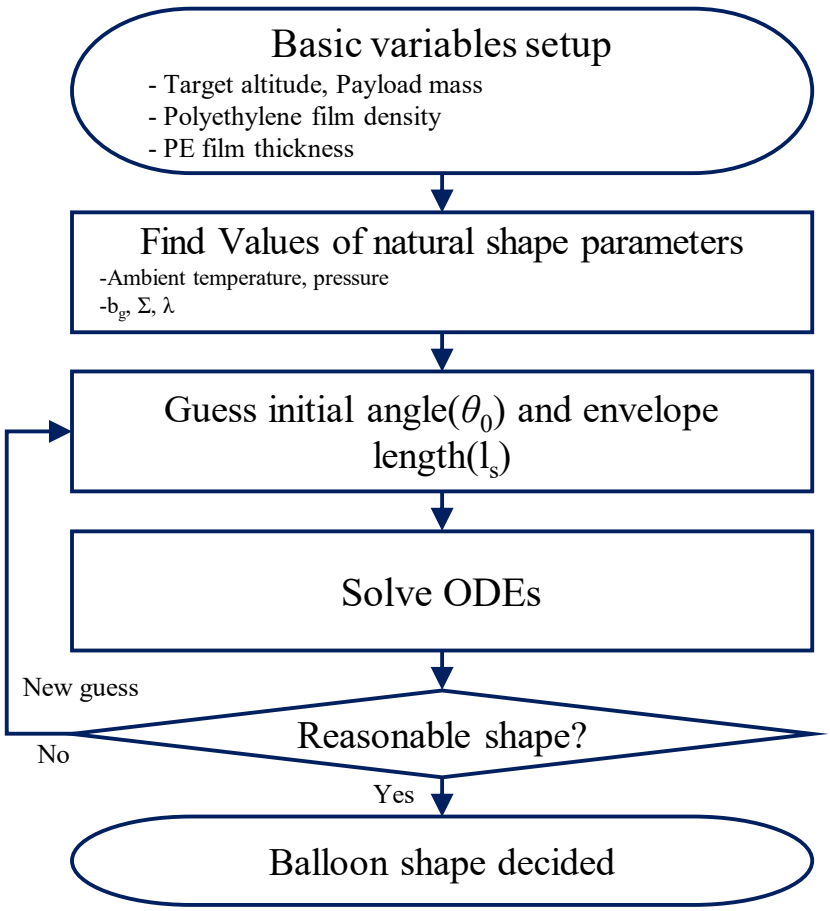

Fig. D1 Flow chart of envelope shape design

Fig.D2 depicts an inflation process of the Natural-shape balloon varies with an increase of an altitude when following conditions: the payload 10kg, target altitude 30km, film density 940kg/m3, and film thickness 20μm. It can be seen that the balloon is in fully expanded at an altitude of 30 km.

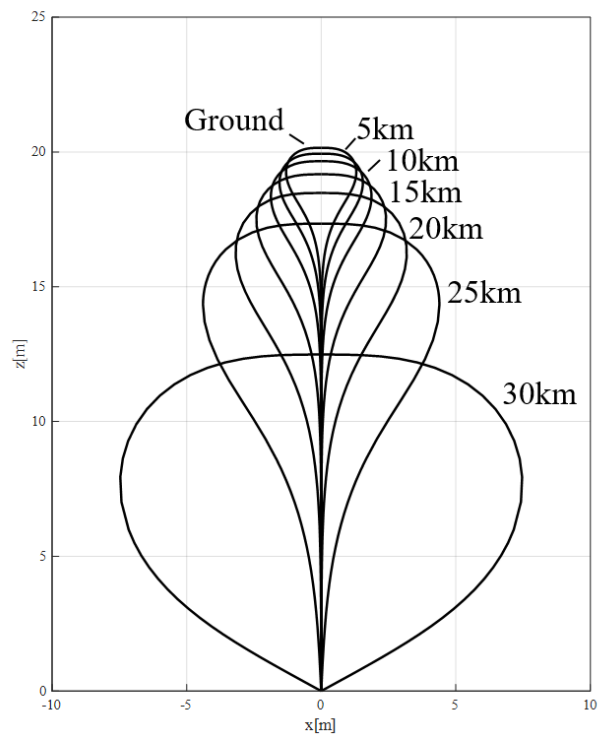

Fig.D2 Designed balloon shape and its variance according to the altitude

[Class: target altitude 30km / payload 50kg]

D.2 Envelope manufacture

To withstand the low-temperature environment during the flight, ultra-thin film materials for envelope production requires following features: low brittleness temperatures, high strength, high elongation percentage, and high tear strength. In this regard, the polyethylene film has been widely used to manufacture the balloon envelope.

A balloon envelope consists of a number of spindle shaped gores which is described in Fig D3. These gores are tailored from a long film and thermally sealed with the neighboring gores by a fine sealing method, as shown Fig D4. The high tensile polyester fibers are bonded upon the thermally bonded gore connection parts in the direction of the meridian that connects the apex of the envelope and the base. Consequently, it distributes the weight of the gondola which is connected to the base of the envelope to prevent ripping. Fig. D5 describes the manufactured envelope of the 10kg / 20km class zero pressure balloon

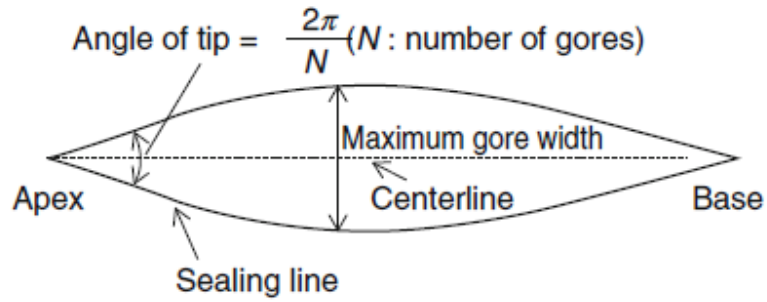

Fig. D3 Shape of a gore [22]

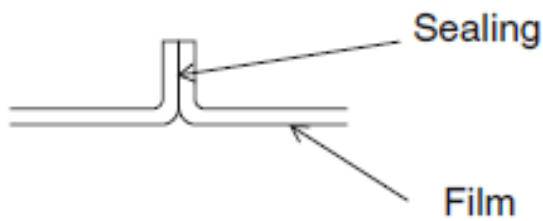

Fig. D4 Fine sealing method for a film

Fig. D5 The manufactured envelope shape

[Class: target altitude 10km / payload 10kg]

D.3 Exhaust valve

An exhaust valve serves to release buoyant gas to reduce buoyancy. This device enables to lower the altitude of a balloon than the pre-planned altitude or to slow down the rate of climb of the balloon during the ascent phase.

The exhaust valve is required to be lightweight and compact due to the limited installation space. As shown in Fig. D6, the exhaust valve is installed at the apex of the balloons which of payload and target altitude are 3kg, 10kg and 10 km, 20km, respectively. However, the two ZPBs described above has a small payload capacity, which imposes burdens on installing an exhaust valve and its associated control electronics in terms of the weight and size constraints. Therefore, a compact and lightweight spring-loaded exhaust valve was implemented. This spring-loaded exhaust valve serves to prevent the rupture of the envelope in case of the venting duct is malfunctioning, not for controlling the altitude of the balloon.

On the other hand, since the target balloon (50kg / 25km class) has a larger payload capacity than the aforementioned balloons, a solenoid exhaust valve of the normally closed (NC) type is implemented to adjust the altitude and the ascending speed. This prototype of the solenoid type exhaust valve for the 50kg / 25km class balloon is expected to be installed at the balloon apex with the disk-shaped fitting plate, as shown in Fig. D7. This plate is used not only for fastening the ends of the load tape and film but also for mounting the prototype solenoid exhaust valve.

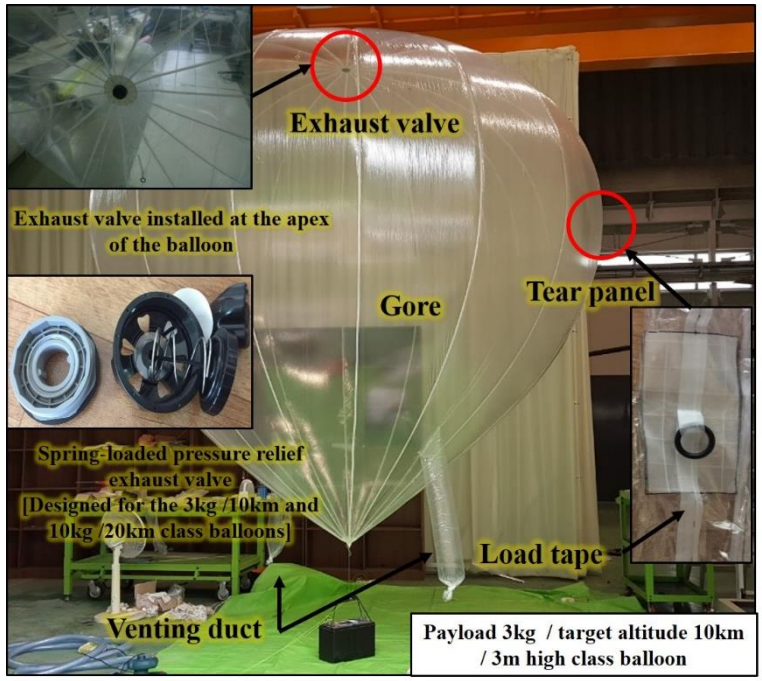

Fig. D6 The exhaust valve and tear panel configuration

Fig. D7 Solenoid exhaust valve for 50kg / 25km class balloon

This solenoid valve is designed to operate by the telecommand from the ground station via UHF frequency band. Once the UHF transceiver of the onboard telecommunication system receives the command signal from the ground station, the MCU relay the command to the exhaust valve via the Zigbee wireless protocol to control the open or closing of the exhaust valve.

The electronics driving the solenoid valve consists of three PCBs as shown in Fig.D8. It is consists of the Zigbee sensor layer to receive and transmit the open or close command, MCU layer to control solenoid valve according to the received command, and power source to operate the electronic equipment.

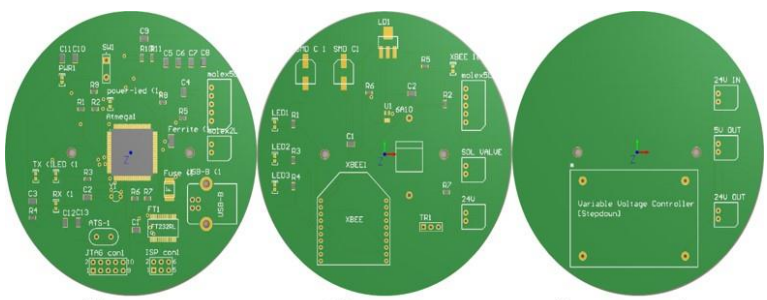

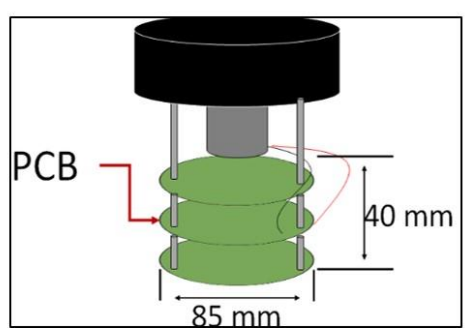

Fig. D8 PCB parts for the exhaust valve

Appendix E: Sub-systems for safety

E.1 ATC transponder

Air Traffic Control transponder is a standard equipment installed in an aircraft for aviation safety. When the ATC transponder receives an interrogation signal from the Secondary Surveillance Radar (SSR) of the air traffic control system, it sends back its identification code and altitude information (Fig. 53(a)). Thus, the location and pressure altitude of a scientific balloon is identified by Air Traffic Controllers. Consequently, Air Traffic Controller keep the balloon location informed to other aircraft pilots so that they can be safe from a balloon flight. Fig. E1 depicts the Becker ATC transponder installed the SNUBALL [68].

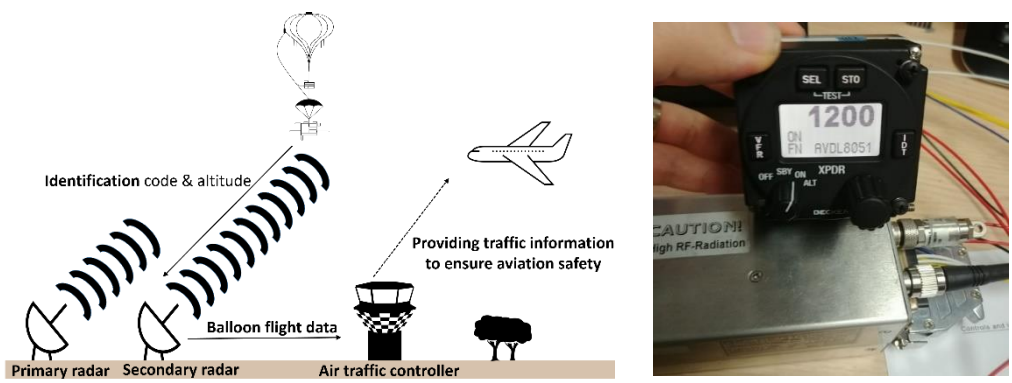

Fig. E1 The functional diagram of the ATC and BECKER ATC transponder

Appendix F: Employed components and cost list

Table F1 presented the required budget for a ZPB balloon campaign. After the success of the sea recovery operation, the cost of a balloon campaign can be reduced for next time depending on the condition of electronics and equipment.

Table F1 Cost breakdown for a ZPB balloon campaign

Components		COST($)	Notes
Envelope	Envelope	7,114	7m/ 10kg class 5ea
	Helium	890	47 liter high pressure gas cylinder
Parachute	-	353	16 ft diameter
Separator	TT&C electronics	675	
	Pacific scientific	1,848	
	Cable cutter		
	Tender descender	60	
	TT&C electronics	1,048	
	Transponder	4,890	
Gondola	Active buzzer	60	
	Iridium backup tracker	380	
	Autoinflation buoy	400	
Other required hardware	-	2,000	
Rent-a-ship	-	2,000	per day
Rent-a-car	-	180	per day
Total		21,898	

All the component models and prices are can be found in the following URL : https://drive.google.com/file/d/1rTJLKw_KOiXjY_BAqcmWVr7yzOZo2px-/view?usp=sharing

References

[1] M. Casolino, "The JEM-EUSO Program to Study UHECR from Space," presented at the Proceedings of 2016 International Conference on Ultra-High Energy Cosmic Rays (UHECR2016), 2018.

[2] W. V. Jones, "Evolution of scientific ballooning and its impact on astrophysics research," *Advances in Space Research,* vol. 53, no. 10, pp. 1405-1414, 2014.

[3] Tibor Kremic, Karl Hibbitts , Eliot Young, Robert Landis, Keith Noll, and K. Baines, "Assessing the Potential of Stratospheric Balloons for Planetary Science," presented at the 2013 IEEE Aerospace Conference, Big Sky, MT, USA, 13 May 2013, 2013.

[4] P. B. Voss, L. R. Hole, E. F. Helbling, and T. J. Roberts, "Continuous In-Situ Soundings in the Arctic Boundary Layer: A New Atmospheric Measurement Technique Using Controlled Meteorological Balloons," *Journal of Intelligent & Robotic Systems,* 2012.

[5] M. Schwarzbach, S. Wlach, and M. Laiacker, "Modifying a scientific flight control system for balloon launched UAV missions," presented at the 2015 IEEE Aerospace Conference, Big Sky, MT, USA, 08 June 2015, 2015.

[6] H. Kimm, J. S. Kang, B. Bruinga, and H. S. Ham, "Real Time Data Communication Using High Altitude Balloon Based on Cubesat Payload," *Journal of Advances in Computer Networks,* vol. 3, no. 3, pp. 186-190, 2015.

[7] A. D. Simpson, O. A. Rawashdeh, S. W. Smith, J. D. Jacob, W. T. Smith, and J. E. Lumpp, "BIG BLUE: high-altitude UAV demonstrator of Mars airplane technology," presented at the 2005 IEEE Aerospace Conference, Big Sky, MT, USA, 19 December 2005, 2005. Available: https://ieeexplore.ieee.org/abstract/document/1559753

[8] J. A. Gaskin, I. S. Smith, and W. V. Jones, "Special Issue on Scientific Balloon Capabilities and Instrumentation," *Journal of Astronomical Instrumentation,* vol. 03, no. 02, 2014.

[9] S. Louvel, J. Evrard, and S. Montminy, "Assessment of the Last Two STRATO SCIENCE Campaigns in Timmins, Canada," presented at the SpaceOps 2016 Conference, 2016.

[10] E. S. Seo *et al.*, "Cosmic-ray energetics and mass (CREAM) balloon project," (in English), *Advances in Space Research,* vol. 33, no. 10, pp. 1777-1785, 2004.

[11] K. Yamada *et al.*, "Deployment and Flight Test of Inflatable Membrane Aeroshell Using Large Scientific Balloon," in *21st AIAA Aerodynamic Decelerator Systems Technology Conference and Seminar*, 2011, p. 2579.

[12] S. Katikala, "GOOGLE™ PROJECT LOON," *RIVIER ACADEMIC JOURNAL,* vol. 10, 2014.

[13] T. M. Randolph, R. Mullenax, C. Schwantes, and D. R. B. Steven W. Sell, "The First Balloon Flight of the Low Density Supersonic," presented at the 2015 IEEE Aerospace Conference, Piscataway, NJ, 2015.

[14] H. Fuke *et al.*, "Developments of the Sliding Launcher and Related Facilities for the New Japanese Balloon Base," *Transactions of the Japan Society for Aeronautical and Space Sciences, Space Technology Japan,* vol. 7, no. ists26, pp. Tm_7-Tm_11, 2009.

[15] A. Vargas, D. Levesque, V. Dubourg, S. Lafrance, and R. Grenier, "Qualification of the new French balloon system and the new Canadian launch site," presented at the AIAA Balloon Systems Conference, 2014.

[16] T. Fields, M. Heninger, J. LaCombe, and E. Wang, "In-flight Landing Location Predictions using Ascent Wind Data for High Altitude Balloons," presented at the AIAA Balloon Systems (BAL) Conference, 2013.

[17] (2016). *NASA/TM-2016-219148, Avionics and Power Management for Low-Cost High-Altitude Balloon Science Platforms*. Available: https://ntrs.nasa.gov/search.jsp?R=20160011507

[18] Margarita Safonova *et al.*, "An Overview of High-Altitude Balloon Experiments at the Indian Institute of Astrophysics," *Astronomical and Astrophysical Transactions (AApTr),* vol. 29, no. 3, pp. 397-426, 2016.

[19] K. Gozlan, Y. Reuveni, K. Cohen, B. Ben-Moshe, and E. Berliner, "Cost-Effective Platforms for Near-Space Research and Experiments," in *Space Flight*, 2018.

[20] J. P. Vernier *et al.*, "BATAL: The Balloon Measurement Campaigns of the Asian Tropopause Aerosol Layer," *Bulletin of the American Meteorological Society,* vol. 99, no. 5, pp. 955-973, 2018.

[21] A. Simpson, J. Jacob, S. Smith, O. Rawashdeh, J. Lumpp, and W. Smith, "BIG BLUE II: Mars Aircraft Prototype with Inflatable-Rigidizable Wings," presented at the 43rd AIAA Aerospace Sciences Meeting and Exhibit, 2005.

[22] N. Yajima, T. Imamura, N. Izutsu, and T. Abe, *Scientific Ballooning*. Springer, 2009.

[23] H. Zell. (2017, 30 September). *Types of Balloons*. Available: https://www.nasa.gov/scientific-balloons/types-of-balloons

[24] W. V. Jones, "Recent Developments in Scientific Research Ballooning," *Nuclear Physics B - Proceedings Supplements,* vol. 166, pp. 217-222, 2007.

[25] T. Yoshida. (2003, 17 May). *A New World of Scientific Balloons*. Available: http://global.jaxa.jp/article/interview/vol42/index_e.html

[26] S. Westerlund, M. Abrahamsson, G. Florin, and C. Lockowandt, "Esrange Space Center – A European Rocket and Balloon Launch and Operation Site North of The Arctic Circle," presented at the 15th International Conference on Space Operations, 2018.

[27] V. Dubourg *et al.*, "3 balloon campaigns in 10 months - 3 Outback balloon flights in a fortnight: a challenge made true!," presented at the 15th International Conference on Space Operations, 2018.

[28] H. Fuke *et al.*, "A new balloon base in Japan," (in English), *Advances in Space Research,* vol. 45, no. 4, pp. 490-497, Feb 15 2010.

[29] Center for International Earth Science Information Network - CIESIN - Columbia University and Information Technology Outreach Services - ITOS - University of Georgia, "Global Roads Open Access Data Set, Version 1 (gROADSv1)," ed. Palisades, NY: NASA Socioeconomic Data and Applications Center (SEDAC), 2013.

[30] A. Doi *et al.*, "A balloon-borne very long baseline interferometry experiment in the stratosphere: Systems design and developments," *Advances in Space Research,* vol. 63, no. 1, pp. 779-793, 2019.

[31] A. Vargas, V. Dubourg, P. Raizonville, and P. Cocquerez, "The CNES Balloon Program : 2017 - 2019," presented at the AIAA Aviation 2019 Forum, 2019.

[32] J. Nishimura, N. Yajima, H. Akiyama, M. Ejiri, R. Fujii, and S. Kokubun, "Polar patrol balloon," *Journal of Aircraft,* vol. 31, no. 6, pp. 1264-1267, 1994.

[33] K. You, B. Won, and S. Jeong, "Design and Wind Tunnel Test of Airfoil for Mars Exploration Aircraft," in *KSAS 2018 Spring Conference* 2018, pp. 42-43: The Korean Society for Aeronautical & Space Sciences (KSAS).

[34] *ENFORCEMENT DECREE OF THE RADIO WAVES ACT,* M. o. S. a. ICT, 2016.

[35] V. Anmireddy *et al.*, "Telemetry, telecommand and safety sub-systems for scientific ballooning from Hyderabad," *Advances in Space Research,* vol. 46, no. 7, pp. 960-967, 2010.

[36] A. Kumar, S. C. Sati, and A. K. Ghosh, "Design, Testing, and Realisation of a Medium Size Aerostat Envelope," *Defence Science Journal,* vol. 66, no. 2, 2016.

[37] P. Clark *et al.*, "An open source toolkit for the tracking, termination and recovery of high altitude balloon flights and payloads," *Journal of Instrumentation,* vol. 14, no. 04, pp. P04003-P04003, 2019.

[38] R. J. Leopold and A. Miller, "The IRIDIUM communications system," *IEEE Potentials,* vol. 12, no. 2, pp. 6-9, 1993.

[39] A. G. C. Guerra, A. S. Ferreira, M. Costa, D. Nodar-López, and F. Aguado Agelet, "Integrating small satellite communication in an

autonomous vehicle network: A case for oceanography," *Acta Astronautica,* vol. 145, pp. 229-237, 2018.

[40] R. S. M. S. Ltd, "RockBLOCK v2 -Developer Guide," Rock Seven Mobile Services Ltd, Ed., ed, 2016.

[41] Y. Shoji *et al.*, "Marine Search-and-Recovery Operation of Scientific Balloons in Japan," (in English), *Journal of Astronomical Instrumentation,* vol. 06, no. 02, Jun 2017.

[42] (2019, 30 September). *HAMMAR*. Available: https://www.cmhammar.com/products/personal-safety-mob/lifejacket-inflator/

[43] (2019, 30 September). *Ship Model Basin: Towing Tank* Available: http://ship.snu.ac.kr/index.php?mid=E_Education

[44] Y. Lee and K. Yee, "Numerical Prediction of Scientific Balloon Trajectories While Considering Various Uncertainties," *Journal of Aircraft,* vol. 54, no. 2, pp. 768-782, 2017.

[45] (30 September). *Global Forecast System (GFS)*. Available: https://www.ncdc.noaa.gov/data-access/model-data/model-datasets/global-forcast-system-gfs

[46] (2019). *Flight safety regulations for aeroplanes-unmanned Free Balloons Operation*. Available: http://www.molit.go.kr/USR/I0204/m_45/dtl.jsp?gubun=4&search=&search_dept_id=&search_dept_nm=&old_search_dept_nm=&psize=10&search_regdate_s=&search_regdate_e=&srch_usr_nm=&srch_usr_num=&srch_usr_year=&srch_usr_titl=&srch_usr_ctnt=&lcmspage=1&idx=16015

[47] *Annex 2 to the Convention on International Civil Aviation, Rules of the Air,* I. C. A. O. (ICAO).

[48] T. Yamagami *et al.*, "Semi-dynamic launching method for scientific balloons," *Advances in Space Research,* vol. 30, no. 5, pp. 1145-1148, 2002.

[49] A. Denney, "Iridium Satellite Based Global Communications for High Altitude Scientific Ballooning," presented at the AIAA Balloon Systems Conference, 2007.

[50] Margaret M. McMahon and R. Rathburn, "MEASURING LATENCY IN IRIDIUM SATELLITE CONSTELLATION DATA SERVICES," US Naval Academy, 2005.

[51] F. Bekkadal, "Arctic Communication Challenges," *Marine Technology Society Journal,* vol. 48, no. 2, pp. 8-16, 2014.

[52] I. S. Smith, "The NASA Balloon Program: looking to the future," *Advances in Space Research,* vol. 33, no. 10, pp. 1588-1593, 2004.

[53] W. V. Jones, "Global balloon flight obstacles and opportunities," *Advances in Space Research,* vol. 33, no. 10, pp. 1600-1607, 2004.

[54] (2019). *GSFC-E-DAA-TN69959, NASA Wallops Overview of Rideshare Mission Integration Capability*.

[55] G. Russo *et al.*, "Unmanned Space Vehicle Program: DTFT In Flight Experiments," presented at the 18th ESA Symposium on European Rocket and Balloon Programmes and Related Research, Visby, Sweden, 3-7 June 2007, 2007.

[56] Y.-J. Cho *et al.*, "Vertical Analysis of Wind Speed over South Korea for the Flight Safety of HALE UAV," *Journal of the Korea Institute of Military Science and Technology,* vol. 19, no. 4, pp. 551-558, 2016.

[57] T. Strganac, "Wind study for high altitude platform design," presented at the 3rd Lighter-Than-Air Systems Technology Conference, 1979.

[58] J.-W. A. Wang *et al.*, "Sensitivities of the NCEP Global Forecast System," *Monthly Weather Review,* vol. 147, no. 4, pp. 1237-1256, 2019.

[59] V. S. R. Prasad, C. Johny, P. B. Mali, S. K. Singh, and E. N. Rajagopal, "Global retrospective analysis using NGFS for the period 2000–2011," in *CURRENT SCIENCE*, 2017, vol. 112, no. 2.

[60] J. A. Roney, "Statistical wind analysis for near-space applications," *Journal of Atmospheric and Solar-Terrestrial Physics,* vol. 69, no. 13, pp. 1485-1501, 2007.

[61] K. Ulgen and A. Hepbasli, "Determination of Weibull parameters for wind energy analysis of ?zmir, Turkey," *International Journal of Energy Research,* vol. 26, no. 6, pp. 495-506, 2002.

[62] H. Fuke, "Recent Highlights of Scientific Ballooning in Japan," (in English), *Journal of Astronomical Instrumentation,* vol. 06, no. 02, Jun 2017.

[63] Y.-J. Cho *et al.*, "The Analysis of Meterological Environment over Jeju Moseulpo Region for HALE UAV," *Journal of the Korea Institute of Military Science and Technology,* vol. 18, no. 4, pp. 469-477, 2015.

[64] R. Palumbo, "A SIMULATION MODEL FOR TRAJECTORY FORECAST, PERFORMANCE ANALYSIS AND AEROSPACE MISSION PLANNING WITH HIGH ALTITUDE ZERO PRESSURE BALLOONS," Doctor, University of Naples Federico II, 2007.

[65] R. Farley, "BalloonAscent: 3-D Simulation Tool for the Ascent and Float of High-Altitude Balloons," presented at the AIAA 5th ATIO and16th Lighter-Than-Air Sys Tech. and Balloon Systems Conferences, 2005.

[66] R. Palumbo, M. Russo, E. Filippone, and F. Corraro, "ACHAB: Analysis Code for High-Altitude Balloons," presented at the AIAA Atmospheric Flight Mechanics Conference and Exhibit, 2007.

[67] H. Du, M. Lv, L. Zhang, W. Zhu, Y. Wu, and J. Li, "Energy management strategy design and station-keeping strategy optimization for high altitude balloon with altitude control system," *Aerospace Science and Technology,* vol. 93, 2019.

[68] (30 September). *Becker Avionics*. Available: http://www.becker-avionics.com/portfolio/bxp6401-mode-s-transponder/

초 록

안전 문제 및 회수 가능성에 관계없이 과학 풍선의 회수를 위한 합리적인 방법은 해상 회수 전략이다. 해상 회수 전략은 Japan Aerospace Exploration Agency (JAXA) 및 the Institute of Space and Astronautical Science (ISAS)가 수십 년 동안 개척한 독특한 회수 방법이다. 이 방법은 대기 관측 및 우주 환경 시뮬레이션과 같은 일본의 다양한 과학 및 공학 연구 임무 달성에 기여해왔다. 그러나, JAXA /ISAS가 오랜 기간 동안 해상 회수 전략을 수행해 왔음에도 불구하고 저자가 아는 한 이 회수 방법의 희귀성으로 인해 해상 회수에 적합한 풍선 시스템 설계 및 제조에 관해 출판된 연구는 거의 없다.

이러한 점에서, 본 연구에서는 해상 회수을 위해 설계된 소형 영압력기구(ZPB) 플랫폼을 위한 시스템 개발과정 및 비행시험에 대한 자세한 설명이 제시되었다. 해상회수용 벌룬시스템 제작을 위해 해상 통신, 방수, 단락 방지 및 부력을 신중하게 고려하여 비용효율적인 상용 (COTS) 제품을 사용하는 소형 ZPB 플랫폼을 개발하였다. COTS 제품을 사용하여 전체 비용 절감뿐만 아니라 원격 측정, 추적 및 명령 (TT&C) 시스템의 크기를 최소화하여 휴대성을 향상시킬 수 있었다.

벌룬 시스템 개발과 함께 해상회수에 중점을 둔 벌룬 캠페인 절차를 수립하였다. 이를 위해 5년간(2014~2018)의 계절풍에 따른 기구의 이동 경향을 수치 궤적 예측 프로그램을 이용하여 조사하였다. 시뮬레이션 결과를 반영하여 울릉도의 지리적 이점을 활용한 대한민국 동해에서의 ZPB 운영 절차를 제안하였다. 개발된 벌룬 시스템의 신뢰성을 검증하기 위해 해상 회수 전략을 포함한 4번의 비행 테스트를

수행하였다. 개발된 소형 ZPB 플랫폼은 해상 회수 전략을 포함한 4 차례의 비행 테스트를 통해 만족스러운 성능과 시스템 안정성을 보여주었다.

Keywords: Scientific balloon, High Altitude Balloon, Flight Test, Tracking, telemetry and command system, Sea recovery

주요어 : 고고도 과학 기구, 비행 시험, 추적, 원격측정 및 명령 시스템, 해상회수

학 번 : 2016-30182